RECONSTRUCTION OF ENVIRONMENTAL AND CLIMATE DYNAMICS USING MULTI-PROXY EVIDENCE FROM PALAEOSOLS OF THE WESTERN CAPE, SOUTH AFRICA

PETER NDUBUISI EZE

Thesis Presented for the Degree of

DOCTOR OF PHILOSOPHY (PhD)

In the

Department of Environmental & Geographical Science

Faculty of Science

UNIVERSITY OF CAPE TOWN

November 2013

“If I have seen further, it is by standing on the shoulders of giants” ~Isaac Newton.

“Every soil has a story to tell” ~ National Aeronautics & Space Administration (NASA).

DECLARATION

I declare that this thesis is the findings of my own research work. It is being submitted for the Degree of Doctor of Philosophy (PhD) in Environmental and Geographical Science, Faculty of Science at the University of Cape Town. The works of other authors cited were duly acknowledged. To the best of my knowledge and believe, this thesis has not been in the past, or is being submitted, for a Degree or examination at another university.

……

Peter Ndubuisi Eze

Cape Town

November 2013

ABSTRACT

Like many of the world's subtropical regions, the Western Cape of South Africa is highly sensitive to oscillations in the earth's climate system triggered by major tectonic changes, local variations in orbital forcing, better known as Milankovitch cycles, and its position at the interface between temperate and tropical circulation systems. Regrettably, a dearth of reliable and continuous palaeoenvironmental records means that relatively little is known about how regional environments have been impacted over centennial to multi-millennial timescales. Palaeosols constitute an important stratigraphic marker for past environments and may provide useful validation of pedogenic and other earth system process models. However, the characterisation and analysis of palaeosols has been a largely neglected source of information in the Western Cape, South Africa. This thesis aims to improve the understanding of the environments and climate dynamics using evidences from palaeosols.

Various palaeosol-based proxies including geochemistry, mineralogical, macro- and micromorphological, $\delta^{13}C$ and $\delta^{18}O$ isotope, and selected physico-chemical properties of palaeosols were studied and records obtained for four sites in the Western Cape. A number of chemical weathering indices and geochemical climofunctions were used to calculate weathering intensities, pedogenesis, palaeotemperature and palaeoprecipitation for the various locations using geochemical and stable isotope data.

Results of this study indicate that palaeosol-based proxies have the potential to provide snapshots into the palaeoenvironments and palaeoclimate of Western Cape and may complement previous studies done with other proxies such as pollens and diatoms. For example, the interpretation of the pedofeatures (calcareousness, vertic, gleyic, illuviation) - from the micromorphology - of the palaeosols suggests cyclic patterns of erosion and deposition that correlate with climate changes

of the past. Podzolization and laterization are the principal pedogenic processes responsible for the red palaeosol formation at the Cape Peninsula, while calcification and salinization are accountable for the Quaternary palaeosols. Inferences of gleization and lessivage are only evident in the mid-Miocene palaeosol at Langebaanweg. At LBW, pedogenesis was more advanced in the Mid-Miocene and Early Pliocene layers signifying a more humid and warmer climate with more stable landscape. Two major regional climate cycles were evident at the Cape Peninsula: relatively warm and humid subtropical climate which gave rise to the pedogenically modified buried red palaeosol and dry semi-arid Mediterranean climate under which the soils overlying the stone line is currently forming, as seen from the poor horizonation and translocation of materials. Clay mineral assemblages suggest the Quaternary palaeoclimate of the Western Cape has been predominantly characterised by low precipitation and active coastal erosion, which jointly accounted for poor soil profile development. This is in agreement with the early reports obtained from marine records of the African continent (e.g. deMenocal, 2005). A cross plot of the $\delta^{13}C$ and $\delta^{18}O$ of the carbonate palaeosols indicates they all formed under strong marine influence and C3 plants have been dominant since late Quaternary.

Caution is required when using geochemical weathering indices to obtain palaeoclimate information from the palaeosol sequences because weathering indices are not only sensitive to climate but also to soil age, and geochemical and mechanical overprinting. Moreover, the degree of weathering decreases with soil depth; in an eroded palaeosol profile, the most strongly weathered upper part may have been removed so that only the weathering index of the lower part is available. In the Western Cape, more palaeosol samples are required to validate the applicability of the tested geochemical climofunctions.

ACKNOWLEDGEMENT

Immense thanks are due to my supervisor, Professor Michael Meadows, whom provided me with the opportunity and advice which made this thesis a reality. His unalloyed passion and enthusiasm for palaeoenvironmental research has positively reshaped my academic career. I owe you more than I can say.

I would also like to thank Dr. Dave Roberts of the South African Council for Geosciences for his field guidance and productive criticism of the manuscripts which gave this thesis a face-lift. Dr. Pippa Haarhoff granted me the permission to sample at the West Coast Fossil Park, and I am indebted to her.

For providing valuable assistance including, literature, interpretation of thin sections and geochemical climofunction models, I wish to say a very huge thank you to: Drs. Sue McLaren, Karolina Leszczynska, Marcelo Krause, Rosa Poch, Lesogo Khomo and Frank Eckardt.

Palaeontological Scientific Trust through its Scatterlings of Africa programme and the University of Cape Town Postgraduate Funding Office provided the funding to undertake this study and I am profoundly thankful.

To my office mates, friends and colleagues: thanks for the valuable company, moral support and generally for making my stay in the EGS department so enjoyable. Special mention needs to be made for Chinecherem Nwankwo and Ester Lourens for their outstanding support and encouragement.

Most importantly, I would like to extend my utmost gratitude to my parents and siblings. Their love, unflinching support, and above all, believe in me were fundamental to the completion of this thesis, and it would not have happened without them. This thesis is dedicated to my father who fostered my love for academic excellence. The beauty of a thing done is to have done it. I owe you all.

Finally, I would like to say that; ***truth shall always stand and love is the greatest gift of all***.

TABLE OF CONTENTS

LIST OF FIGURES

LIST OF TABLES

CHAPTER 1

GENERAL INTRODUCTION

1.1. Historical aspects of palaeopedology

In recent decades, there has been growing recognition of the significance of fossilized soils/ palaeosols (Retallack, 1998) and the branch of this study is called "palaeopedology", the name of which is derived from ancient Greek word (*πεδου, πεδου*) for ground (Retallack, 2001). Also, Retallack (1998) argues that, while palaeosols have featured prominently as an object of study since the very beginning of modern geology (e.g. Hutton, 1795; Playfair, 1802; Webster, 1826), the term "palaeopedology" and a greater part of its theoretical basis has evolved essentially as a branch of soil science. The International Union of Soil Science (IUSS) upgraded palaeopedology as one of its principal focus areas, from a working group to a fully fledged commission; in recognition of the growing global interest in palaeosol research.

The study of palaeosols has multidisciplinary dimensions reflecting the broad interest of this field for geoscientists including geologists, stratigraphers, sedimentologists, geochemists, geographers, palaeoclimatologists and pedologists (Catt, 1990; Retallack, 1990; Retallack, 1998). Consequently, this has led to disparities in the definition of palaeosols; for example, palaeosols can be regarded as, among other opinions as to their nature and origin, natural boundaries in complex stratigraphic sequences (e.g. Morrison, 1978), indicators of previous atmospheric composition (e.g. Holland, 1984), fossil soils of earlier ecosystems (e.g. Retallack, 1990) or simply buried soils (e.g. Soil Survey Staff, 2006. The operational definition of palaeosols used in this study however, is that they are pedogenic formations of past geologic time. A further corollary is that they archive the ancient environmental conditions which shaped their formation.

1.2. Overview of palaeosols in relation to pedogenic processes

The processes that shape soils and landscape formation are a complex interaction between surficial geological formations and the ecosystem (Retallack, 2001). Jenny's (1994) functional-factorial soil formation model identifies five major factors responsible for the state of pedogenesis. They are climate, organisms, topography (relief), parent material and time. Amongst these factors, the role of climate on soil genesis has been proved very significantly by various researchers and many soil classification systems are based on major climatic parameters. Exploring palaeosols is therefore one means by which we might interpret the palaeoenvironmental and palaeoclimatic oscillations in time and space. A caveat is that these factors tend to be interdependent and may be difficult to isolate in natural settings.

Climate especially plays an important role in the chemical weathering of parent materials and re-distribution of soluble constituents in soils and palaeosols (Blum and Törnqvist, 2000; Gibbard and Lewin, 2002; McCarthy and Plint 2003; Salcher et al., 2010). Precipitation, temperature and evapotranspiration are play significant role in soil development and are considered as the most active and primary the active climatic parameters which are commonly and widely used in modelling the nature and degree of pedogenesis/ pedogenic processes (Finke, 2011).

Landscape topography influences microclimate, hydro-dynamics, and material redistribution processes that critically influence the nature of soils and vegetation patterns (Van Breemen and Buurman, 2002; Siebert et al., 2007; Eze at al., 2010). Aspects of topography considered in soil formation are slope length and steepness, erosion/ sedimentation and local variants of temperature, precipitation and evaporation (Finke, 2011). Monogenetic and/ or polygenetic

palaeosols are formed at varying rates of sediment supply, drainage, pedoclimate and geomorphic surface stability (Fig. 1.1).

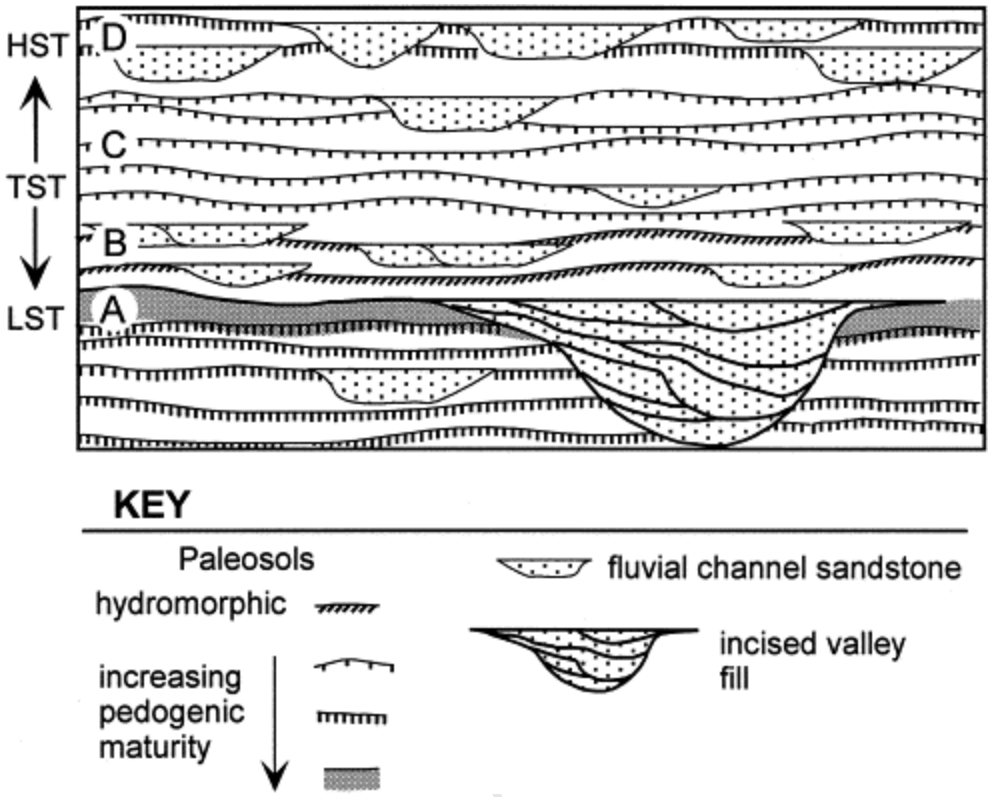

Fig. 1.1. Schematic diagram showing Wright and Marriott (1993) model of pedogenic development related to the sea-level cycle. (A) The lowstand systems tract (LST) is characterized by channel incision and strongly developed and well-drained paleosols that form on terraces. (B) Early in the TST, hydromorphic paleosols may form because base level is rising; channel sandstones may overlap because accommodation space is still low. (C) Increased accommodation space in the TST produces rapid sediment accumulation and weakly developed soils. (D) The HST is characterized by low accommodation space, thus, well-developed paleosols (Kraus, 1999).

Properties that have been used as indicators of pedogenesis include, but are not limited to, clay accumulation (Birkeland, 1999), accumulation of $CaCO_3$ (Alonso-Zarza and Silva, 2002; Alonso et al., 2004; Alonzo-Zarza and Wright, 2010), and Fe oxide content and composition (Favre et al., 2002; Smeck et al., 2003; Thompson et al., 2006). Field properties have been combined to form an index (Gupta and Rao, 2001; Brown et al., 2003; Price and Velbel 2003) and a simpler index (degree of reddening) has also been used as an indication of duration of

pedogenesis (Wondafrash et al., 2005; Ben-Dor et al., 2006). Pedogenic silica accumulation has also been classified into evolutionary stages on a qualitative basis and used as an indicator of pedogenesis (Kendrick and Graham, 2004; Sommer et al., 2006).

1.3. Identification of palaeosols

Palaeosols intercalated in sedimentary sequences can be very challenging to distinguish from the enclosing sediments where pedogenesis is not advanced. Three macromorphological features are used in identifying palaeosols: root traces, horizons, and structures (Retallack, 1988; 2005). However, it becomes important to determine whether a horizon in the palaeosol formed on *in situ* parent material, or from transported material/ pedosediments (McCarthy, 1998). Further, one should be cautious while identifying very ancient palaeosols (e.g. Precambrian) because most times, their original chemistry is altered due to mechanical and geochemical diagenesis overprinting (Gall, 1992; Demko et al., 2004).

Micromorphological features of *in situ* soils are characterised by homogeneous pedogenic facies recognised by at least one of the following features: (i) undisturbed features from soil floral and faunal activity, such as channels with root residues and excrement; (ii) a pedogenic b-fabric; (iii) pedogenic microstructures; (iv) one or more types of undisturbed pedofeatures (Fedoroff et al., 2010). On the other hand, pedosediments are recognised by: (i) an absence of *in situ* biogenic features, but the occasional presence of fragmentary faunal or floral remains; (ii) a massive microstructure, and occasionally a structure dominated by packing of rounded aggregates and/ or (iii) preserved sedimentary features (Fedoroff et al., 2010 and Mücher et al., 2010).

Palaeosols in most cases are not preserved as complete and undisturbed profiles but features such as truncations, stone lines and superimposed allochtonous materials on genetic horizons can detect such discontinuities (Fedoroff et al., 2010). Palaeosols are commonly classified into three major types on the basis of their position in a stratigraphic section and in the landscape namely buried, relict and exhumed soils (Birkeland, 1999). Buried soils are those which were not affected by later pedogenesis since the time they formed because they got buried by younger sediments. Non-buried or relict soils are at the land surface since the time of their initial formation and they may or may not have acquired their properties sometime in the past whereas exhumed soils were formerly buried but then exposed to current pedogenesis.

1.4. Classification of palaeosols

Palaeosol classification, in a manner similar to other disciplines, is primarily aimed at grouping similar palaeosols based on observable and measurable properties, thereby improving systemisation of knowledge and enhancing communication amongst palaeopedologists. A widely accepted classification of palaeosols has yet to emerge because palaeosols are modified in various ways after burial (Mack et al., 1993; Buurman, 1998; Kraus, 1999; Nettleton et al., 1998; Nettleton et al., 2000; Sheldon and Tabor, 2009).

Krause (1999) compiled three widely used basic classification systems have been widely used (Kraus 1999): United States Soil Taxonomy (Soil Survey Staff 2006; Soil Survey Staff 2010) system based on modern analogues; the classification system of Duchaufour (1982) and the palaeosol-specific taxonomy given by Mack et al. (1993). The first two approaches are largely based on a large number of modern diagnostic soil properties such as cation exchange capacity, pH, base saturation, argillic horizon and compaction that are not preserved in palaeosols (Retallack 2001; Sheldon and Tabor, 2009). Interpretative criteria for horizon

designation and taxonomic classification of palaeosols based on these two approaches are detailed in Tables 1.1 and 1.2.

Table 1.1. Interpretive criteria for horizon designation of the palaeosols.

Category	Symbol	Definition*	Identifying Properties**
Master Horizons	A	Surface horizon. Accumulation of humified organic matter mixed with mineral fraction	A surface horizon that is darker in colour with finer ped structure than lower horizons
	E	Surface horizon. Underlies an A horizon and is characterised by less organic matter, less sesquioxides (Fe_2O_3 and Al_2O_3), or less clay than underlying horizons.	Lighter relative colour than bounding horizons as a result of abundant quartz. Kaolinisation of feldspar grains.
	B	Subsoil horizon. Shows discernible enrichment in clay, carbonates, sesquioxides, organic matter or obliterated parent material structure.	Change of colour relative to the parent material. Increase in relative ped size.
	C	Parent material.	Preserves most depositional structures
Intergrade Master Horizons	AB	As above, but with A horizon characteristics dominant	
	EB	As above, but with E horizon characteristics dominant	
Subordinate Descriptors	g	Gleying from iron reduction	Lower chroma colour, usually 2 or less.
	k	Accumulation of carbonates	Carbonate nodules and elevated $CaO + MgO/ Al_2O_3$ ratios.
	t	Accumulation of clay	Presence of silicate clay forming coatings on ped faces, argillans in thin section, and elevated Al_2O_3 / SiO_2 ratios.
	w	Development of colour and structure only	Subsoil change in colour and structure relative to surrounding horizons or parent material and does not have significant illuvial accumulations

*Adapted from the FAO (2006); **Adapted from Soil Survey Staff (2010) and Retallack (1997)

Table 1.2. Interpretive criteria for soil taxonomic classification of the palaeosols

USDA Nomenclature	Definition*	Diagnostic Criteria
Argillic	Diagnostic horizon. A subsoil horizon that has at least 1.2 times as much clay as does some horizons above it, or 3% more clay content if the eluvial layer has > 15% clay, or 8% more clay if the eluvial layer has > 40% clay	Bt horizons that qualify
Calcic	Diagnostic horizon. A subsoil horizon that is at least 15cm thick, has secondary accumulation of carbonates (nodules) and contains > 5% carbonate nodules	Bk horizons that qualify
Cambic	Diagnostic horizon. A subsoil horizon of very fine sand or finer with some weak indication of constituent accumulation that is not enough to qualify as other subsoil diagnostic horizons.	Bw horizons that qualify
Ochric	Diagnostic horizon. A mineral surface horizon with colour values>5 dry or >3 moist**.	A horizons that qualify
Inceptisol	Soil taxonomic order. Soils that have not developed features diagnostic for other orders but beyond those permitted for entisols	Ochric horizon over a cambic or calcic subsoil, but without argillic horizon
Entisol	Soil taxonomic order. Soils that have little pedogenic development.	Weak ochric horizon development only, root traces

*From Soil Survey Staff (2010)

The palaeosol-specific nomenclature given by Mack et al., (1993) is a hierarchical system that draws fundamentally from six observable pedogenic features or processes: organic matter content, horizonation, redox conditions, *in situ* mineral alteration, illuviation of insoluble minerals and accumulation of soluble minerals.

1.5. Late Cenozoic palaeoclimates of the Southern Hemisphere

The climate of the early Neogene in the Southern Hemisphere was warmer than present, more humid and characterised by intermittent cooling (Steppuhn et al., 2006; Table 1.3) and carbon dioxide concentrations are reported to have varied between 300 and 600 ppm (Tripati et al., 2009). Global average temperatures were markedly higher than today and subsequent global climatic cooling in the Miocene brought about an increase in seasonality, which affected environments worldwide (Fedorov et al., 2006). The middle Miocene (Middle Miocene Climatic Optimum; MMCO) was the last prolonged warming of the Cenozoic era between 17 to 14.7 Ma (Shunk et al., 2009; Majewski and Bohaty, 2010). The MMCO was in operation for approximately 4 million years with 100 – 400 kyr variations in climatic parameters, and overall globally low ice volumes (Holbourn et al., 2007).

Table 1.3. Late Cenozoic palaeoclimate of the Southern Hemisphere

Era	Climate	Why?	Reported by
Early –middle Miocene (23 – 17 Ma)	Warm	Substantial increase in both surface and bottom temperatures of Sub-Antarctic waters reflects Periods of global warming; Neogene temperature Maximum at 19.5 – 17 Ma	Shackleton and Kennett, 1975; Kennett, 1986, Miller et al., 1987
Mid Miocene - late Miocene (17 – 11 Ma)	Cool	Abrupt cooling phase from 17 to 14 Ma linked to rapid expansion of East Antarctic ice sheet (EAIS) and associated cooling of high latitude waters; marked increase in meridional temperature gradients.	Shackleton and Kennett, 1975; Kennett, 1977, 1986; Miller et al., 1987
Late Miocene (approx 11 – 6.2 Ma)	Intermittent cool-warm	General cooling trend initiated in middle Miocene continues but is punctuated by brief episodes of climatic warming at 10.5 Ma, 9 – 8.5 Ma and 7.6 – 6.6 Ma.	Kennett, 1986; Kennett and Barker, 1990; Barron et al., 1991
Early Pliocene (5 – 3 Ma)	Warm	Higher than present CO_2 concentration	Jansen et al 2007
Mid Pliocene (3.3 – 3.0 Ma)	Warm	Elevated CO_2 levels in the atmosphere	Jansen et al 2007
Late Pliocene – Recent (2.4 – 0 Ma)	Cool	2.4 Ma event marks onset of bipolar glaciations	Kennett and Barker 1990; Hodell and Warnke, 1991
Last Glacial maximum (21ka)	Cool	Changes in greenhouse gas forcing and ice sheet conditions.	Jansen et al 2007

1.6. Rational and Justification

Palaeoenvironmental evidence for southwestern South Africa remains spatially and temporally sparse as palaeoclimatic proxy records are scarce and often discontinuous or brief (Chase and Meadows, 2007). Hitherto, the characterization and analysis of palaeosols has been a largely neglected source of information along the west coast of South Africa.

Furthermore, arid regions comprise more than a third of Earth's landscapes and sustain nearly two billion people (UNCCD, 2003), yet the pedogenic processes and thresholds that result in arid soils and landscapes have not been fully understood. In comparison to humid soils, which largely reflect the hydrolysis of minerals and the loss of alkalis from the soil profile, arid landscapes are distinct because their soil profiles typically reflect a net influx of ions to the Earth's surface over time. This influx, combined with alkaline soil solutions and fluctuating moisture conditions, produces a variety of unique authigenic mineral assemblages (Francis et al., 2007) including (but not limited to) carbonates, chlorides, iron and/or manganese oxides, nitrates, and sulfates, as well as unusual, fibrous phyllosilicate species such as palygorskite and sepiolite. Because important geochronologic, pedogenic, and climate change data are coded into the geochemistry of each authigenic species, this range of compositionally different minerals plays a pivotal role in understanding palaeoclimatic and palaeoenvironmental dynamics.

Soils, like organisms evolve and change with time. It is therefore very important that both modern soils and palaeosols are studied equally in order to improve our understanding of climate change and its impacts on the ecosystem. Palaeosols may constitute a stratigraphic marker for the past environment and may provide useful validation of pedogenic and other earth processes' models. There is also a growing global need to update existing knowledge using modern technological advancement, which gives room for more accurate and precise data.

1.7. Aim and Objectives

The overarching aim of this research, therefore, is to improve the understanding of the South African coastal palaeoenvironments and palaeoclimate dynamics from the detailed studies palaeosol-sediment-sequences.

Specific **OBJECTIVES** include:

i) To characterise the selected palaeosols and parent sediments on the basis of their macro and micro- -morphological, physical, mineralogical and geochemical properties.

ii) To interpret depositional history, evaluation of pedogenic pathways and geomorphic processes (autogenic and allogenic) that shaped the geomorphology of the study areas.

iii) Landscape and palaeoenvironmental reconstruction including: mineral provenance, weathering intensity, palaeovegetation, and palaeohydrology.

iv) Palaeoclimatic reconstruction including, estimation of ancient MAP, MAT and atmospheric CO_2 levels from the stable C and O isotope ratios of the palaeosol/ pedogenic carbonates.

1.8. Thesis layout

This thesis is a compilation of various research papers at various stages of publication culminating from the study of palaeosol-sediment sequences at four locations: Langebaanweg Fossil Park, Koeberg sea cliff, Goukamma coastal barrier and Cape Peninsula. Each chapter has a detailed description of the location and research methodology.

CHAPTER ONE: General introduction including a brief discussion on the science and core concepts of palaeopedology.

CHAPTER TWO: Geochemistry and palaeoclimatic reconstruction of a palaeosol sequence at Langebaanweg, South Africa.

CHAPTER THREE: Mineralogy and micromorphology of palaeosol and pedofacies from Langebaanweg, South Africa: Palaeoenvironmental interpretation**.**

CHAPTER FOUR: Stable isotope geochemistry and mineralogy of Late Quaternary Palaeosols from South African Coasts: Palaeoenvironmental Reconstructions**.**

CHAPTER FIVE: Evaluation of pedogenesis and palaeoenvironmental conditions of a palaeosol associated with stone line in the Cape Peninsula, South Africa.

CHAPTER SIX: Synthesis, summary and conclusion with suggestions for further research foci.

Together, these studies address the complex pedological, geochemical and mineralogical properties of palaeosols as well as their great potential for in-depth scientific study of the palaeoenvironments and palaeoclimate. Although based in the Western Cape of South Africa, this study has implications for comparison and interpretation of varying palaeosols worldwide. The choice of sites for this study from a variety of settings and ages actually would help achieve the aim because it indicates the diversity of environments from which palaeosol information can be extracted and used to interpret palaeoenvironments. Moreover, since calcic horizons (calcretes) have been observed in different and varied environmental settings, they may provide specific implications for the study of calcic palaeosols, and/or phyllosilicate minerals in non-pedogenic, depositional environments.

Reference

Alonso, P., Dorronsoro, C., Egido, J., 2004. Carbonatation in palaeosols formed on terraces of the Tormes river basin (Salamanca, Spain). Geoderma 118, 261-276.

Alonso-Zarza, A.M., Wright, V., 2010. Calcretes. Developments in Sedimentology 61, 225-267.

Alonso-Zarza, A., Silva, P., 2002. Quaternary laminar calcretes with bee nests: evidences of small-scale climatic fluctuations, Eastern Canary Islands, Spain. Palaeogeography Palaeoclimatology Palaeoecology, 178,119-135.

Ben-Dor, E., Levin, N., Singer, A., Karnieli, A., Braun, O., Kidron, G., 2006. Quantitative mapping of the soil rubification process on sand dunes using an airborne hyperspectral sensor. Geoderma 131, 1-21.

Birkeland, P., 1999. Soils and geornorphology. 3rd edition. Oxford University Press, New York. 430pp.

Blum, M.D., Törnqvist, T.E., 2000. Fluvial responses to climate and sea-level change: a review and look forward. Sedimentology 47 (Suppl. 1.), 2–48.

Brown, D.J., Helmke, P.A., Clayton, M.K., 2003. Robust geochemical indices for redox and weathering on a granitic laterite landscape in Central Uganda. Geochimica Cosmochimica Acta 67, 2711-2723.

Buurman, P., 1998. Classification of paleosols--A comment. Quaternary International 51, 17-20.

Catt, J.A., 1990. Paleopedology manual. Quaternary International **6**, 1–95pp.

Chase, B. M., Meadows, M. E., 2007. Late Quaternary dynamics of southern Africa's winter rainfall zone. Earth-Science Reviews 84(3-4), 103-138.

Duchaufour, P., 1982. Pedology: Pedogenesis and Classification. Allen and Unwin, Boston, MA,. Translated by T.R. Paton.

Demko,T.M., Currie, B.S., Nicoll, K.A., 2004. Regional paleoclimatic and stratigraphic implications of paleosols and fluvial/overbank architecture in the Morrison Formation (Upper Jurassic), Western Interior, USA, Sedimentary Geology 167, (3–4), 115-135.

Eze, P.N., Udeigwe, T.K. and Stietiya, M.H., 2010. Distribution and potential source evaluation of heavy metals in prominent soils of Accra Plains, Ghana. Geoderma, 156, 357-362.

FAO, 2006. Guideline for Soil Description, 4th edition. FAO, Rome, Italy (109 pp.).

Fedorov, A., Dekens, P., McCarthy, M., Ravelo, A., Barreiro, M., Pacanowski, R. and Philander, S., 2006. The Pliocene paradox (mechanisms for a permanent El Niño). Science 312, 1485-1489.

Favre, F., Tessier, D., Abdelmoula, M., Genin, J., Gates, W. and Boivin, P., 2002. Iron reduction and changes in cation exchange capacity in intermittently waterlogged soil. European Journal of Soil Science 53, 175-183.

Fedoroff, N., Courty, M., and Guo, Z., 2010. Palaeosoils and Relict Soils. In:Stoops, G., Marcelino, V., AND Mees, F. (Eds.). Interpretation of micromorphological features of soils and regoliths. Elsevier Science. pp. 623-654.

Finke, P.A., 2011. Modeling the genesis of luvisols as a function of topographic position in loess parent material. Quaternary International 265, 3-17.

Francis, M.L., Fey, M.V., Prinsloo, H.P., Ellis, E., Mills, A.J., Medinski, T.V., 2007. Soils of Namaqualand: Compensations for aridity, Journal of Arid Environments 70 (4), 588-603.

Gall, Q., 1992. Precambrian paleosols in Canada. Canadian Journal of Earth Sciences 29 (12), 2530–2536.

Gibbard, P., Lewin, J., 2002. Climate and related controls on interglacial fluvial sedimentation in lowland Britain. Sedimentary Geology, 151,187-210.

Gupta, A.S., Rao, S.K., 2001. Weathering indices and their applicability for crystalline rocks. Bulletin of Engineering Geology And the Environment 60, 201-221.

Holland, H. D., 1984. The Chemical Evolution of the Atmosphere and Oceans: Princeton Series in Geochemistry: Princeton, New Jersey, Princeton University Press, 582 pp.

Holbourn, A., Kuhnt, W., Schulz, M., Flores, J.A., Andersen, N., 2007. Orbitally-paced climate evolution during the middle Miocene. Earth Planetary Science Letters 261, 534-550.

Hutton, J., 1795. Theory of the Earth, with Proofs and Illustrations. Edinburgh, W. Creech Vol. 2 p. 567.

Jenny, H., 1994. Factors of Soil Formation: A System of Quantitative Pedology. New York: Dover Press. (Reprint, with Foreword by R. Amundson, of the 1941 McGraw-Hill publication). pdf file format.

Kendrick, K.J., Graham, R.C., 2004. Pedogenic silica accumulation in chronosequence soils, southern California. Soil Science Society of American Journal 68, 1295-1303.

Kraus, M.J., 1999. Paleosols in clastic sedimentary rocks: their geologic applications. Earth-Science Review 47, 41-70.

Mack, G.H., James, W.C., Monger, H.C., 1993. Classification of paleosols. Geological Society of America Bulletin 105, 129-136.

Majewski, W., Bohaty, S.M., 2010. Surface-water cooling and salinity decrease during the Middle Miocene climate transition at Southern Ocean ODP Site 747 (Kerguelen Plateau). Marine Micropaleontology 74, 1-14.

McCarthy, P.J., Martini, I.P., Leckie, D.A., 1998. Use of micromorphology for palaeoenvironmental interpretation of complex alluvial palaeosols: an example from the Mill

Creek Formation (Albian), southwestern Alberta, Canada. Palaeogeography Palaeoclimatology Palaeoecology 143, 87-110.

McCarthy, P.J., Plint, A.G., 2003. Spatial variability of palaeosols across Cretaceous interfluves in the Dunvegan Formation, NE British Columbia, Canada: palaeohydrological, palaeogeomorphological and stratigraphic implications. Sedimentology 50, 1187-1220.

Morrison, R. B., 1978. Quaternary soil stratigraphy concepts, methods and problems. In: W.C. Mahaney, Editor, Quaternary Soils, Geoabstracts, Norwich 77–108 pp.

Mücher, H., van Steijn, H., Kwaad, F., 2010. Colluvial and mass wasting deposits. In Stoops, G., Marcelino, V., Mees, F. (eds.), Interpretation of Micromorphological Features of Soils and Regoliths. Elsevier, Amsterdam, pp. 37–48.

Munsell color company, 2000. Munsell soil Colour Charts, Rewashable Edition. Gretag MAcbeth, 617 Little Britain Road, New Windsor, NY12533.

Nettleton, W., Olson, C., Wysocki, D., 2000. Paleosol classification: problems and solutions. Catena 41, 61-92.

Nettleton, W., Brasher, B., Benham, E., Ahrens, R., 1998. A classification system for buried paleosols. Quaternary International 51, 175-183.

Playfair, J., 1802. Illustrations of the Huttonian Theory of the Earth. In: Cadell & Davies and W. Creech, London and Edinburgh p. 529.

Price, J.R. and Velbel, M.A., 2003. Chemical weathering indices applied to weathering profiles developed on heterogeneous felsic metamorphic parent rocks. Chemical Geology 202, 397-416.

Retallack, G.J., 1990. Soils of the Past. In: Unwin-Hyman, London p. 520.

Retallack, G.J., 1997. A colour guide to paleosols. John Wiley and Sons, Chichester, 175 p

Retallack, G.J., 1998. Core concepts of paleopedology. Quaternary International 51-52, 203-212.

Retallack, G., 2001. Soils of the past, an introduction to paleopedology: Blackwell science Ltd. Second edition. 404 pp

Salcher, B.C., Faber, R., Wagreich, M., 2010. Climate as main factor controlling the sequence development of two Pleistocene alluvial fans in the Vienna Basin (eastern Austria) - A numerical modelling approach. Geomorphology 115, 215-227.

Seibert, J., Stendahl, J., Sørensen, R., 2007. Topographical influences on soil properties in boreal forests. Geoderma 141, 139-148.

Sheldon, N.D., Tabor, N.J., 2009. Quantitative paleoenvironmental and paleoclimatic reconstruction using paleosols. Earth-Science Reviews 95, 1-52.

Shunk, A.J., Driese, S.G., Farlow, J.O., Zavada, M.S., Zobaa, M.K., 2009. Late Neogene paleoclimate and paleoenvironment reconstructions from the Pipe Creek Sinkhole, Indiana, USA. Palaeogeography Palaeoclimatology Palaeoecology 274, 173-184.

Smeck, N.E., Torrent, J., Duiker, S.W., Lal, R., Rhoton, F.E., 2003. Iron (hydr) oxide crystallinity effects on soil aggregation. Soil Science Society of American Journal 67, 606-611.

Soil Survey Staff, 2010. Keys to Soil Taxonomy, Eleventh ed. USDA-Natural Resources Conservations Service, Washington, DC 341.

Soil Survey Staff, 2006. Keys to Soil Taxonomy, Tenth ed. Soil Conservation Service, USDA, Blacksburg, VA.

Sommer, M., Kaczorek, D., Kuzyakov, Y., Breuer, J., 2006. Silicon pools and fluxes in soils and landscapes—a review. Journal of plant nutrition and soil science 169, 310-329.

Steppuhn, A., Micheels, A., Geiger, G., Mosbrugger, V., 2006. Reconstructing the Late Miocene climate and oceanic heat flux using the AGCM ECHAM4 coupled to a mixed-layer ocean model with adjusted flux correction. Palaeogeography Palaeoclimatology Palaeoecology 238, 399-423.

Thompson, A., Chadwick, O.A., Rancourt, D.G. and Chorover, J., 2006. Iron-oxide crystallinity increases during soil redox oscillations. Geochimica Cosmochimica Acta 70, 1710-1727.

Tripati, A.K., Roberts, C.D., Eagle, R.A., 2009. Coupling of CO_2 and ice sheet stability over major climate transitions of the last 20 million years. Science, 326, 1394-1397.

UNCCD, 2003. Report of the Conference of the Parties on its Sixth Session, Held in Havana 25 August to 5 September 2003. Doc. ICCD/COP (6)/11 of 3.

Van Breemen, N. and Buurman, P., 2002. Soil Formation. Kluwer Academic Pub. 404 pp.

Webster, T., 1826. Observations on the Purbeck and Portland Beds. Transactions of the Geological Society London **2**, 37–44.

Wondafrash, T.T., Sancho, I.M., Miguel, V.G. and Serrano, R.E., 2005. Relationship between soil color and temperature in the surface horizon of Mediterranean soils: A laboratory study. Soil Science 170, 495-503.

Wright, V. P., Marriott, S.B., 1993. The sequence stratigraphy of fluvial depositional systems: the role of floodplain storage. Sedimentary Geology 86, 203–210.

CHAPTER TWO

GEOCHEMISTRY AND PALAEOCLIMATIC RECONSTRUCTION OF A PALAEOSOL SEQUENCE AT LANGEBAANWEG, SOUTH AFRICA

Abstract

Neogene Langebaanweg (LBW) palaeosol-sediment-sequences at the West Coast of South Africa are well known for their well-preserved rich palaeontological heritage. The palaeosols developed on estuarine/ marine/ coastal alluvial deposits stacked on each other, ranging in age from the Mid-Miocene to Quaternary. Elemental mobility and redistribution based on major and minor element geochemistry of 11 horizons of the ~18m sequences were studied to evaluate the degree of chemical weathering, a major process of soil formation; and to reveal important palaeoenvironments in which the palaeosols developed. Elemental geochemistry was carried out on <2 mm samples by X-ray fluorescence spectrophotometry. The carbonate horizons (Bk and 2Bkmb2) were dominated by CaO (mean wt. % = 32.77), while the other horizons had preponderance of SiO_2 (>50 % mean wt.). Two (WI-1 and WI-2) of the four weathering indices applied to evaluate weathering intensity proved unsuitable for use in an alluvial palaeosol-sediment sequences such as LBW. Chemical index of alteration (CIA) and chemical index of weathering (CIW) values were relatively more consistent in distribution pattern across the pedocomplex, but caution should be applied when using them in similar cases. The pedogenic carbonate horizons on average had the lowest values for both CIA and CIW (1.12 to 2.60) suggesting more advanced weathering. Plots of geochemical ratios (quantifying pedogenic processes) against depth show striking variations among and within the palaeosol and sediment sections. Soil formation was more advanced in the Mid-Miocene and Pliocene than in the Quaternary suggesting a more humid and warmer climate than present. We evaluated selected geochemical climofunctions and conclude that more data are obviously needed for a more robust calibration of the models in Langebaanweg palaeosols.

Keywords: calcretes, isotopes, geochemistry, paleoclimate, pedogenesis, Langebaanweg

2.1. Introduction

Palaeosols form at the interface of the past landscape and atmosphere and therefore have the potential to archive the climatic and environmental conditions at their time of formation (Soil Survey Staff, 1999). Like modern soils, palaeosols formed under the complex interaction of climate and organisms on a parent material over time on a given topography (Jenny, 1941; Birkeland, 1999). The rates of soil formation (pedogenesis) are most significantly affected by temperature and precipitation, for example water and warmth speed up the rate of alkaline and alkaline earth metal cation (Ca, Mg, Na, K) depletion at the expense of refractory elements such as Aluminum (Sheldon et al., 2002). These two important climate variables therefore exert control over chemical weathering and elemental mobility within the pedon (Nesbit and Young, 1989; Kumaravel et al., 2009). In addition to being a key process of soil formation through disintegration of parent rocks, chemical weathering is also important in geochemical element cycling (Ji et al., 2004) as it leads to the release of elements such as carbon and sulphur to the earth system. Unlike most marine-based proxies, which provide only indirect records of climatic conditions, soils/palaeosols are formed at the Earth's surface and are in more direct contact with the environmental and climate conditions at the time of their formation.

In places where there is a paucity of other palaeoenvironmental proxies, such as pollen or marine geochemical and palaeontological evidence, palaeosols may prove very valuable for palaeoclimate reconstruction (Retallack, 2008). Naturally, a combination of wide range of multi-proxies is always significant in getting robust palaeoenvironmental insights. Recent advances in palaeopedology (the study of palaeosols) suggest that it has evolved from being largely a qualitative science reliant on field observations to a quantitative technique based endeavour (e.g. Yang et al., 2004; Adams et al., 2011; Óskarsson et al., 2012). While palaeosol characteristics,

such as clay mineralogy and micromorphology have facilitated qualitative reconstructions, however, study of geochemical properties of palaeosols are emphasized and desirable for providing better quantitative quantifiable information on the trends of various climate parameters.

Quantitative techniques involving the use of bulk palaeosol geochemistry have been widely applied in the reconstruction of various palaeoenvironmental and palaeoclimatic conditions (e. g. (Prochnow et al., 2006; Kumaravel et al., 2009) and this has led to remarkable advances in the applicable areas. Scientists have developed proxies for the interpretation of pedogenic processes such as salinization, lessivage, gleization; and climate parameters including mean annual precipitation (MAP), mean annual temperature (MAT), the composition of palaeo-atmosphere (e.g. ρCO_2), (Sheldon and Tabor, 2009). Geochemical climofunctions, as with other quantitative empirical factorial models, aims to explain the influence of climate parameters such as temperature and precipitation on soil formation and maturity (Yoo and Mudd, 2008). The application of weathering indices and geochemical climofunctions has recently been intensively reviewed by Sheldon and Tabor (2009) and it emerges that the major problem with the use of such indices in palaeoclimatic and palaeoenvironmental reconstruction stems from the fact that palaeosols may be genetically affected by post-burial alteration. While chemical properties such as base saturation and cation exchange capacity (CEC) are not preserved in palaeosols because of post burial alteration (Retallack, 1994, 1997, 2001), bulk chemical composition appears more stable in the face of diagenesis and metamorphic alterations (Mora et al., 1996). Geochemical climofunctions, when compared with results from other proxies found in palaeosols and fossil plants have always produced reliable results for palaeoenvironmental and palaeoclimate reconstruction (Sheldon and Tabor, 2009).

The late Cenozoic depositional environment of Langebaanweg (LBW), South Africa, continues to provide insights into the region's palaeoclimate. Internationally renowned for its rich palaeontological and geo-archaeological heritage (Hendy, 1982; Roberts et al., 2011; Stynder, 2011), the stratigraphy of the West Coast Fossil Park sediments at Langebaanweg reveals several palaeosol layers interbedded by pedosediments of varying diagenetic degrees (Roberts, 2006a; Roberts et al., 2011). Without doubt, LBW presents one of the richest palaeosol sequences on the West Coast of South Africa in which a substantial number of pedogenically modified layers have been preserved under varied Late Cenozoic climates. Also clay mineralogy and micromorphology of the palaeosols has been done to infer their palaeoenvironments and associated climates (Chapter three). Herein, major emphasis is on the bulk geochemical studies in different pedofacies of the palaeosols. From field observations, the palaeosol profiles of the LBW pedocomplex are often truncated by phases of erosional and depositional processes thereby making the preservation of the upper horizons (O/A/E) incomplete. The close association between pedogenesis and sedimentation at LBW consequently gave rise to the formation of a multi-story palaeosol which are both compound (stacked profiles separated by sediments) and composite (profile with an overlap and overprinting of pedogenesis). Unlike compound palaeosols, pedogenic events in the composite profile are difficult to distinguish solely on the basis of field observable features due to pedogenic overprinting. Herein, the nature and degree of such overprinting has been investigated on the basis of geochemical properties of these palaeosols. Thereafter, several chemical weathering indices to reconstruct their relationships to various climofunctions such as MAP and MAT as done by Sheldon et al. (2002) and Adams et al. (2011), and evaluate several of the indices as compiled by Sheldon and Tabor (2009).

2.2. Geographical and geological setting

The West Coast Fossil Park at Langebaanweg is located approximately 120 km north of Cape Town. The exposed palaeosol-sediment-sequences are situated at latitude 32°57.784″ S and longitude 18°06.367″ E (Fig. 2.1). Its elevation is approximately 30m above sea level. This site is notable for a number of mid- to late Quaternary palaeontological sites, for example, Elandsfontyn (where the partial cranium of early archaic *Homo sapiens*, "Saldanha man" was discovered by Singer and Wymer (1968), Langebaan (the site of last interglacial fossil human footprints, Roberts, 2009), and the Middle Stone Age (~250–25 ka) sites of Hoedjiespunt, Sea Harvest, Yzerfontein and Duinefontyn (Hendey, 1981; Roberts and Berger, 1997; Halkett *et al*., 2003). The climate of LBW is generally semi-arid to arid and falls within the winter rainfall zone of South Africa (Hopley et al., 2006).

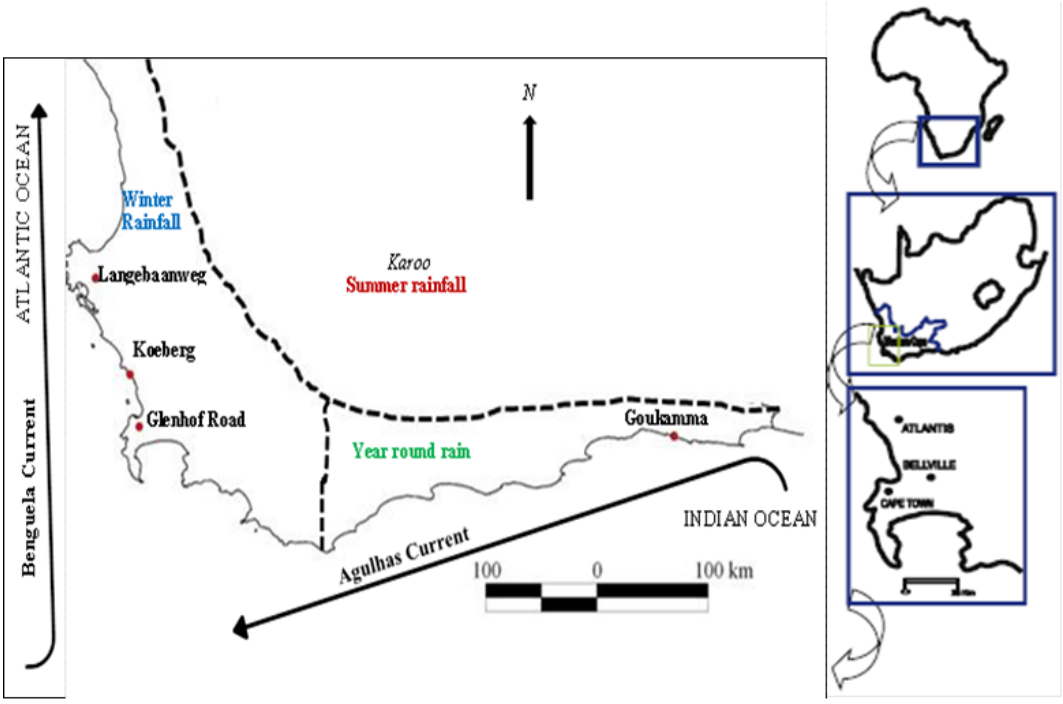

Fig. 2.1. Map of Langebaanweg, Western Cape South Africa

The geology of LBW consists of a calcareous aeolian deposit of the Langenbaan formation (Fm) and Springfontyn Fm underlain by the Varswater Fm of the Sandveld group (Roberts et al., 2011) (Fig. 2.2). The Varswater formation is further subdivided into four members, viz: the Langeenheid Clayey Sand (LCSM), the Konings Vlei Gravel (KGM), the Langeberg Quartz Sand (LQSM) and the Muishond Fontein Pelletal Phosphorite Members (MPPM) (Roberts et al., 2011). A lithostratigraphic summary (Fig. 2.2) of the fossil park shows the spatio-temporal relationships in approximate thickness, lithology, and depositional environment of the palaeosol-sediment sequences.

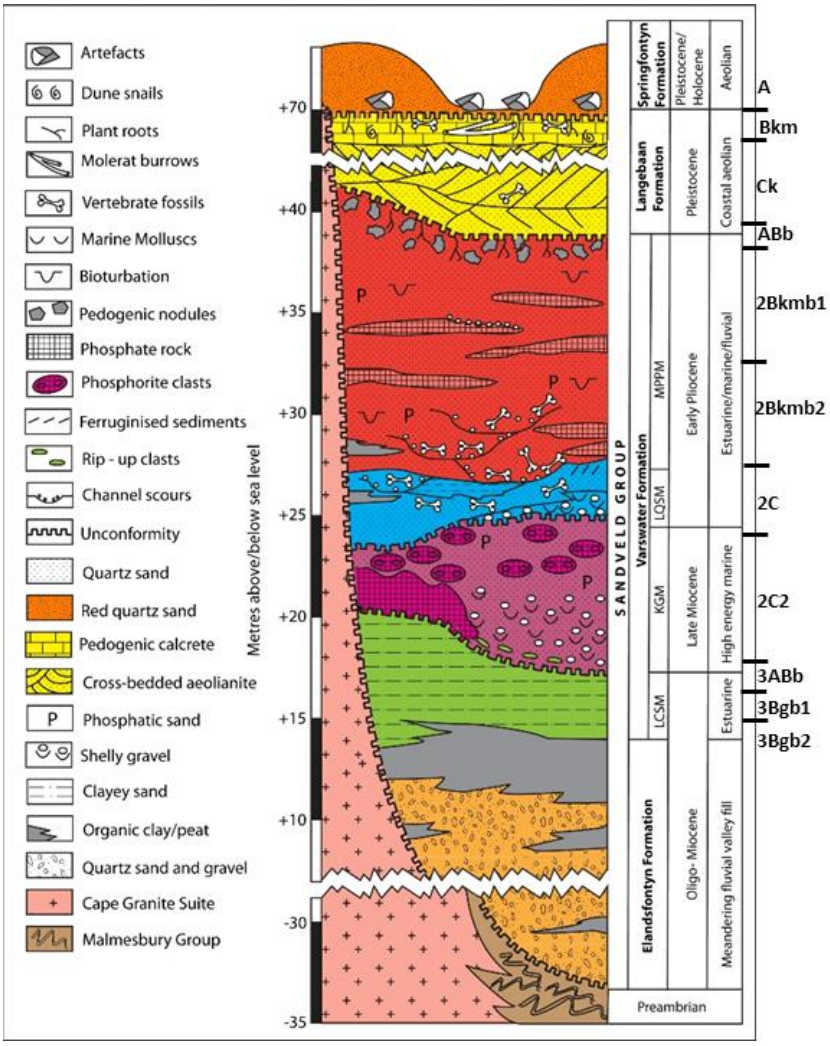

Fig. 2.2. Summary of the stratigraphic column of LBW geology (After Roberts et al., 2011).

2.3. Materials and Methods

2.3.1. Field sampling

The defunct quarry was cleaned by scraping off the exposed surfaces to avoid taking any weathered/ altered samples. Undisturbed clods and/or core samples were taken from each horizon of the palaeosol-sediment sequences. These samples were specifically marked for thin section preparation for micromorphological studies. The LBW excavation was not continuous along the same plane and to complete the sampling, the exposed surfaces to a depth of 30 m was sampled along two subsections: the so-called "high wall" and "low wall" (Fig. 2.2; and Fig. 2.4, in a higher resolution) which are separated by an interbedded thick layer of unweathered pelletal phosphorite rock. Detailed, multiple sampling was done for further laboratory investigations. In the field, colour was described using the Munsel soil colour chart (Munsell Color Company, 2000), while the general macromorphological properties were described in accordance with the guidelines for soil profile description (FAO, 2006).

2.3.2. Laboratory methods

Pretreatment of samples included gently grinding to break up clods and subsequently passing the material through a 2mm sieve to separate gravel and roots/rhizomes from the 2mm soil fraction. Dry and moist colours were determined using Munsell colour system. For soil pH, a soil/ deionized water solution ratio of 1: 2.5 was used and the values read from digital FieldScout SoilStik pH metre. Calcium carbonate content of samples was determined by the gravimetric method as described by the U.S. Salinity Laboratory Staff (1954). Standard pellets of 5g were made out of homogenised samples for total elemental oxide compositions by X-ray fluorescence spectrophotometry at the Geological Sciences Department of the University of Cape Town.

Weight percentages given by XRF were recalculated to molar ratios, following Sheldon et al. (2002), for use in chemical weathering analyses. Quantitative grain sizes were determined using a Malvern Longbed Mastersizer. New Gasbench II method was used to analyze for stable isotopes ($\delta^{18}O$ and $\delta^{13}C$) composition of calcrete palaeosols at the Archaeometry Research Laboratory, University of Cape Town. Reported values are the average of measurements taken in triplicates.

2.3.3 Weathering indices and geochemical climofunctions

Soil geochemical indices such as Rb/Sr, Sr/Ba, Na/K, CaO/Al_2O_3 have been adjudged to be more sensitive to palaeoclimatic changes than magnetic susceptibility and grain size (Chen et al., 1998, 1999; Yang et al., 2004). To evaluate pedogenic processes quantitatively across the pedocomplex, a range of proxies were used (Table 2.1). The Chemical Index of Alteration (CIA) of Nesbit and Young (1982), Chemical Index of Weathering (CIW or CIA-K), which is a modified version of CIA takes care of post-burial addition of K by metasomatism and/ or illitization of clay minerals in soils by removing K in the equation, and two weathering indices (WI-1 and WI-2) of Darmody et al. (2005) were used to quantitatively evaluate the intensity of chemical weathering in the soils and pedosediments. Dataset for WI-1 and WI-2 were obtained from modern soils with granitic parent materials, although their wider application to soils developed on other parent materials are yet to be demonstrated.

$$WI\text{-}1 = (Si+Ca)/(Fe+Ti) \quad \text{...equation 1}$$

$$WI\text{-}2 = (Si+Ca)/(Fe+Ti+Al) \quad \text{…equation 2}$$

Table 2.1. Molecular weathering and pedogenesis proxies

Proxy	Formula	Rationale	Pedogenic process
Salinization	$\frac{K+Na}{Al}$	Alkali elements as soluble salts not removed from the soil horizon (Nesbitt and Young, 1984)	Salinization
Provenance	Ti/Al	Ti is most readily lost by physical weathering, whereas Al is lost by chemical weathering (Sheldon and Tabor, 2009)	Acidification (~pH)
Leaching	Ba/Sr	Sr has higher solubility than Ba (Sheldon and Tabor, 2009)	Leaching/hydrolysis
Calcification	$\frac{CaO+Mg}{Al}$	Alkaline earth elements are lost compared with Al during pedogenesis (Nesbitt and Young 1984, Sawyer, 1986)	Calcification
Sericitization	K_2O/Al_2O_3	plagioclases and other minerals are replaced by sericite through the effect on rocks of low temperature thermo-geochemistry (Nesbitt and Young, 1984)	Hydrolysis
Clayeyness	Al/Si	the higher the value of this ratio, the more weathered or clayey the soil is because Al accumulates as clay minerals form in soils (Sheldon and Tabor, 2009)	Hydrolysis

Using the soil dataset of Marbut (1935) compiled from soils in the USA and modern measurements of MAP, the CIA without potash index of Sheldon et al. (2002) was used to calculate palaeoprecipitation. It calculates mean annual precipitation (MAP) from K_2O free CIA as follows:

MAP = [14.265 (CIA-K) - 37.632] …equation 3

where CIA-K = [(Al_2O_3 / Al_2O_3 + CaO + Na_2O) x 100] (molar abundance).

The climofunction of Retallack (2005b) was also applied for Bk horizons. The relationship:

P (mm yr^{-1}) = − 0.013D^2 + 6.45D + 137.2 …equation 4

Note that "D" is depth to Bk horizon**.** This was developed and tested on moderately developed soils with carbonate nodules formed on unconsolidated parent materials (e.g. alluvium or loess), and which were undisturbed by human activity. Estimation of MAP using geochemical analysis of Fe-Mn nodules (Stiles et al., 2001) was also applied to horizons with iron oxide nodules. The dataset for this model was obtained from a modern climosequence developed on the Texas Gulf Coastal Plain. MAP was calculated as follows:

P (mm yr^{-1}) = 654.4 + 31.5Fe_{TOT} …equation 5

where Fe_{TOT} as a whole number % value of total iron oxide content and R^2 = 0.92 for the empirical relationship. This relationship was developed from a dataset of modern climosequence on the Texas Gulf Coastal Plain in the United States. Most of the soils there were Vertisols forming under modern MAP (Stiles et al., 2001).

Palaeotemperature was estimated by the solution of the two equations that link the stable oxygen isotopic composition of meteoric water and pedogenic carbonate to ambient temperature (Zheng *et al.* 1987):

$\delta^{18}O_{H2O} = 0.31T - 13.9$ …equation 6

whereas $\delta^{18}O_{H2O}$ = -1.361+0.955 $\delta^{18}O_{CaCO3}$ (R^2 = 0.98). And from Cerling and Quade (1993)

$\delta^{18}O_{cc}$ (‰, PDB) = 0.49T−12.65 …equation 7

2.4. Results

2.4.1. Age and properties of the palaeosols

The Langebaanweg pedocomplex comprises palaeosol and pedosediment layers deposited by different phases of water and wind activities. The age of the section ranges from Middle Miocene (established by correlation stratigraphy) to OSL confirmed Holocene aeolian sediments (Fig. 2.2, Roberts et al., 2011). The composite Mid-Miocene profile is the oldest. It is buried by Late Miocene high energy marine deposits of phosphate rocks, which also have phosphate sands which have undergone some diagenesis. The compound palaeosols overlying the phosphate materials are of Early to Late Pliocene age. A Pleistocene coastal aeolian is sandwiched between the uppermost Pliocene palaeosol and a late Pleistocene pedogenic calcrete horizon (Bk).

Horizonation, ped morphology, root traces and ichnofossils are characteristics of the palaeosols. Results of the macromorphology and selected physico-chemical properties (Table 2.2) show striking variations in properties such as depth of horizon, colour, particle size distribution and $CaCO_3$ contents of the palaeosols. For example, the buried Mid-Miocene palaeosol profile (3ABb, 3Bgb1 and 3Bgb2) showed strong indications of pedogenesis, with few tiny root traces, reddish brown mottles and a loamy texture with high pH. The Pliocene palaeosol profile (ABb, 2Bkmb1 and 2Bkmb2) has strong indications of pedogenesis observed from several pedogenic features (calcareous concretions, both large and small root traces, and vertic properties). A conspicuous feature of the Pliocene palaeosol profile is the abrupt change in colour from dark reddish brown (5YR 3/4) of the 2Bkmb1 to white (2.5Y 8/1) of the 2Bkmb2

Table 2.2. Selected physico-chemical properties of Langebaanweg palaeosol-sediment-sequences

Horizon	Depth (cm)	Lithofacies	Munsel colour (moist)	Colour description	Sand (<2mm, g kg^{-1})	Silt (<2mm, g kg^{-1})	Clay (<2mm, g kg^{-1})	Texture (ISSS)	pH (H_2O)	$CaCO_3$ (g kg^{-1})
A	0-15	aeolian	5YR 3/2	dark reddish brown	908	22	70	sand	8.3	183
Bk	15-33	calcrete	5Y 7/1	light gray	638	137	225	clay loam	9.2	437
Ck	33-120	aeolian	2.5 Y 5/4	light olive brown	907	22	71	sand	7.7	218
2ABb	120-138	fluvial?	7.5YR 5/4	brown	899	11	90	loamy sand	9.5	238
2Bkmb1	138-348	calcrete	5YR 3/4	dark reddish brown	729	41	230	sandy clay loam	9.2	475
2Bkmb2	348-397	calcrete	2.5Y 8/1	white	473	184	343	sandy clay loam	9.3	626
2C	397-997	phoscrete	2.5Y 8/2	pale yellow	-	-	-	-	-	-
2C2	997-1597	cal-phosphate sand	-	-	613	150	228	sandy clay loam	8.6	-
3ABb	1597-1607	estuarine	5YR 4/6	yellowish red	712	63	225	sandy clay loam	7.9	-
3Bgb1	1607-1641	estuarine	10YR 6/3	pale brown	264	112	624	clay	8.0	-
3Bgb2	1641-1700+	estuarine	10YR 6/6	brownish yellow	562	113	325	sandy clay loam	8.3	-

-: Not determined

horizon (Table 2.2). The 120 cm light olive brown (2.5Y 5/4) bedded coastal aeolian sediment has only undergone some diagenesis and there is insufficient evidence to indicate any degree of pedogenesis was seen in the layer. Apparently, the Late Quaternary deposits have shown a moderately developed Bk horizon with an accumulation of calcareous nodules with 33cm depth of the pedocomplex. The Quaternary Bk horizon has abundant nodules, root traces and burrows, but is not as strongly cemented as the Pliocene 2Bkmb1 and 2Bkmb2 horizons. Soil pH fluctuated down the sequences, although it is alkaline throughout. Higher pH values were recorded in the horizons with carbonates.

2.4.2. Geochemical distribution

Major and minor element data are provided in Tables 3 and 4 respectively. A total of 13 major and 19 minor elements were analyzed for the palaeosols and pedosediments. The sum of all soil components (major elements as oxides + loss on ignition + air-dried moisture) averaged 998± 2 g kg^{-1}, indicating excellent analytical precision. Silica (SiO_2) is the dominant major oxide in all the samples, followed by calcium oxide. Fluctuations across the pedocomplex characterize the distribution of major elements, with no uniform pattern. However, there are remarkably low amounts of magnesium, calcium and sodium in the ABb horizon. Loss on ignition (LOI) was as high as 210 to 310 g kg^{-1} in the carbonate enriched horizons. Of the 19 minor elements determined, S, Sr, Y and Zr are the most abundant. The geochemical and isotopic compositions of the palaeosols provide an appropriate context for two additional pedological and palaeoenvironmental interpretations, namely (1) weathering intensity/ pedogenesis, and (2) applicability of climofunctions as discussed below.

Table 2.3. Major oxides composition of LBW palaeosol-sediment-sequences

Horizon	SiO_2	TiO_2	Al_2O_3	Fe_2O_3	MnO	MgO	CaO	Na_2O	K_2O	P_2O_5	SO_3	Cr_2O_3	NiO	LOI*
		(%)												
A	88.70	0.19	1.18	0.14	0.01	0.03	4.07	0.05	0.42	0.26	0.02	0.00	0.00	4.08
Bk	46.68	0.05	1.00	0.01	0.01	0.47	27.43	0.28	0.48	0.86	0.13	0.01	0.00	21.98
Ck	37.82	0.06	0.90	0.22	0.01	0.39	32.36	0.28	0.42	1.03	0.15	0.01	0.00	25.64
2ABb	91.35	0.33	1.95	0.51	0.00	0.07	1.82	0.17	0.72	0.56	0.00	0.01	0.00	1.46
2Bkmb1	69.26	0.26	3.08	6.59	0.01	0.33	7.66	0.76	0.57	3.71	0.09	0.01	0.00	5.11
2Bkmb2	25.58	0.10	0.59	0.37	0.01	0.80	38.53	0.22	0.15	0.88	0.25	0.00	0.00	31.52
2C	80.91	0.21	1.20	0.01	0.01	0.02	8.73	0.09	0.40	5.40	0.03	0.01	0.01	2.11
2C2	54.53	0.19	1.18	0.62	0.01	0.22	25.30	0.36	0.39	12.64	0.28	0.00	0.00	3.69
3ABb	68.53	0.26	5.71	3.77	0.00	0.53	4.92	1.29	0.59	3.18	0.09	0.02	0.00	5.13
2Btb1	63.23	0.22	5.66	1.33	0.01	0.44	9.94	1.00	0.48	6.38	0.15	0.01	0.00	4.93
2Btb2	87.87	0.24	3.70	2.07	0.01	0.11	0.97	0.19	0.39	0.68	0.00	0.01	0.00	2.19

*: LOI – Loss on Ignition in a furnace at 950 ^{o}C (= chemically bound H_2O and CO_2)
Fe_2O_3 is expressed as total Fe

Table 2.4. Minor elements composition of Langebaanweg palaeosol-sediment-sequences

	Mo	Nb	Zr	Y	Sr	Rb	U	Th	Pb	Zn	Cu	Ni	Co	Mn	Cr	V	Sc	Ba	S
	---------- (ppm) ----------																		
A	<0.4	3.0	261.9	12.2	124.4	18.0	<0.9	<0.9	6.8	5.7	<0.8	<1.0	<2.2	56.2	44.4	14.5	<2.1	121.0	251.4
Bk	<0.4	3.8	53.4	9.5	737.6	18.9	2.9	<0.9	4.6	7.3	1.4	<1.0	<2.2	11.3	25.2	5.2	<2.1	100.1	1405.3
Ck	<0.4	4.9	84.9	12.4	713.5	17.0	2.0	<0.9	4.5	9.5	1.7	<1.0	<2.2	15.4	50.1	12.6	<2.1	153.6	1140.0
2ABb	<0.4	8.4	470.3	21.3	108.6	30.0	<0.9	4.0	7.5	6.4	<0.8	5.1	<2.2	158.7	105.0	37.1	6.2	262.3	107.7
2Bkmb1	<0.4	19.7	318.0	88.0	1273.0	15.1	12.3	<0.9	4.1	5.3	13.8	45.2	2.8	46.8	92.7	155.6	3.1	171.5	1276.6
2Bkmb2	<0.4	4.9	112.4	18.0	633.6	5.8	<0.9	<0.9	2.5	4.7	2.5	<1.8	<2.2	19.1	22.4	12.3	<2.1	149.6	1671.1
2C	<0.4	10.2	242.0	40.8	536.5	18.5	12.1	2.2	8.4	9.4	<1.4	<1.8	<2.2	70.1	44.0	22.8	<2.1	147.3	1108.6
2C2	<0.4	7.1	182.7	31.1	569.7	12.2	10.6	<0.9	6.5	9.2	4.4	5.0	<2.2	61.7	43.2	39.7	<2.1	133.0	1622.5
3ABb	<0.4	6.1	158.5	49.6	249.4	37.2	<0.9	7.5	8.8	12.2	2.4	17.9	<2.2	110.2	173.2	99.5	9.7	126.4	1130.0
3Btb1	<0.4	3.3	96.2	24.0	231.6	40.3	4.0	4.0	9.5	10.8	<0.8	5.2	<2.2	43.1	81.3	48.7	2.6	100.7	1670.8
2Btb2	<0.4	2.2	114.9	15.7	69.9	30.8	<0.9	4.2	9.0	8.5	<0.8	6.1	<2.2	56.3	74.0	73.4	7.9	144.2	1055.2

2.4.3. Weathering intensity

Results of the four weathering intensity indices (CIA, CIW, WI-1 and WI-2) used for evaluation of the pedogenesis are presented in Table 2.5. Plots of various geochemical ratios against depth show the patterns (Fig. 2.3) of five pedogenic processes (salinization, leaching, provenance, calcification and sericitization) and clayeyness (Al/Si) (Table 2.5) across the palaeosol-sediment sequences. The Mid-Miocene palaeosols have relatively high clay contents compared to the overlying sections. Salinization and calcification parameters vary directly with carbonate accumulation in the palaeosol horizons. The Pleistocene coastal aeolian horizon (Ck) is the least affected by salinization, base loss, calcification and sericitization, reflecting eodiagenesis (the earliest stage of diagenesis at shallow depths) and this is therefore not a pedogenically modified horizon. In those horizons which are pedogenically modified to a greater degree, the sericitization curves show a little decrease with depth indicating the weathering of feldspars during soil forming processes.

The application of four weathering indices for evaluation of pedogenesis/ weathering intensity in LBW locality suggests that WI-1 and WI-2 of Darmody et al. (2005) are not suitable as the trends are inconsistent and did not complement pedogenic trends with depth. The indices CIA and CIW both indicate a more uniform pattern across the sequences. They suggest more intense weathering at the Mid-Miocene palaeosols followed by the Early Pliocene palaeosols.

2.4.4. Climofunctions

The results of the mean annual precipitation and mean annual surface temperature (Table 2.5) from climofunctions of Zheng et al. (1987), Cerling and Quade (1993), Retallack (2005b), Stiles et al., (2001) and Sheldon et al., (2002) show some differences. The Sheldon et al. (2002) model

Table 2.5. Geochemical weathering indices and climofunctions of LBW palaeosol-sediment-sequences

Horizon	Al/Si	Ti/Al	K+Na/Al	CIA	CIW	WI-1	WI-2	$\delta^{13}C$	$\delta^{18}O$	$\delta^{18}H_2O$	MAT (^{o}C)	MAP (mm yr^{-1})
A	0.02	0.18	0.62	15.94	17.49	209.51	53.05	-	-	-	-	-
Bk	0.02	0.06	1.15	2.55	2.60	1120.92	73.15	-0.49	-1.77	-3.05	35[a], 22[b]	231[c]
Ck	0.03	0.08	1.17	1.97	2.00	214.97	61.25	-	-	-	-	-
2ABb	0.02	0.19	0.70	33.77	41.97	79.36	27.73	-	-	-	-	-
2Bkmb1	0.05	0.10	0.64	20.00	21.24	7.94	5.92	-	-	-	-	800[d]
2Bkmb2	0.03	0.19	0.90	1.12	1.12	122.96	62.13	-2.63	-8.70	-9.67	14[a], 8[b]	663[d], 670[c]
2C	0.02	0.20	0.63	8.73	9.15	331.69	57.37	-	-	-	-	-
2C2	0.02	0.18	0.94	3.25	3.30	79.60	37.12	-	-	-	-	-
3ABb	0.09	0.05	0.48	37.85	40.32	12.73	6.11	-	-	-	-	614[e]
3Bgb1	0.10	0.04	0.38	26.65	27.63	34.52	9.03	-	-	-	-	488[e]
3Bgb2	0.05	0.07	0.24	62.84	70.13	26.24	11.76	-	-	-	-	881[e]

[a]: Zheng et al., 1987; [b]: Cerling and Quade, 1993; [c]: Retallack, 2005; [d]: Stiles et al., 2001; [e]: Sheldon et al., 2002

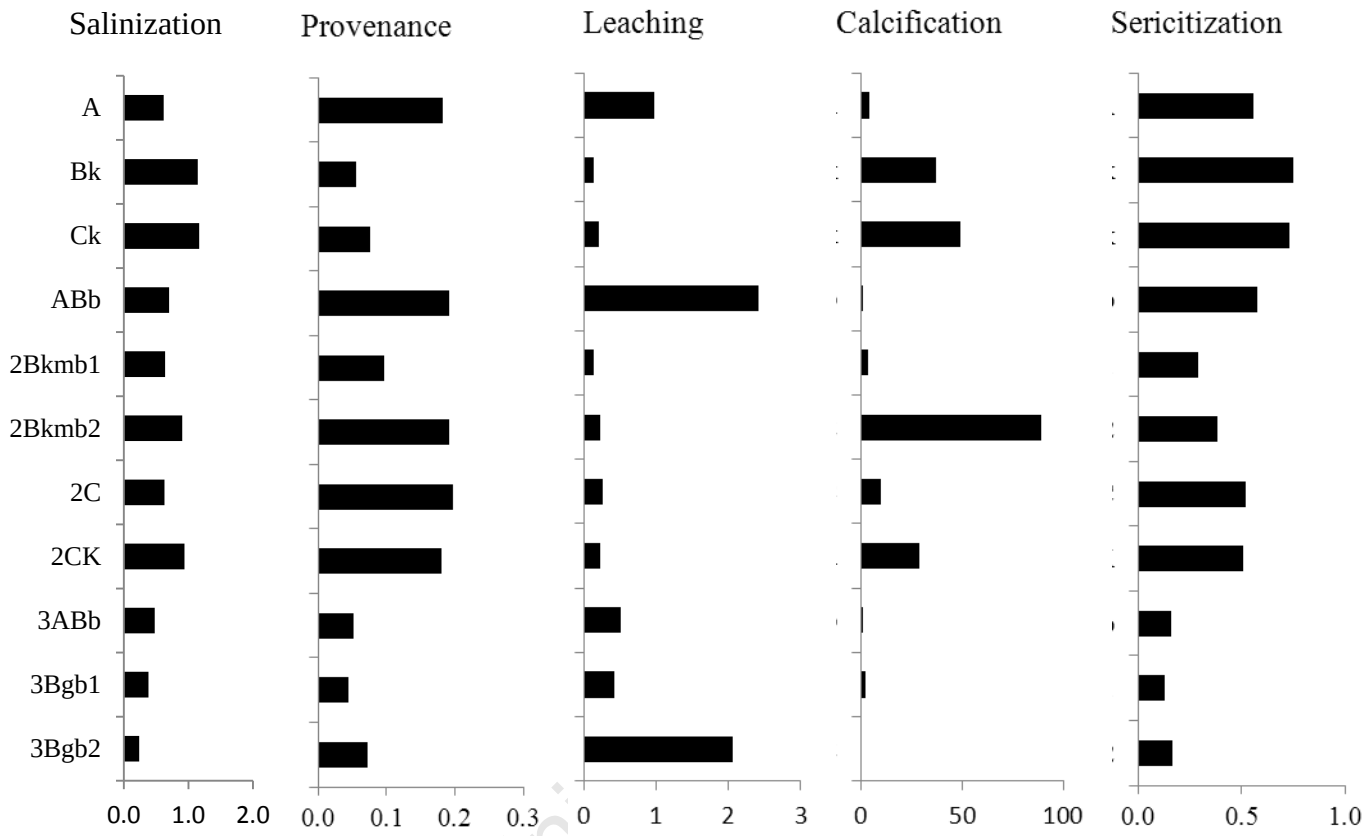

Fig. 2.4. Plot of geochemical ratios depicting different pedogenic processes against depth in the LGW sequences

was used for the Mid-Miocene palaeosol section (3ABb-3Bgb1-3Bgb2). The resulting MAP outputs vary from 614 to 881 mm. Plots of the data against various pedogenic processes (base loss and leaching) show strong positive correlations (Fig. 2.4) that point to fidelity of the calculated MAP. Since the Pliocene section is calcrete-enriched, we applied the geochemical function of Retallack (2005b) and Stiles et al., (2002). In this case, the values obtained for MAP ranged from 663 to 800 mm, suggesting a somewhat overlapping annual precipitation regime with the Mid-Miocene palaeosols. Similarly, the model suggests the Quaternary section (Bk) horizon has a MAP of 231 mm. This indicates a semi-arid environment which corresponds approximately to the contemporary situation at LBW.

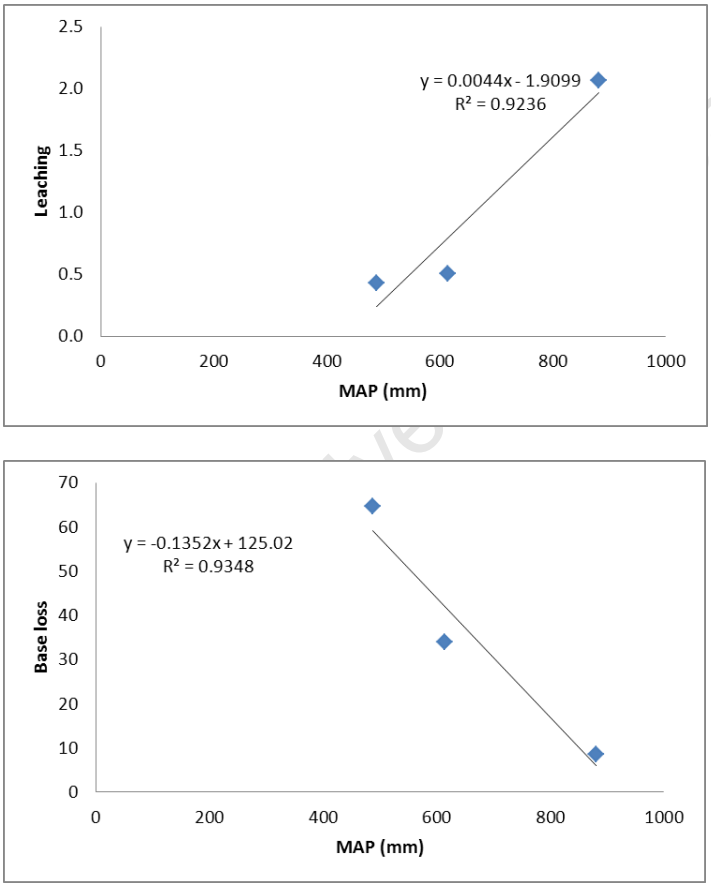

Fig. 2.5. Correlation between MAP and pedogenic processes (leaching and base loss)

For MAT, we resorted to the method of calculating the formation surface temperature of carbonate palaeosols of Zheng et al., (1987) and Cerling and Quade (1993) from $\delta^{18}O$ isotope values. Like the calculated MAP, the calculated MATs also do show variations across the models. Both models yielded 35 ^{o}C and 22 ^{o}C respectively for the Quaternary Bk horizon. We are however, not able to fully validate their applicability due to the limited size of the data base. Nevertheless, the MAT results suggest a higher surface temperature of formation for the Quaternary palaeosol (Bk) horizon than the Pliocene carbonate horizon (2Bkmb2) which was 14^{o}C and 8 ^{o}C (for Zheng et al., 1987 and Cerling and Quade, 1993 models respectively).

2.5. Discussion

As reported by Roberts et al (2011), the ages of the pedogenically modified layers of the pedocomplex are Mid-Miocene, Pliocene, and Pleistocene. Periods of high sedimentation rate explain why there are deposits of alluvial material sandwiching the palaeosols. As a rule of thumb, the more advanced the evidence of pedogenesis, the longer the palaeo surface was stable and/or the higher temperature and precipitation favouring chemical weathering. The transitional ABb horizon which has evidently been eroded from the A horizon is most likely the source of the iron oxide which bestowed the dark reddish brown colour to the 2Bkmb1 horizon. Since 2Bkmb2 has a lower sand content (Table 2.2), implicitly, it has higher surface area, which makes it impossible to get enough iron oxide by illuviation to impart red colouration. Dissolution of carbonates from shells and other marine organisms deposited by marine/fluvial/aeolian would increase the soil pH through the production calcium bicarbonate.

The prominence of SiO_2 and CaO may relate to the fact that coastal sand is the parent material. As often is the case, there are marine shells in these deposits which are dissolved by acidification resulting in carbonates and diagenetic carbonate horizons. Weathering and

diagenesis emerge as the principal factors that determined the transformation and transfer of the chemical elements with time. More reddish horizons have the highest iron oxide content. The red colour of the horizons therefore precipitated from hematite as suggested in the XRD results of a parallel study (Chapter three). The high quantities of sodium, calcium and magnesium in both the older and more recent horizons suggests that they still contain more weatherable primary minerals, mainly alkali feldspar and pyroxene group minerals inherited from the parent materials. Loss on ignition (LOI) varies directly in relation to carbonate-enriched horizons because of the presence of hydroxyl-rich secondary minerals and organic carbon. Field observation showed that the palaeosols and sediments have very low organic matter. Therefore, 21 to 32% of the palaeosol carbonate mass is attributable to loss of structural hydroxyls, consistent with their gibbsitic-chloritic clay mineralogy. For comparison, the theoretical LOI of gibbsite is 346 g kg^{-1} and chlorite is 204 g kg^{-1} (Klein and Dutrow, 2007).

Parent material (alluvial sand) and intermittent inflow of ocean water are likely to have influenced the mobilization and redistribution of chemical elements in LBW area. Silica and titanium depletion are most prominent in the horizons (Bk, 2Bkmb1, 2Bkmb2, 3Bgb1 and 3Bgb2), where there is more advanced evidence of pedogenesis. Additions of alkalis and alkaline earths (Na, K, Mg and Ca) are higher in these same horizons, reflecting the situation that continued weathering in these horizons may have fixed these elements through surface adsorption and exchange onto secondary clay minerals, or incorporation into structural sites of clays (Nesbitt et al., 1980). The buried Mid-Miocene palaeosols have relatively high clay contents compared to the overlying sections. Possibly, its all-year-round near-saturation water content could have promoted clay deposition on the palaeo erosional 3ABb horizon via sedimentary differentiation with water as the agent. The provenance of clay minerals in this

section further supports their deposition as a result of transportation rather than chemical weathering processes (Fig. 2.3). Leaching is well pronounced in the Ck horizon, probably because of its coarse sandy texture (Table 2.2) (e.g. Lee et al. 2002). There are remarkably low amounts of magnesium, calcium and sodium in the ABb horizon suggesting a higher degree of weathering and leaching.

WI-1 and WI-2 values were not consistent across the pedocomplex. These indices could therefore be adjudged as unsuitable for evaluating weathering intensity. We argue that since these models were developed from dataset of soils with granitic parent materials and this is not the case for LGW sequences, the differences in parent materials may be accountable for their unsuitability. Earlier study by Kahmann et al. (2008) had compared results from a couple of indices and also found that WI-1 and WI-2 showed remarkably poor agreement with other weathering indices and also estimates of MAP derived from CIA-K values. As opined by Sheldon and Tabor (2009), WI-1 and WI-2 have not been widely tested on soils and palaeosols. More testing obviously needs to be done to determine their wider applicability or to know if they are only applicable to granitic parent materials.

A number of quantitative climofunctions have been developed to determine palaeo rainfall and palaeo-temperature using geochemical and stable isotope proxies from palaeosols. The applicability and reproducibility of reliable results from these relationships would greatly depend on the similarity of the palaeosols studied with the ones from which the functions were developed. All the geochemical climofunctions evaluated in this study were developed from soils and palaeosols from the Northern Hemisphere. It is believed that if all the operational parameters including depth to soil horizon and morphology are valid, the climofunctions should be applicable to soils and palaeosols from anywhere in the globe. The palaeosols vary in

morphology and this makes uniform application of the models across the entire sequences unsuitable. A few number of palaeosol samples (3) are obviously insufficient to advocate for continued use of this climofunction in Southern Africa.

Even though the MAP and MAT seem to be in agreement with the global trend of climatic fluctuation (e.g. Zachos et al., 2001) and strong influence of short term climate fluctuations (possibly originating at high latitudes) on the continental record in the temperate/subtropical zone at the southwestern tip of Africa (Roberts et al., 2013), however it is desirable a more robust database based on increased number of palaeosols/ soils is required as this would increase the degree of freedom thereby improving precision. The Early Pliocene palaeosols have a well-developed 2Bk horizon with a spectacular development of calcretes indicating prolonged arid/ semi-arid palaeo conditions, although the calculated MAP >660 mm does not suggest aridity. The complex relationship between pedogenesis and calcretization therefore needs further detailed studies including other calcrete horizons within LBW and its environments. The Quaternary palaeosols, from the calculated MAT, formed at a higher temperature than the Pliocene palaeosols indicating their likely formation within an interglacial. The major inherent limitations in the application of geochemical climofunctions to palaeosols remain that the degree of weathering decreases with soil depth; in an eroded palaeosol, the most strongly weathered upper part may have been removed so that only the weathering index of the lower part is available.

2.6. Conclusions

The following are the major conclusions of the present studied LBW palaeosol-sediment sequences:

1. Differences in the types palaeosols intercalated between sedimentary levels at LBW indicate both changes in sedimentary conditions and climate oscillations and the duration of each period determined the degree of pedogenesis of a particular layer. Soil formation was more advanced in the Mid-Miocene and Early Pliocene layers indicating a warm, humid climate with greater landscape stability.
2. To evaluate weathering intensity/ pedogenesis using CIA and CIW indices in palaeosol-sediment-sequences with alluvial parent material, like the LBW sediments and has been found quite reliable as compared to the WI-1 and WI-2 weathering indices of Darmody et al. (2005) which seemed very inconsistent and hence unsuitable.
3. Great care is required when using geochemical weathering indices for obtaining palaeoclimatic information from palaeosols sequences in a setting like LBW because these weathering indices are not only sensitive to climate but also to soil age. Moreover, the degree of weathering decreases with soil depth; in an eroded palaeosol profile, the most strongly weathered upper part may have been removed so that only the weathering index of the lower part is available. Hence, both soil age and erosion need careful examination and evaluation before deducing palaeoclimatic information using geochemical weathering indices in LBW like palaeosols.

References

Adams, J. S., Kraus, M. J., Wing, S. L., 2011. Evaluating the use of weathering indices for determining mean annual precipitation in the ancient stratigraphic record. Palaeogeography Palaeoclimatology Palaeoecology 309(3-4), 358–366.

Birkeland, P.W., 1999. Soils and Geomorphology. Oxford University Press, New York, 430p.

Chadwick, O.A., Brimhall, G.H., Hendricks, D.M., 1990. From a black to a gray box — a mass balance interpretation of pedogenesis. Geomorphology 3, 369–390.

Cerling, T. E., 1984. The stable isotopic composition of modern soil carbonate and its relationship to climate, Earth and Planetary Science Letters, 71 (2) 229-240.

Cerling, T.E., Quade, J., 1993. Stable carbon and oxygen isotopes in soil carbonates. In: McKenzie, J.A., Savin, S. (Eds.), Climate Change in Continental Isotopic Records. Geophysics Monograph, vol. 78. American Geophysical Union, Washington (DC), pp. 217–231.

Chen, J., Ji, J.F., Qiu, G., Lu, H., 1998. Geochemical studies on the intensity of chemical weathering in Luochuan loess–paleosol sequence, China. Science in China 41, 235–241.

Chen, J., An, Z.S., Head, J., 1999. Variation of Rb/Sr ratios in the loess–paleosol sequences of central China during the last 130,000 years and their implications for monsoon paleoclimatology. Quaternary Research 51, 215–219.

Darmody, R.G., Thorn, C.E., Allen, C.E., 2005. Chemical weather and boulder mantles, Kärkevagge, Swedish Lapland. Geomorphology 67, 159–170.

Ding, Z.L., Sun, J.M., Yang, S.L., Liu, T.S., 2001. Geochemistry of the Pliocene red clay formation in the Chinese Loess Plateau and implications for its origin, source provenance and paleoclimatic change. Geochimica et Cosmochimica Acta 65, 901–913.

Du, X., Rate, A.W., Gee, M., 2010. Geochemical mass-balance in intensely weathered soils, Darling Range, Western Australia. 19th World Congress of Soil Science, Soil Solutions for a Changing World 1 – 6 August 2010, Brisbane, Australia. Published on DVD.

Food and Agricultural Organisation (FAO), 2006. Guideline for Soil Description, 4th edition. FAO, Rome, Italy (109 pp.).

Fox, D.L., Koch, P.L., 2003. Tertiary history of C4 biomass in the Great Plains, U.S.A. Geology 31, 809–812.

Halkett, D., Hart, T., Yates, R., Volman, T.P., Parkington, J.E., Klein, R.J., Cruz, Uribe, K., Avery, G., 2003. First excavation of intact Middle Stone Age layers at Ysterfontein, western Cape province, South Africa: implications for Middle Stone Age ecology. Journal of Archaeological Science 30, 955-971.

Hendey, Q.B., 1982. Langebaanweg: A Record of Past Life. South African Museum, Cape Town. 71 pp.

Hopley, P. J., Latham, A. G., Marshall, J. D., 2006. Palaeoenvironments and palaeodiets of mid-Pliocene micromammals from Makapansgat Limeworks, South Africa: A stable isotope and dental microwear approach, Palaeogeography Palaeoclimatology Palaeoecology 233, (3–4) 235-251.

Jenny, H., 1941. Factors of soil formation. McGraw-Hill, New York, 281p.

Ji, H.B., Wang, S.J., Ouyang, Z.Y., Zhang, S., Sun, C.X., Liu, X.M., Zhou, D.Q., 2004. Geochemistry of red residua underlying dolomites in karst terrains of Yunnan-Guizhou Plateau I. The formation of the Pingba profile. Chemical Geology 203, 1-27.

Kahmann, J.A., Seaman III. J., Driese, S.G., 2008. Evaluating trace elements as paleoclimate indicators: multivariate statistical analysis of late Mississippian Pennington Formation Paleosols, Kentucky, USA. Journal of Geology 116, 254-268.

Klein, C., Dutrow, B. 2007. Mineral science. John Wiley and Sons, Inc., Hoboken, NJ. 675 pp.

Kumaravel, V., Sangode, S., Siddaiah, N.S., Kumar, R., 2009. Major element geochemical variations in a Miocene-Pliocene Siwalik paleosol sequence: Implications to soil forming processes in the Himalayan foreland basin. Journal of the Geological Society of India 73, 759–772.

Lee, D.H., Cody, R.D., Kim, D.J., Choi, S., 2002. Effect of soil texture on surfactant-based remediation of hydrophobic organic-contaminated soil. Environment international, 27(8), 681–8.

Ma , J.L., Wei, G.H., Xu, Y.G., Long, W.G., Sun, W.D., 2007. Mobilization and re-distribution of major and trace elements during extreme weathering of basalt in Hainan Island, South China. Geochimica et Cosmochimica Acta 71, 3223-3237.

Mora, C.I., Driese, S.G., Colarusso, L.A., 1996. Middle to late Paleozoic atmospheric CO2 levels from soil carbonate and organic matter. Science 271, 1105–1107.

Nesbitt, H.W., Young, G.M., 1984. Prediction of some weathering trends of plutonic and volcanic rocks based on thermodynamic and kinetic considerations. Geochimica et Cosmochimica Acta. 48, 1523–1534.

Nesbitt, H.W., Young, G.M., 1989. Formation and Diagenesis of weathering profiles. Jour. Geol., 97,129-147.

Nesbitt, H.W., Markovics, G., Price, R.C., 1980. Chemical processes affecting alkalis and alkaline earths during continental weathering. Geochimica et Cosmochimica Acta 44, 1659-1666.

Munsell Color (2000) Munsell soil color charts. Gretag Macberth, New York.

Óskarsson, B. V., Riishuus, M. S., Arnalds, Ó., 2012. Climate-dependent chemical weathering of volcanic soils in Iceland. Geoderma, 189-190, 635–651. doi:10.1016/j.geoderma.2012.05.030

Prochnow, S. J., Nordt, L. C., Atchley, S. C., Hudec, M. R., 2006. Multi-proxy paleosol evidence for middle and late Triassic climate trends in eastern Utah. Palaeogeography, Palaeoclimatology, Palaeoecology, 232(1), 53–72.

Retallack, G.J., 1994. The environmental factor approach to the interpretation of paleosols. In: Amundson, R., et al. (Ed.), Factors in soils formation: A fiftieth anniversary retrospective. Soil Science Society of America Special Publication, vol. 33, pp. 31–64.

Retallack, G.J., 1997. Palaeosols in the upper Narrabeen Group of New South Wales as evidence of Early Triassic palaeoenvironments without modern analogues. Australian Journal of Earth Sciences 44, 185–201

Retallack, G.J., 1999. Post-apocalyptic greenhouse paleoclimate revealed by earliest Triassic paleosols in the Sydney Basin, Australia. Geological Society of America Bulletin 111, 52–70.

Retallack, G.J., 2001. Soils of the Past. Blackwell, Oxford. 600pp.

Retallack, G.J., 2005. Pedogenic carbonate proxies for amount and seasonality of precipitation in paleosols. Geology 33, 333–336.

Roberts, D.L., 2006. Lithostratigraphy of the Sandveld Group. S. Afr. Committee Stratigr. Lithostratigraphic Ser. 9, 25–26

Roberts, D.L., Berger, L., 1997. Last interglacial c.117 kyr human footprints, South Africa. S. Afr. J. Sci. 93, 349–350.

Roberts, D.L., Matthews, T., Herries, A.I.R., Boulter, C., Scott, L., Dondo, C., Mtembi, P., Browning, C., Smith, R.M.H., Haarhoff, P., Bateman, M.D., 2011. Regional and global context of the Late Cenozoic Langebaanweg (LBW) palaeontological site: West Coast of South Africa. Earth-Science Reviews 106, 191–214.

Roberts, D.L., Sciscio, L., Herries, A.I.R., Scott, L., Bamford, M.K., Musekiwa, C., Tsikos, H., 2013. Miocene Fluvial Systems and Palynofloras at the Southwestern Tip of Africa: Implications for Regional and Global Fluctuations in Climate and Ecosystems, Earth Science Reviews 124, 184-201.

Sayyed, M.R., Hundekari, S.M., 2006. Preliminary comparison of ancient bole beds and modern soils developed upon the Deccan volcanic basalts around Pune (India): potential for paleoenvironmental reconstruction. Quaternary International 156– 157, 189–199.

Sawyer, E.W., 1986. The influence of source rock type, chemical weathering and sorting on the geochemistry of clastic sediments from the Quetico metasedimentary belt, Superior Province, Canada. Chemical Geology 55, 77–95.

Sheldon, N. D., 2006. Abrupt chemical weathering increase across the Permian–Triassic boundary. Palaeogeography, Palaeoclimatology, Palaeoecology, 231(3-4), 315–321.

Sheldon, N.D., Retallack, G.J., Tanaka, S., 2002. Geochemical climofunctions from North America soils and application to paleosols across the Eocene–Oligocene boundary in Oregon. Journal of Geology 110, 687–696.

Sheldon, N. D., Tabor, N. J., 2009. Quantitative paleoenvironmental and paleoclimatic reconstruction using paleosols. Earth-Science Reviews, 95, 1–52.

Singer, R., Wymer, J., 1968. Archaeological investigations at the Saldanha skull site in South Africa. S. Afr. Archaeol. Bull. 23: 63-74.

Soil Survey Staff., 1999. Soil Taxonomy. Natural resources Conservation Service, USDA, 8th edition. Government printing office, Washington.

Stiles, C.A., Mora, C.I., Driese, S.G., 2001. Pedogenic iron-manganese nodules in Vertisols: a new proxy for paleoprecipitation? Geology 29, 943–946.

Stynder, D. D., 2011. Fossil bovid diets indicate a scarcity of grass in the Langebaanweg E Quarry (South Africa) late Miocene/early Pliocene environment. Paleobiology, 37(1), 126–139.

United States Salinity Lab. Staff., 1954. Methods for soil characterization. In: Diagnosis and improvement of saline and alkali soils. Agr. Handbook 60, USDA, Washington, D.C. pp 83-147.

Yang, S. Y., Li, C. X., Yang, D. Y., Li, X. S., 2004. Chemical weathering of the loess deposits in the lower Changjiang Valley, China, and paleoclimatic implications. Quaternary International, 117(1), 27–34.

Yoo, K., Mudd, S. M., 2008. Toward process-based modeling of geochemical soil formation across diverse landforms: A new mathematical framework. Geoderma, 146(1-2), 248–260.

Zachos, J., Pagani, M., Sloan, L., Thomas, E., and Billups, K. 2001. Trends, rhythms, and aberrations in global climate 65Ma to present. Science 292: 686-693.

CHAPTER THREE

CLAY MINERALOGY AND MICROMORPHOLOGY OF PALAEOSOLS AND PEDOFACIES FROM LANGEBAANWEG, SOUTH AFRICA: PALAEOENVIRONMENTAL INTERPRETATION

Abstract

Palaeosol-sediment-sequences at the West Coast Fossil Park in Langebaanweg, South Africa have a stratigraphy extending over ten horizons/ layers occupying a total depth of some 17 metres ranging from Mid-Miocene to Holocene. Six of these horizons qualify as palaeosols. The mineralogical assemblages and micromorphology of the palaeosols and pedofacies are explored with the objective of interpreting and reconstructing the palaeoenvironment of the locality. Physico-chemical parameters, mineralogical properties and micromorphology (soil thin sections and quartz grain exoscopy) of the palaeosols and pedofacies were analyzed using routine laboratory methods. The layers were designated according to the FAO and Soil Survey Staff systems. An alternating stack of palaeosols and sediments suggests repeated cyclic palaeoenvironment climate changes. Rhizoliths in the Pleistocene Ck layer affirms a shallow standing palaeowatertable during the Pliocene. Remarkable differences are observed in the mineralogical assemblages of the palaeosols and sediments. Palaeosols of the Middle Miocene have mixed clay mineralogy of halloysite, chlorite, muscovite mica, and kaolinite – an indication that the clay sources could be from different parent materials which may have taken place during transportation. Allophane and imogolite in the Early Pliocene palaeosols are stream-deposited while palygorskite and sepiolite along with high pH status of the soil environments indicate aridic/ dry environmental conditions. Pedofeatures (calcareousness, vertic, gleyic, illuviation) suggest cyclic patterns of erosion and deposition, which in turn are conformable with palaeoenvironmental and climatic changes. Vertic properties of the palaeosols were observed from their open porphyric c/f-related distribution, blocky microstructure and striated b-fabrics. The reddish Mid-Miocene palaeosols and Pliocene pedogenic calcretes formed under subtropical and Mediterranean climate conditions, while the pedosediments represent a (semi) arid climate.

Keywords: Palaeoenvironments, micromorphology, clay mineralogy, climate change, calcretes.

3.1. Introduction

Like modern soils, palaeosols, show characteristics that reflect the conditions under which they form, such as: climate, organisms, topography and parent material all of which influence their development. In recent years, palaeosols have provided increasingly useful and reliable proxies through which scientists are able to reconstruct palaeoenvironmental and palaeoclimatic dynamics (Mack and James, 1994; Blum, 2005; Sheldon and Tabor, 2009). There are many palaeosol environmental proxies, including clay mineralogy (e.g. Nedachi et al., 2005; Srivastava et al., 2009; Presley et al., 2010; Du et al., 2010; Rostási et al., 2011; Hong, 2012; Watanabe et al., 2012), micromorphology (e.g. Kemp, 2103; Todisco and Bhiry, 2008; Khormali and Kehl, 2011), and scanning electron microscopy (e.g. Xie et al., 2013; Mahaney et al., 1988; Mahaney and Vortisch, 1989; Retallack and Krinsley, 1993), which have been successfully applied in the palaeoenvironmental and palaeoclimate reconstruction through careful description and interpretation of various pedogenic properties of soils and palaeosols.

Clay minerals are products of chemical weathering. They are formed when parent material interacts with water at or near the surface of the earth (Velde, 1995). Consequently, they are of secondary origin in soils and do not necessarily reflect the primary compositions of the genetic parent material from which they formed. Varying degrees of geothermal, hydrothermal and contact metamorphic conditions promote the formation of different clay minerals (Velde, 1995; Thiry, 2000). In soils, there are diverse processes capable of forming different types of clay minerals (Birkeland, 1984) and the formation of clay minerals during pedogenesis is the most fundamental among these processes such that temperature, precipitation and drainage exert the foremost controls on clay mineral formation (Blaise, 1989).

In general, five assumptions form the basis for using pedogenic clay proxies for palaeoclimate reconstruction, viz.: (1) clay mineral formation is a function of climate; (2) once formed in a weathering environment, clay minerals are stable and do not change subsequently as long as the climate remains unchanged (pre-burial stability); (3) there is a uniformity of clay mineral accumulation throughout a weathering profile; (4) once present and buried, clay minerals are stable (post-burial stability); (5) uniform sensitivity of clay minerals towards environmental factors (Singer, 1984). Through the sensitivity of clay minerals to environmental and climatic factors is variable, however clay minerals present in palaeosols in well-defined environmental situations, have been adjudged suitable for palaeoclimate interpretation (Velde, 1995).

Micromorphology is the identification, description and interpretation of the components, features and fabrics of soils and sediments at a microscopic level (Bullock et al., 1985; Stoops et al., 2010). It provides a lead into the operational pedogenic processes, hydrology and geology of soils and sediments. Although micromorphology has been applied extensively to an understanding of past and present environmental processes a combination of field and bulk analytical data provides a stronger platform for soil genesis interpretation. One major interpretative problem associated with micromorphology is the acceptance by scientists of the distinctiveness of some pedofeatures-pedogenic process-macroenvironment relationships. It is true that such relationships are often not fully understood, indeed, a growing body of evidence suggests that different local and regional blends of pedogenetic processes and/or environments may produce similar horizons and pedofeatures (Stoops et al., 2010). Nevertheless, holistic interpretations of pedogenic features, including micromorphology, may provide important insights into key processes related to environmental controls such as clay illuviation, calcite redistribution and the formation of cryogenic microstructures (Kemp, 1999).

The West Coast Fossil Park at Langebaanweg (LBW), South Africa, is a regionally and globally importantlate Neogene geoarcheological site renowned for its well preserved buried fossils extending to circa 5.1 Ma (Olson, 1984; Roberts et al., 2011). Typical of coastal sedimentary environments (Roy et al., 2012; Panagiotaras et al., 2012; Parkinson et al., 2012), the geomorphology, soils and sediments of the West Coast Fossil park vicinity have been subjected to several cycles of fluvial, aeolian and marine processes over time, including sediment transport, coastal erosion and biogeochemical processes, which have shaped their characteristics. Global sea level changes in response to tectonics and climate change are believed to have had a significant impact on the geomorphology of this locality and the fossil animal remains deposited during a marine transgression have been very intensively studied giving rise to detailed palaeoenvironmental reconstructions (Hendy, 1982; Roberts et al., 2011). Quarry excavation at this site has revealed a lithostratigraphic section with pedogenically modified horizons (Roberts, 2006a; Roberts et al., 2011). The exposed surfaces, based on relative stratigraphy and OSL consists of early Pliocene pedogenically modified buried soils at the bottom of the section through to Holocene aeolian sediments at top of the profile.

Hitherto, the West Coast Fossil Park has been extensively studied mainly for its rich palaeo-biodiversity (e.g. Hendey, 1982; Manegold, 2010; Scott et al., 2011), and complex stratigraphy e.g. (Roberts, 2006d; Roberts et al., 2011). The study of palaeosol-based proxies including clay mineralogy and micromorphology has largely been ignored in southern Africa generally and the important fossil-bearing site at Langebaanweg which certainly warrants intense palaeoenvironmental studies. Chase and Meadows (2007) opined that palaeoenvironmental evidence for southern Africa remains largely incomplete as palaeoclimatic proxy records are scarce and often discontinuous. In fact, it is largely demonstrated that palaeosols archive reliable

and finer scale palaeo- climatic and environmental imprints (May et al., 2008; Sheldon and Tabor, 2009; Von Suchodoletz et al., 2009), hence it can be hypothesized that a combination of geomorphic and pedogenic processes have continued to shape the development of a palaeosols-sediment-sequences with horizons of varying degrees of pedogenic and diagenetic alterations which may prove significantly valuable in the reconstruction of the palaeoclimate of the West Coast Fossil Park and broader region. The overarching aim of this study, therefore, is to improve the understanding of palaeoenvironments and palaeoclimate dynamics of the exposed sequence at Langebaanweg using palaeosols. The specific objective is to provide a detailed description and genetic interpretation of the: i) micromorphology of the palaeosols and pedosediments, ii) selected physico-chemical properties, and iii) clay mineralogy.

3.2. Geographical and geological setting

The West Coast Fossil Park is located approximately 120 km north of Cape Town. The exposed palaeosols-sediment-sequences are situated at latitude 32°57.784″ S and longitude 18°06.367″ E (Fig. 3.1) approximately 30m above sea level. The site is also notable as for a number of mid- to late Quaternary palaeontological sites, for example, Elandsfontyn (where the partial cranium of early archaic *Homo sapiens,* "Saldanha man" was discovered (Singer and Wymer, 1968), Langebaan (the site of last interglacial fossil human footprints, Roberts, 2009), and the Middle Stone Age (~250–25 kya) sites of Hoedjiespunt, Sea Harvest, Yzerfontein and Duinefontyn (Roberts and Berger, 1997; Halkett *et al*., 2003). The climate of LBW is generally semi-arid to arid and falls within the winter rainfall zone of South Africa (Hopley et al., 2006).

The geology of LBW comprises Varswater Fm of the Sandveld group overlain by the Springfontyn Fm and calcareous aeolian deposit of the Langebaan Formation (Fm) and underlain

by the Varswater Formation (Roberts et al., 2011) (Fig. 3.2). The Varswater Formation is further subdivided into four members, viz: the Langeenheid Clayey. Sand (LCSM), the Konings Vlei Gravel (KGM), the Langeberg Quartz Sand (LQSM) and the Muishond Fontein Pelletal Phosphorite Members (MPPM) (Roberts et al., 2011). A lithostratigraphic summary (Fig. 2) of the fossil park shows the spatio-temporal relationships, approximate thickness, lithology, and depositional environment of the palaeosol-sediment sequences.

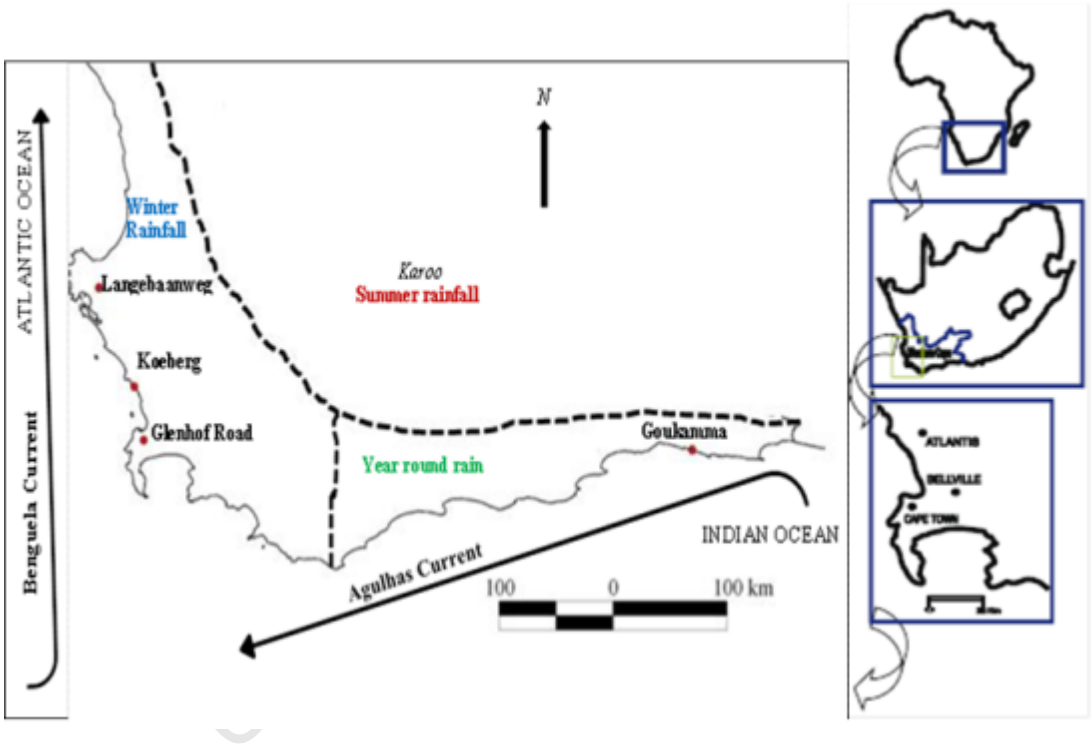

Fig. 3.1. Map of the West Coast Fossil Park, Langebaanweg (LBW).

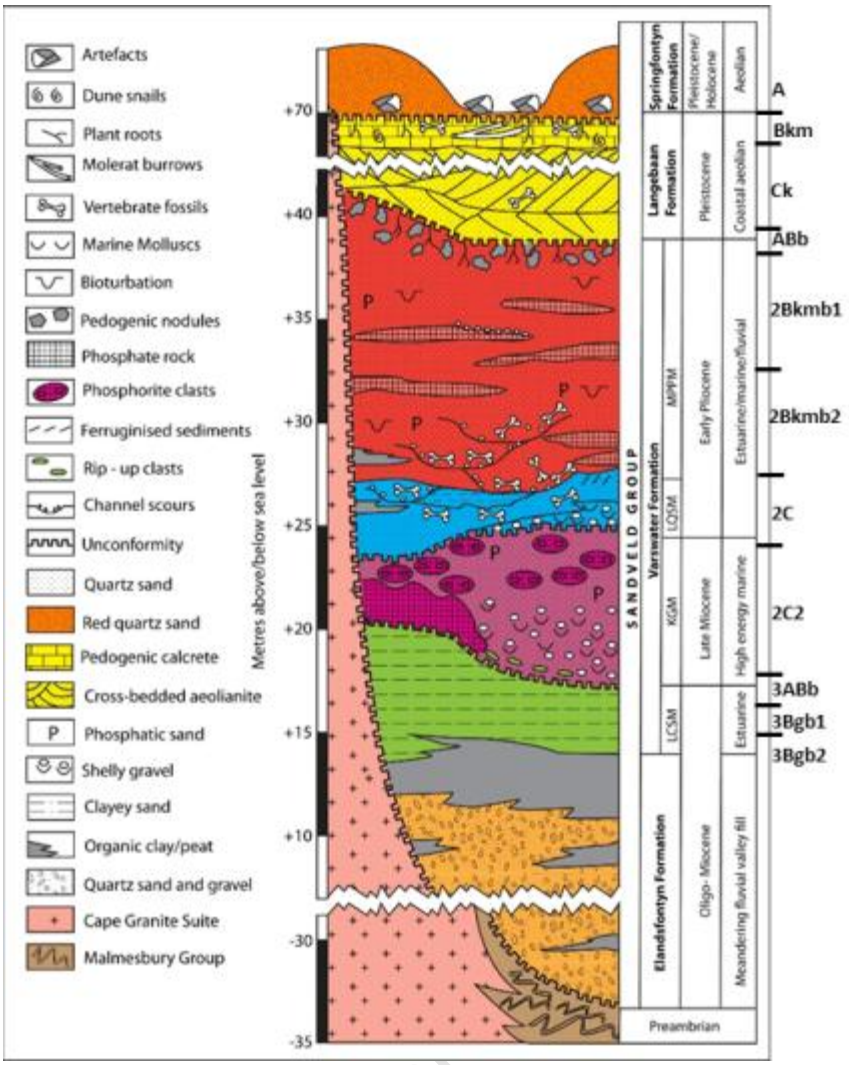

Fig. 3.2. Annotated summary stratigraphic column for LBW (after Roberts et al., 2011)

3.3. Materials and Methods

3.3.1. Field sampling

The Quarry was excavated to fresh exposure by cleaning off the long exposed surfaces so as to avoid weathered/ altered samples. Representative undisturbed and/or core samples were taken from each horizon of the palaeosol-sediment sequences (Fig 3.3 for thin section preparations. Additionally, bulk sampling from each horizon was done for laboratory analyses. It

was not possible to sample the LBW excavation along the same plane due to a rocky layer so in order to facilitate a complete study of the exposed surfaces to a depth of 30 m, samples were taken in two subsections: the so-called "high wall" and "low wall" (Fig. 3.3) which are separated by an interbedded thick layer of unweathered pelletal phosphorite rock.. In the field, colour was described using Munsell soil colour chart (Munsell colour company, 2000), while the general macromorphological properties were described in accordance with the guidelines for soil profile description (FAO, 2006).

3.3.2. Laboratory analysis

The collected palaesol and pedosediment samples were gently ground to break up clods and subsequently passed through a 2mm sieve in accordance with standards described in van Reeuwijk (2002). Dry and moist colours were determined using a Munsell (2000) color chart (measurements taken in triplicates). The soil redness rating (Hurst, 1977) was calculated using the formula RR= H.C/V where C = Chroma (intensity), V = Value (lightness) and H = Hue (shade) (12.5 for hue 7.5R; 10 for hue 10R; 7.5 for 2.5YR; 5 for 5YR, 2.5 for 7.5YR; and 0 for 10YR of the Munsell colour nomenclature) after Torrent et al., (1980) and Barrón and Torrent (1986). Particle size distribution was measured using the hydrometer method of Bouyoucos (1965). For soil pH(H_2O) and electrical conductivity, a soil/solution ratio of 1: 2.5 was used and the values read from digital pH and Milwaukee SM302 EC meters respectively. Calcium carbonate content of samples was determined by the gravimetric method as described by the U.S. Salinity Laboratory Staff (1954). Clay mineral analyses was conducted using a Phillips PW 3830/40 Generator with a PW 3710 mpd control X-ray diffraction system employing the Xpert data collector/identify software. Micromorphological analyses were carried out on the thin section slides viewed with a polarizing petrographic microscope (Nikon) and images captured

with an Olympus ALTRA 20 camera. Scanning electron microscopy was conducted with the Oxford X-Max silicon drift detector and a high resolution Carl Zeiss Σigma Advanced Analytical Microscope. The energy dispersive spectrum was analyzed with Oxford INCA software. Reported values are the average of measurements taken in triplicates.

3.4. Results

3.4.1. Field observations and pedostratigraphy

The LBW section shows interesting and complex palaeosol-sediment sequences. A higher spatial resolution of the section (Fig. 3.3) whose general stratigraphy (Fig. 3.2) shows that it qualifies as an example of a buried soil with a mantle, i.e. recently transported material lying above a buried horizon. In accordance with the FAO and Soil Survey Staff nomenclature systems, the horizons were delineated. The total height of the exposed palaeosol-sediment sequences is approximately 17 m. At the bottom of the sequences is a mid-Miocene hydromorphic buried soil horizons (3ABgb-3Bgb1-3Bgb2) also developed from the LCSM at the low wall of the pedocomplex (Fig. 3.3). Above these palaeosols is a Late Miocene high marine energy deposit of unweathered/ unaltered phosphocretes which developed from the Varswater formation. After the rocks comes the Early to Late Pliocene 260 cm section which constitutes the ABb-2Bkmb1-2Bkmb2 horizons. The Quaternary "A-Bk-C" (Fig. 3) horizons of overlying Langebaan Fm constitute the mantle of the palaeosols-sediment-sequences and have a characteristic ochric epipedon. Spectacularly prominent in the "C" horizon of the Pleistocene sediment layer are rhizoliths. In summary, the locality consists of three stacks of pedogenically modified layers (Middle Miocene palaeosols, Early to Late Pliocene and uppermost Holocene palaeosol profile) interbedded by pedosediments which have basically undergone diagenesis.

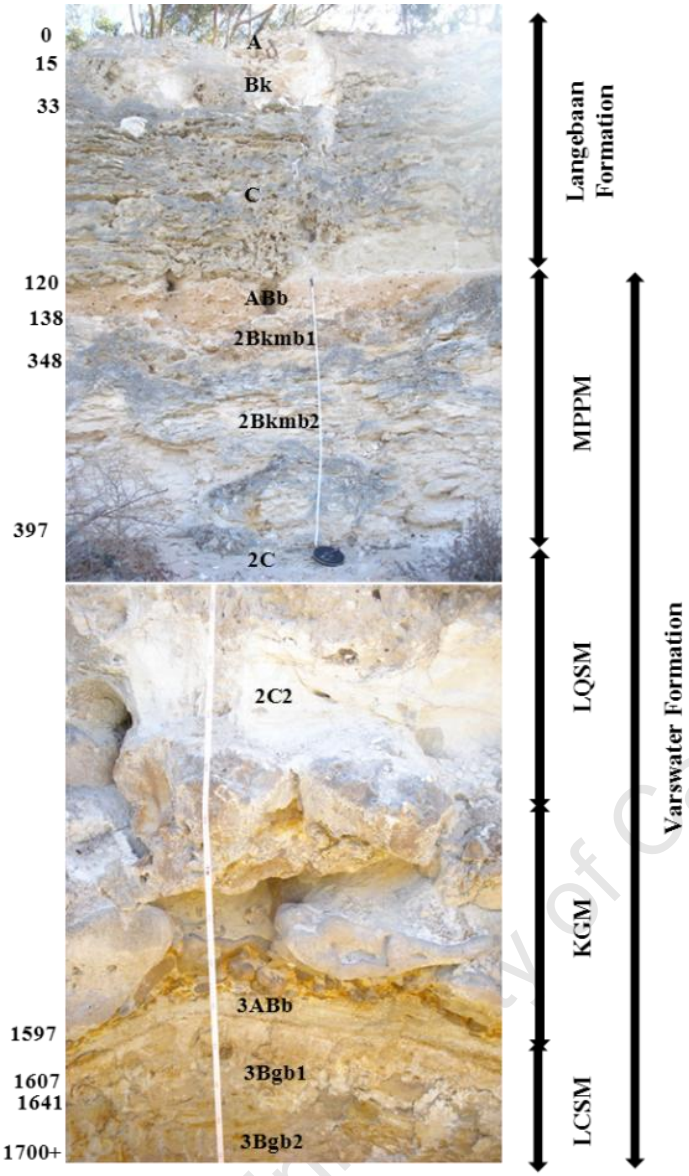

Fig. 3.3. Pedostratigraphic section of the LBW section (depth is in 'cm') showing high and low wall respectively (the thin white straight line demarcates the 'low wall' from the 'high wall').

3.4.2. Physico-chemical properties

Palaeosols were identified by the presence of at least one of: (i) undisturbed features from soil floral and faunal activity, such as passage of features and channels with root residues and excrements; (ii) a pedogenic b-fabric; (iii) a pedogenic microstructure; or (iv) one or more types of undisturbed pedofeatures On the other hand, pedosediments are recognised by: (i) an absence

of *in situ* biogenic features, but the common presence of fragmentary faunal or floral remains; (ii) a massive microstructure, and occasionally a structure dominated by packing of rounded aggregates; or (iii) preserved sedimentary features (Fedoroff *et al*., 2010 and Mücher *et al*., 2010). Throughout the section, strongly contrasting differences in macromorphological properties (Table 3.1) particularly colour and textural characteristics between the palaeosols and pedosediments. The different facies studied comprise aeolian sediments, calcrete palaeosols, phosphocrete and pedogenically modified estuarine sandy deposits at the low wall. The Middle Miocene palaeosols (3ABb-3Bgb1-3Bgb2) on the low wall have colours ranging from yellowish red (5YR 4/6) to brownish yellow (10YR 6/6) with strong evidence of dark yellow mottles, while the Pliocene buried palaeosols (2Bkmb1 and 2Bkmb2) show colours ranging from brown (7.5 YR 5/4) eluvial soil to pale yellow (2.5Y 8/2) calcrete. The Quaternary section is composed of moderately cemented Pleistocene Bk and Ck horizons and a Holocene A horizon- and the colour varies from light olive brown (2.5 Y 5/4) to dark reddish brown (5YR 3/2). Fragments greater than 2mm in diameter are present in some of the horizons (Table 3.1), especially within the interbedded pedosediment layers sandwiching the palaeosols. Where present, and depending on the amount, carbonates were largely responsible for the cementation of both palaeosols and pedosediments. Only palaeosols and pedosediments on the "high wall" reacted to diluted hydrochloric acid, in some cases very markedly.

Table 3.1 Profile description of the macromorphological properties of the LBW pedocomplex

Horizon	Depth (m)	Facies	Colour[1] (moist)	>2mm fragments	Structure[2]	Root	Boundary[3]	Consistency (moist)	Field texture	Cementation	React HCl	other features
A	0-	aeolian	5YR 3/2 (dark reddish brown)	absent	1gr	common	gw	loose	sand	none	moderate	snail shells
Bk	0.15-	calcrete	5Y 7/1 (light gray)	absent	3sbk	common	aw	firm	loamy sand	carbonate	strong	-
Ck	0.33-	aeolian	2.5 Y 5/4 (light olive brown)	very few	3sbk	few	cw	very firm	sand	carbonate	moderate	rhyzolith
2ABb	1.20-	marine	7.5YR 5/4 (brown)	few	1gr	none	cs	friable	sand	none	occasional	burrows
2Bkmb1	1.38-	calcrete	5YR 3/4 (dark reddish brown)	common	3abk	none	gw	very firm	sand	carbonate	occasional	-
2Bkmb2	3.48-	calcrete	2.5Y 8/1 (pale yellow)	absent	3abk	few	gw	firm	clay	carbonate	very strong	burrows
2C	3.97-	phoscrete	2.5Y 8/2 (pale yellow)	abundant	1gr	common	cw	friable	sand	none	none	-
2C2	15.97-	marine	nd	common	blk	none	cw	very firm	blocky	none	none	-
3ABb	16.07	estuarine	5YR 4/6 (yellowish red)	common	2gr.s	few	cs	loose	gr sand	none	none	stone line
3Bgb2	16.41	estuarine	10YR 6/3 (pale brown)	occasional	2sbk	few	cs	firm	loamy sand	none	none	-
3Bgb2	17.00+	estuarine	10YR 6/6 (brownish yellow)	absent	2sbk	few	-	firm	silty clay	none	none	-

[1]nd – not determined

[2] 1– weak; 2 – medium; 3 – strong; gr – granular; sbk – subangular blocky; abk – angular blocky, blk – blocky; Gr. S – gravelly sand

[3] a – abrupt; c – clear; s – smooth; g – gradual; w – wavy

Table 3.2. Selected physico-chemical properties of Langebaanweg pedocomplex

Horizon	Colour (dry)	RR[◊] dry	RR[◊] moist	Sand (<2mm) (g kg^{-1})	Silt (<2mm) (g kg^{-1})	Clay (<2mm) (g kg^{-1})	Texture[ǂ] (IUSS)	pH (H_2O)	EC mS cm^{-1}	$CaCO_3$[*] g kg^{-1}
A	5YR 5/2	2.0	3.3	908	22	70	Sa	8.3	0.08	183
Bk	5Y 8/1	-	-	638	137	225	ClLo	9.2	0.11	437
Ck	2.5Y 7/3	-	-	907	22	71	Sa	7.7	0.06	218
2ABb	7.5YR 7/6	2.1	2.0	899	11	90	LoSa	9.5	0.36	238
2Bkmb1	5YR 5/8	8.0	6.7	729	41	230	SaClLo	9.2	0.46	475
2Bkmb2	2.5 Y 8/1	-	-	473	184	343	SaClLo	9.3	0.62	626
2C2	2.5Y 8/1	-	-	613	150	228	SaClLo	8.6	0.17	nd
3ABb2	5YR 5/6	6.0	7.4	712	63	225	SaClLo	7.9	15.07	nd
3Bgb1	10YR 8/2	0	0	264	112	624	Cl	8.0	11.15	nd
3Bgb2	10YR 6/8	0	0	562	113	325	SaClLo	8.3	2.53	nd

[◊] Redness rating

[ǂ] Sa – sand; ClLo – clay loam; LoSa – loamy sand; SaClLo – sandy clay loam; Cl – clay

[*] nd – not determined

Where applicable, both the wet and dry redness ratings for the pedocomplex follow the same pattern and are highest for the Pliocene palaeosol (Table 3.2). Particle size distribution across the sequence is variable. Both the soils and pedosediments record alkaline soil pH values. Although pH fluctuates down the sequences, the Pliocene palaeosols have higher values than the other samples. Electrical conductivity values of the soils and sediments are low, with the exception of the Middle Miocene palaeosol in the "low wall" section in which conductivity is somewhat higher. Calcium carbonate equivalent values also vary down the sequences of the "high wall" where it is present.

3.4.3. Mineralogy

The x-ray diffractograms of the untreated silt and clay sized fraction (<20 μm) of the samples vary markedly across the palaeosol-sediment sequence (Fig. 3.4). The mid-Miocene palaeosol at the low wall of the section had scanned peaked corresponding to known peaks of greenalite, muscovite, kaolinite and sepiolite at the 3ABb horizon (Fig. 3.4a). The underlying B horizons ('3Bgb1 and 3Bgb2') had mottling, an evidence of hydromorphism in the profile. Both horizons had scanned peaks primarily corresponding to the theoretical peaks of chlorite and kaolinite (Fig. 3.4b, c). Additionally, 3Bgb2 had peaks of none expanding 1:1 clay minerals - halloysite and mica. The two B-horizons of the palaeosol (Bkmb1 and Bkmb2) had low intensity broad peaks corresponding to the known peaks of short range amorphous clay minerals allophane and imogolite respectively. Calcite peaks were also present in the palaeosols (Fig. 3.4d, e). SEM micrographs also confirm the presence of needle fibre shaped and white fluffy calcites in the carbonate palaeosol (Fig. 3.5a, b). The AB horizon of the buried Early Pliocene palaeosol has peaks matching that of mica, dickite, oxides, sepiolite, palygorskite and calcite (Fig. 3.4f). Evidence of layering and neo-formation of clays in this horizon was seen from the SEM (Fig. 3.5b) and the compositional elements from the energy dispersive spectrum (EDS) (Fig. 5c). The gritty Pleistocene aeolian parent material of the mantle (C-horizon) reveals peaks corresponding to calcite only (Fig. 3.4g). The overlying horizon (Bk) has peaks matching smectite, quartz, oxides and sepiolite (Fig. 3.4h). A scanning electron microscopy (SEM) study of the <20 μm 'Bk' sample also reveals the fibrous nature of sepiolite as it appears to coat quartz grains (Fig. 3.5a). The Holocene surface horizon (epipedon of the mantle) has scanned peaks that show primary correspondence with theoretical peaks for quartz, oxides, palygorskite and calcite (Fig. 5i).

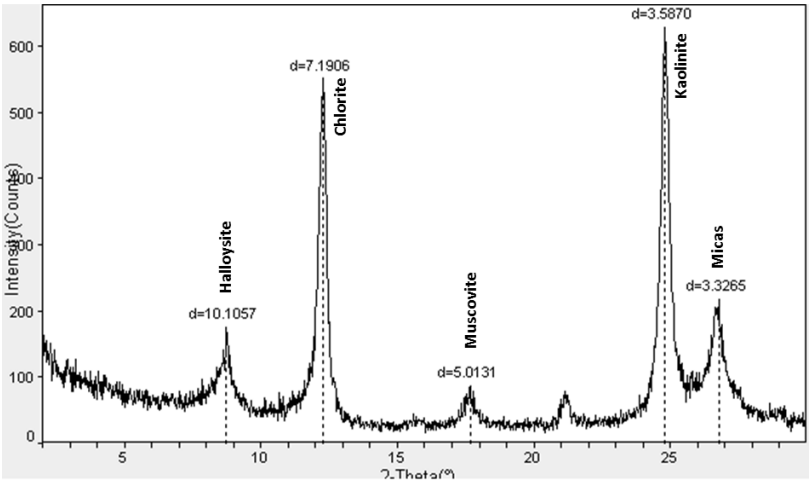

a. 3Bgb2 horizon

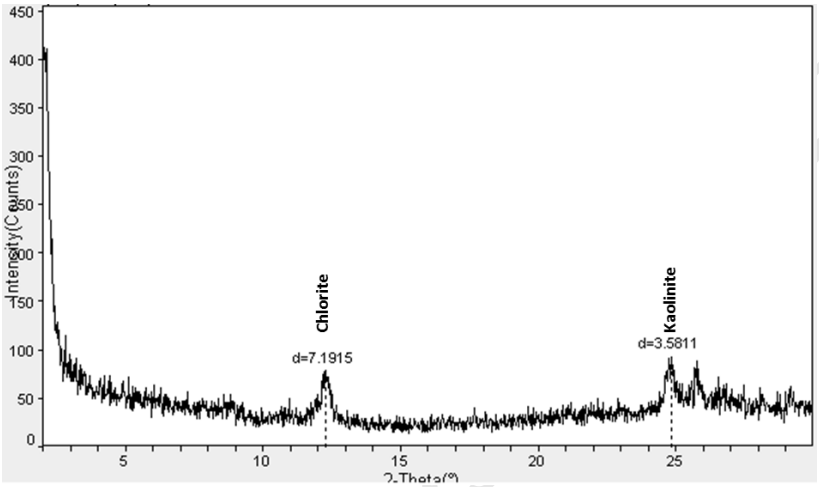

b. 3Bgb1 horizon

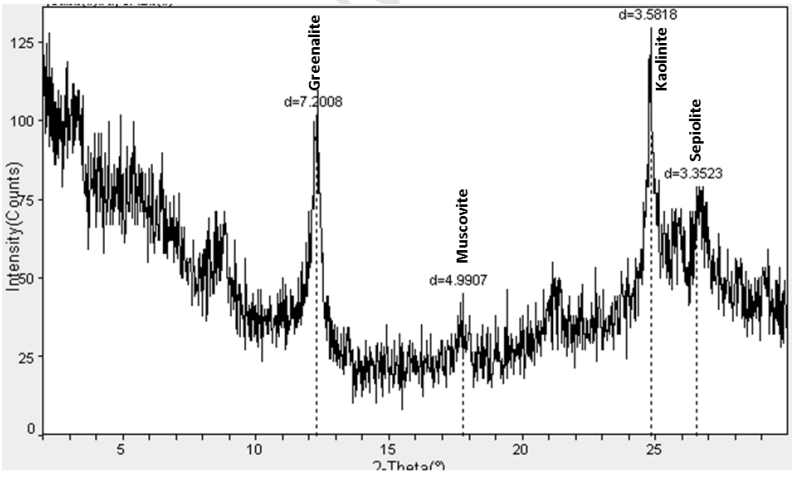

c. 3ABb horizon

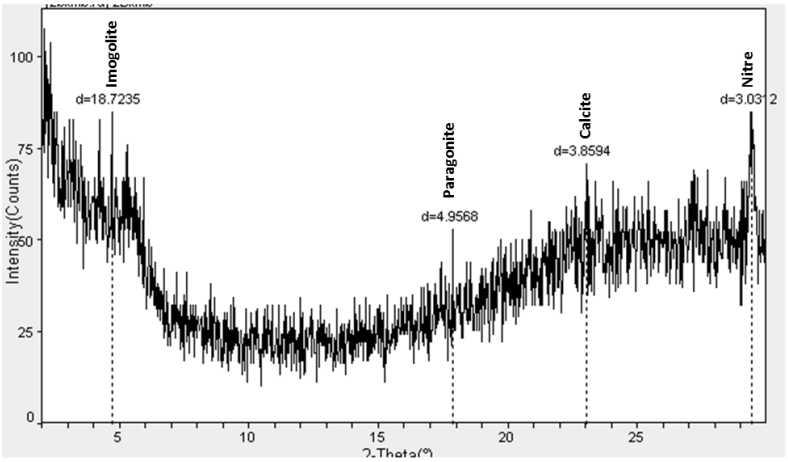

d. Bkmb2 horizon

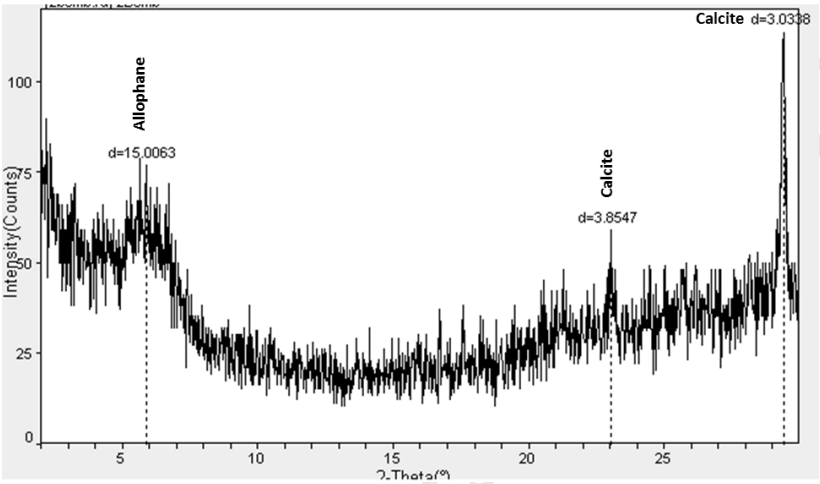

e. Bkmb1 horizon

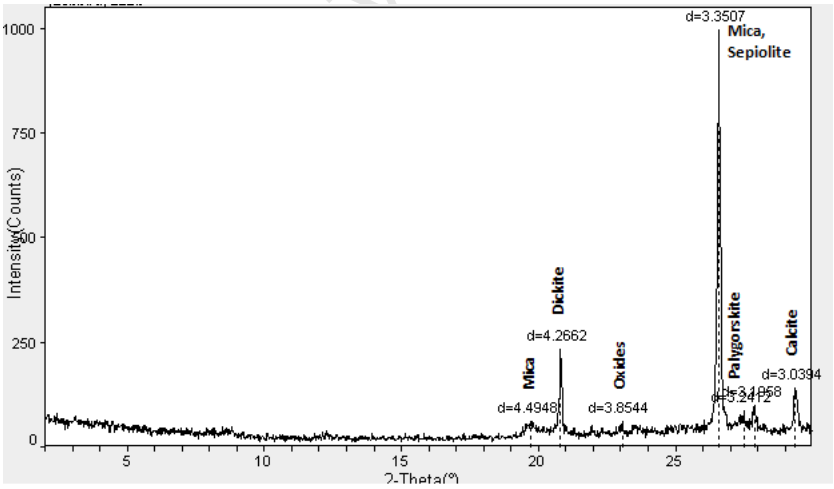

f. 2ABb horizon

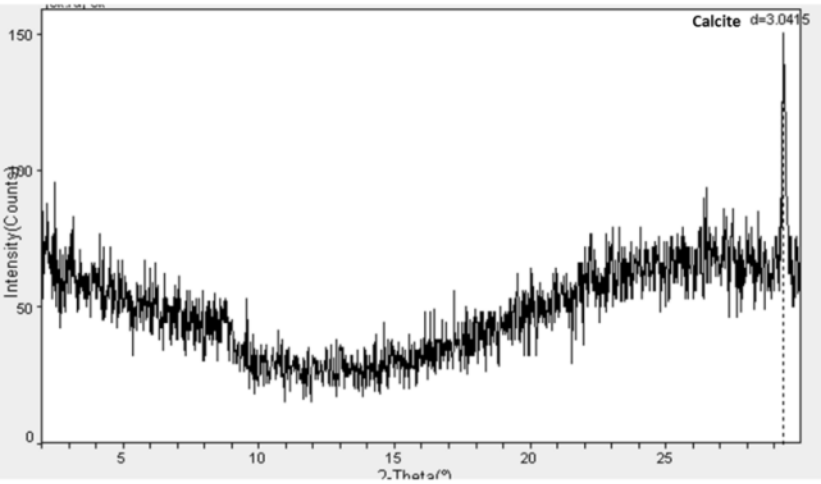

g. Ck horizon

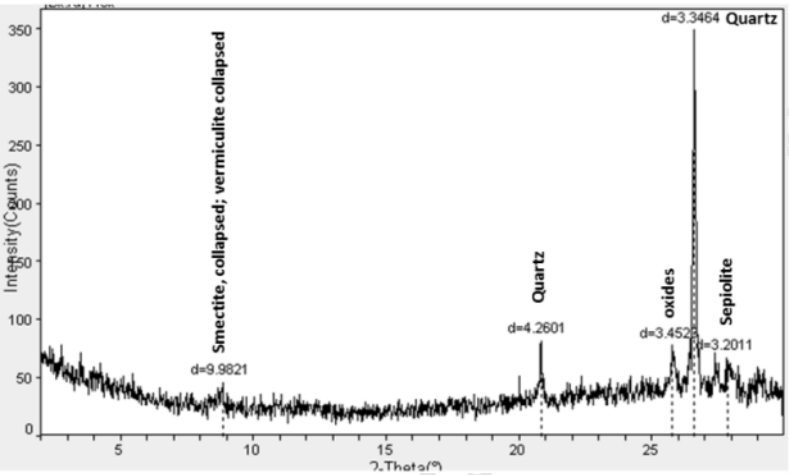

h. Bk horizon

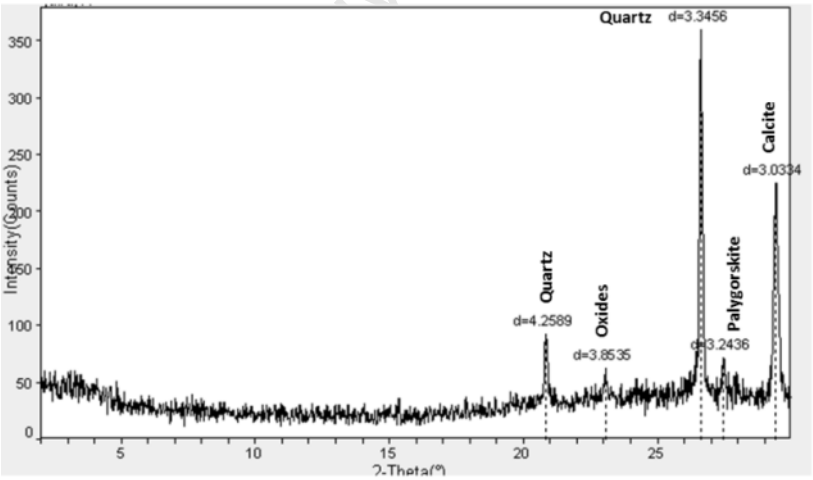

i. A horizon

Fig. 3.4. (a-i). Diffractograms for horizons of the LBW palaeosol-sediment sequences

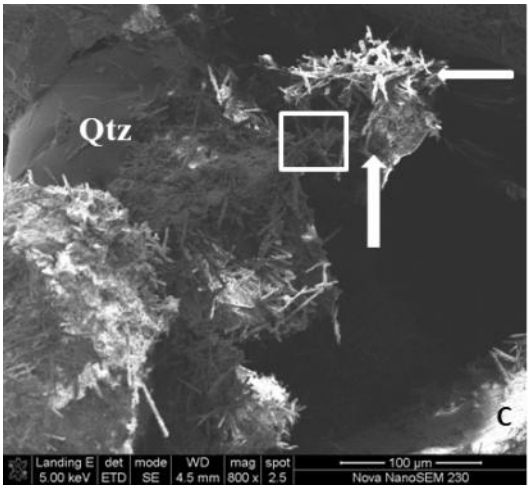

a. Low magnification of the Bk sample showing the coating of the tangential fibrous sepiolite (arrows) on quartz (Qtz) grains, "C": charging.

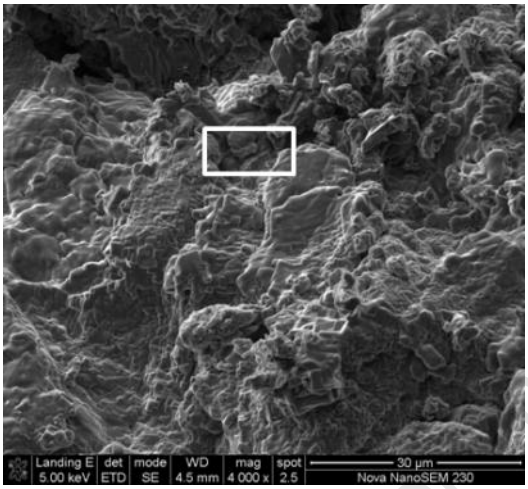

b. Layering and neoformed clay in the 2ABb horizon

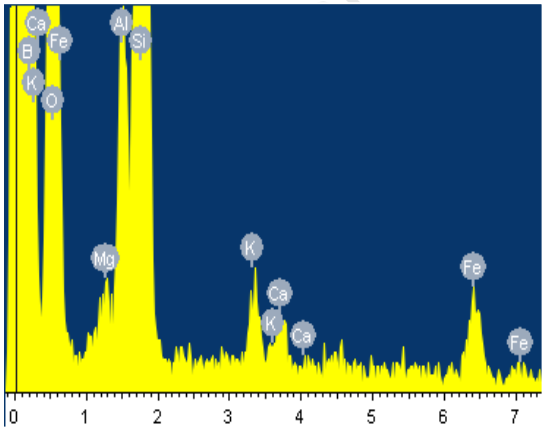

c. Energy dispersive spectrum of the rectangular area highlighted in Fig. 3.5b showing elemental composition

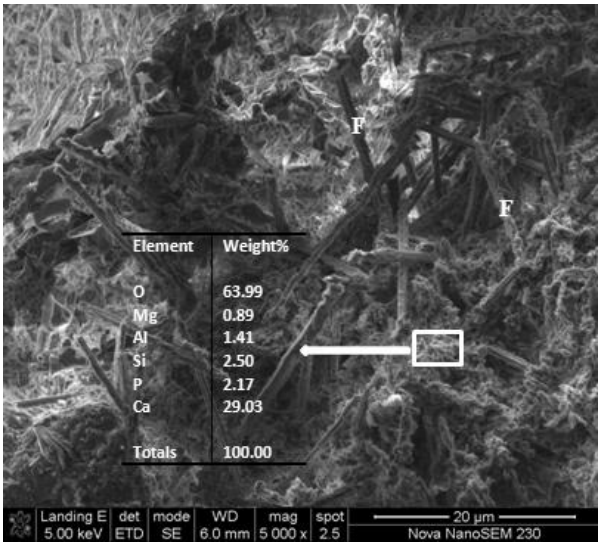

d. Tangential filaments needle fibre calcite of the 2Bkmb1 horizon showing elemental composition (%)

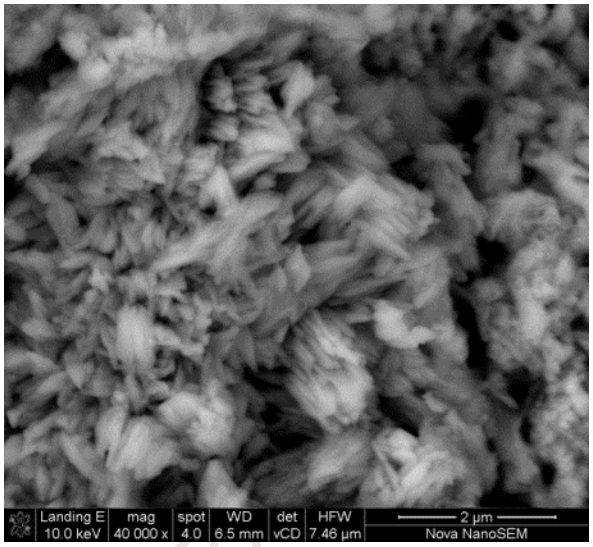

e. High resolution SEM of Bkmb1 showing layering and white fluffy surface coating of calcite mineral.

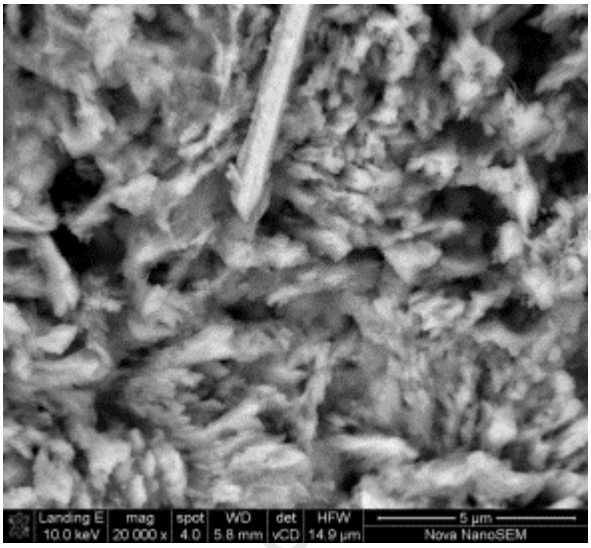

f. High resolution SEM of 2Bkmb2 clays showing abundant white fluffy calcitic fibre.

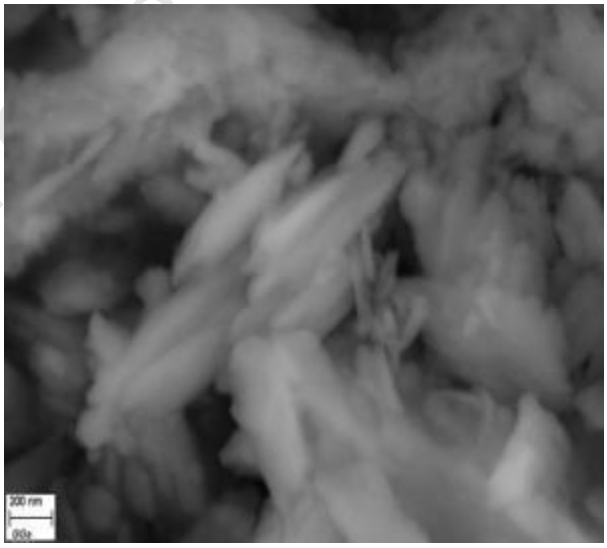

g. A close up higher resolution Σigma SEM of Bkmb2

Fig. 3.5. (a-g). Selected SEM of the granular microstructure palaeosol from LBW

3.4.4. Micromorphology

Only thin sections for the pedogenically modified horizons (3Bgb2, 3Bgb1, 3ABb, 2Bkmb2, 2Bkmb1, and ABb) were prepared as the pedosediments (A, Ck, 2C and 2C2 horizons) have single grains structure which made it very difficult for sampling. Photomicrographs captured under both plane polarized (PPL) and cross polarised lights (Fig. 3.6 a-f) show varying degrees of pedogenesis. A summary of the genetic properties of the palaeosols (Table 3.3) is presented under three subheadings for ease of description, viz. groundmass, voids and microstructure and pedofeatures, and show striking contrasts in composition of the palaeosols and pedosediments.

3.4.4.1. Mineral components

Quartz is the dorminant mineral in the coarse mineral fraction (>100 µm) in all samples. Feldspars (mainly plagioclase) and phosphorite are also common in the Mid Miocene palaeosols in the "low wall" subsection (Fig 3.6a-c). These palaeosols have an intergrain microaggregate structure, complex packing voids with enaulic to chitonic distribution. The overlying Pliocene 2Bkmb1 and 2Bkmb2 palaeosols are dominated by fine to medium (250 – 1000 µm) sand particles which are poorly to moderately sorted with fine monic distribution (Fig. 3.6 d, e). The ABb horizon of the same parent material and epoch comprises a loosely arranged single grain structure, simple packing voids with enaulic to chitonic related distribution (Fig. 3.6f). The Quaternary mantle sediments are well to moderately sorted fine to medium sand particles (>63 – 250 µm). Most of the grains in these horizons are loosely arranged and although there is weak to moderate microaggregate structure in the Pleistocene Bk horizon whose micromorphology is apparently similar with that of 2Bkmb2 (Fig. 3.6d).

3.4.4.2 Marine shell , rhizogenic structure and terrestrial humus characterisation

There is no evidence of marine shell and rhizogenic structure in the middle Miocene palaeosols of the LBW pedocomplex. Marine shells were not observed in the thin section of the Pliocene palaeosols, but macroscopic rhizogenic structures albeit are common. The Pleistocene pedosediment forming on coastal aeolian sediments houses many marine shells which rhizoliths. In general, the palaeosol-sediment-sequences had common to very few organic matter traces. Organic matter pigmentation is seen in the ABb horizon 3ABb samples and proved useful in the designation of such horizons. Traces of soil organic matter, indicated by darker coloured patches are present mostly in the A and Bk horizons of the Quaternary mantle, albeit in very low amounts.

3.4.4.3. Pedological processes

3.4.4.3.1. Mineral component alteration

Evidence of mineral alteration is more pronounced in the palaeosols – "AB" and "B" horizons (Fig 3.6a-f) whereas the mineral components of the pedosediments are relatively unaltered, subrounded to subangular as seen with the aid of hand lens. Additionally, most of the mineral components of the interbedded pedosediments did not show evidence of mechanical cracking fissures, which indicates they were not *in situ* i.e. disturbed and transported. For the palaeosols, there is evidence of advanced chemical weathering of the mineral components as . reddish-brown Fe oxide and/or Fe hydroxide staining commonly occurs along cleavage lines and fractures in grains (Fig. 3.6 a, b).

Table 3.3. Summary of the micromorphological description of the LBW pedocomplex

Horizon	Groundmass	Void and microstructure	Pedofeatures
Bk	**C/F distribution**: gefuric to chitonic; **C/F limit**: clay/sand; **coarse component**: 80% of the t.t.s.a., silt and fine to coarse sand, smooth and spheroidal fracture, shape rounded to subrounded variability within random fabric associated with shape, elongated grains are randomly distributed; **fine component**: b-fabric: 10% t.t.s.a.,	5-10% of the t.t.s.a.; few simple to frequent compound packing voids; **microstructure**: single to bridged grain ped structure	Textural sandy pedofeatures associated with coastal/ aeolian transportation; calcium carbonate coatings around peds; calcium carbonate creates quasi- and hypo-coatings on walls of peds, plant residues
2ABb	**C/F distribution**: enaulic; **C/F limit**: clay/sand; **coarse component**: 80% of the t.t.s.a., silt and fine to coarse sand, smooth and spheroidal fracture, shape subrounded to subangular high variability within random fabric associated with shape, elongated grains are randomly distributed; **fine component**: fabric: crystallitic b-fabric, 15% t.t.s.a.	5% of the t.t.s.a.; few simple packing voids, with common channel voids ; **microstructure**: single to bridged grain structure	Depletion and crystalline pedofeatures associated with iron oxide eluviation and translocation within the soil fabric; iron oxide creates quasi- and hypo-coatings on walls of peds; organic matter pigment
2Bkmb1	**C/F distribution**: porphyric; **C/F limit**: clay/sand; **coarse component**: 70% of the t.t.s.a., silt and fine to coarse sand, smooth and spheroidal fracture, shape subrounded to subangular high variability within random fabric associated with shape, elongated grains are randomly distributed; **fine component**: fabric: striated b-fabric; 25% t.t.s.a., iron	5% of the t.t.s.a.; channel, dominant voids are chambers; **microstructure:** massive	impregnative pedofeatures associated with illuviation and impure clay with hypo coatings around peds; iron oxide creates coatings on walls of peds, plant residues

Table 3.3 continued.

Horizon	Groundmass	Voids and microstructure	Pedofeatures
2Bkmb2	**C/F distribution**: porphyric; **C/F limit**: clay/sand; **coarse component**: 70% of the t.t.s.a., silt and fine to coarse sand, smooth and spheroidal fracture, shape subrounded to subangular high variability within random fabric associated with shape, elongated grains are randomly distributed; **fine component**: fabric: striated b-fabric; 30% t.t.s.a.	5% of the t.t.s.a.; channel, dominant voids are chambers; **microstructure**: massive.	Textural pedofeatures associated with calcium carbonate coatings around peds; CaCO3 creates quasi and hypo-coatings on walls of peds, organic residues.
3ABb	**C/F distribution**: enaulic; **C/F limit**: clay/sand; **coarse component**: 80% of the t.t.s.a., silt and fine to coarse sand, smooth and spheroidal fracture, shape subrounded to subangular high variability within random fabric associated with shape; **fine component**: fabric: crystallitic b-fabric, 15% t.t.s.a.	5% of the t.t.s.a.; compound packing voids, with common chambers voids ; **microstructure**: vughy pore structure.	Depletion and crystalline pedofeatures associated with iron oxide eluviation and translocation within the soil fabric; iron oxide creates quasi- and hypo-coatings on walls of peds, organic matter pigments.
3Bgb1	**C/F distribution**: enaulic; **C/F limit**: clay/sand; **coarse component**: 80% of the t.t.s.a., silt and fine to coarse sand, smooth and spheroidal fracture, shape subrounded to subangular high variability within random fabric associated with shape; **fine component**: fabric: crystallitic b-fabric, 15% t.t.s.a.	5% of the t.t.s.a.; com packing voids, with common channel voids ; **microstructure**: complex: a mixture of vughy and crumb micro structure.	Textural pedofeatures associated with fragments of clay and silt embedded within the soil matrix.
3Bgb2	**C/F distribution**: enaulic; **C/F limit**: clay/sand; **coarse component**: 80% of the t.t.s.a., silt and fine to coarse sand, smooth and spheroidal fracture, shape subrounded to subangular high variability within random fabric associated with shape; **fine component**: fabric: crystallitic b-fabric, 15% t.t.s.a.	5% of the t.t.s.a.; few simple packing voids, with common channel voids ; **microstructure**: complex: a mixture compact and bridged grain structure.	Textural pedofeatures associated with fragments of clay and silt embedded in the soil matrix.

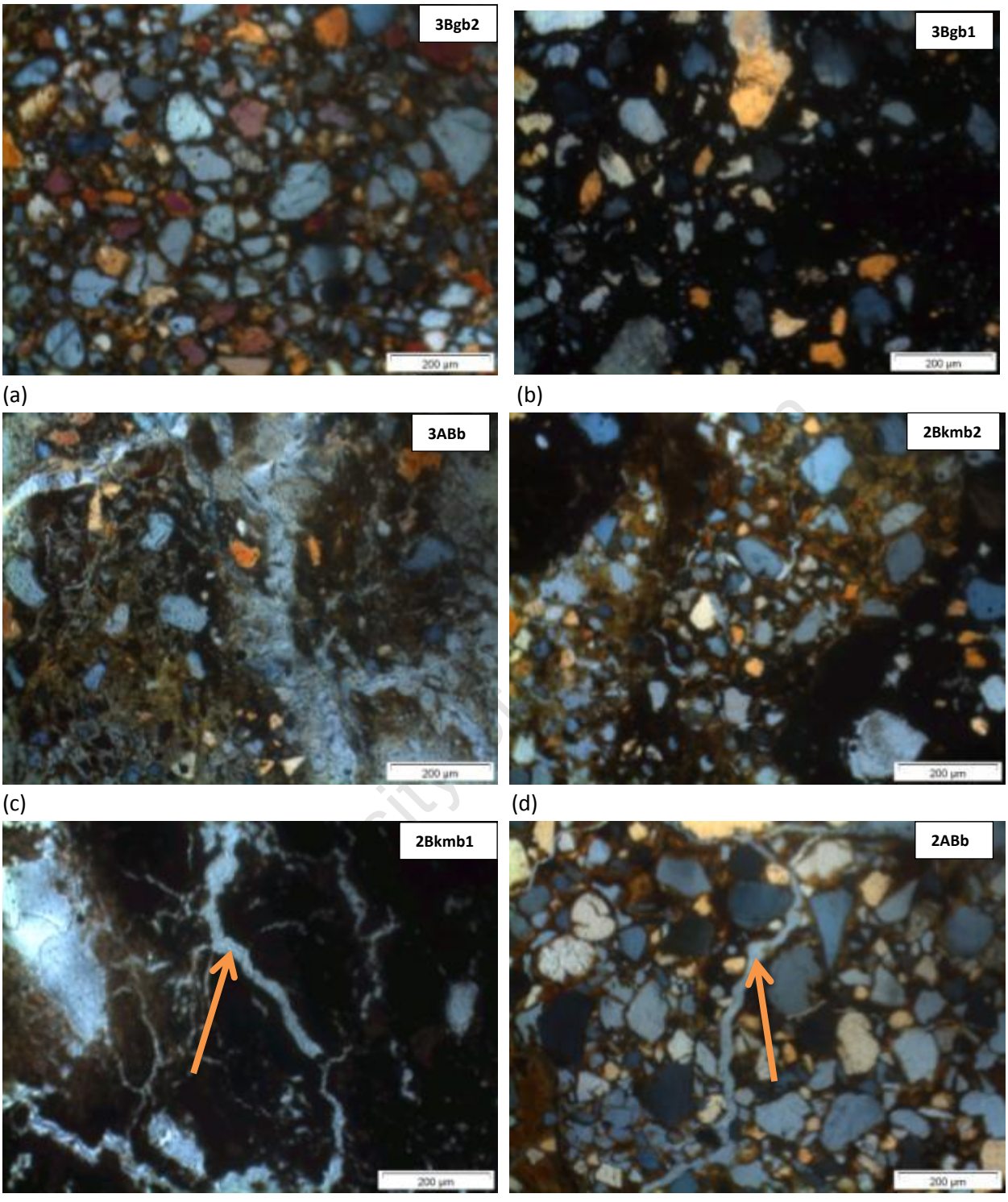

Fig. 3.6. a) Well sorted mineral matrix of quartz and feldspars with clay coatings (3Bgb2, PPL); b) Impregnative redox pedofeatures of iron and manganese oxide hypocoatings and granular matrix with signs of reduction (3Bgb1, PPL); c) Moderately sorted with rounded to sub-rounded particles, with little hierarchy between pedofeatures (calcium carbonate illuvial pedogenic facies, iron oxide coatings and simultaneous faunal activity) (3ABb, PPL); d) Biphase pedogenesis, depletion redox pedofeatures of iron oxide depletion hypocoating and iron oxide quasicoating (2Bkmb2, PPL); e) Impregnative redox pedofeatures of iron oxide hypocoating and granular matrix with no sign of reduction (2Bkmb1, PPL); f) Well sorted granular microstructure with subrounded aggregates and encircling fine grained iron oxide coatings (ABb, PPL). Arrow points to the voids (microsructure) of the paleosols

3.4.4.3.2. Redoximorphic features (redox concentrations)

Evidence for active redoximorphism in the sequences is present only in the Middle Miocene palaeosols (Fig. 3.6a, b). They have abundant reddish, brown-reddish, dark brown to black nodules rich in Fe or Fe-Mn oxide nodules with sharp boundaries. Simple, composite or nucleic nodules are also present. The vertic property of the Pliocene palaeosol (2Bkmb2) as seen from the cracks on the field shows that hydromorphism could have possibly been operational at a time in which lessivage (argilliturbation), high pH and subsequent dessication of the horizon could have lead to a remarkedly cracked horizon. .

3.4.4.3.3. Translocation of fine particles

Based on the features observed from the thin sections there is clear evidence of varying degrees of translocation of fine materials (mostly silt and and clays) across adjacent layers. Texture and drainage conditions are likely the principal factors that influenced the observed faint illuvial features. The higher moisture content of the mid-Miocene palaeosol at the base of the sequences points to a finer particle size distribution which promotes higher water and clay retention in the hygroscopic cappilaries. Since chemical weathering is not advanced in these horizons as seen from earlier study (cf. Chapter 2), we suggest that these finer particles came from sedimentary differentiation of deposited material during Late Miocene high energy marine activities in the area. Translocation of fine materials is also reflected in the redistribution of the chemical components leading to the formation of iron and Mn oxides/ hydroxide nodules within the soil fabrics (Figs. 3.5a-c). Evidence of prolonged translocation of organic to organo-iron coatings is generally rare in the mineral components of the horizons, probably due to erosion. Illuvial features of the Early Pliocene palaeosols indicate a high palaeowatertable and subsequent palaeodrainage.

3.5. Discussion

The palaeosol-sediment-sequences at the West Coast Fossil Park may be classified as a "pedocomplex" – a term that has used in recent literature to describe such alternating sequences of palaeosols and sediments in deltas and alluvial plains (e.g. Srivastava and Parkash, 2002; Feng and Wang, 2005; Fedoroff et al., 2010). Palaeosols and sediments are superimposed upon each other and provide evidence of the inter-penetration of pedofeatures of the overlying into the underlying palaeosols. Roberts et al. (2011) demonstrated that the depositional events of LBW reflect a glacio-eustatic sea level history (Fig 3.7). Apparently, changes in climate and tectonics (i.e. topography) affected the erosional and depositional processes which can be determined from the degree of alteration of the sediments and pedogenesis. A breakdown of sequences of events that lead to the development of the pedocomplex (Fig. 3.7) supports that 3ABb, 3Bgb1 and 3Bgb2 section of the pedocomplex formed during Mid-Miocene sea level rise and deposition (Fig. 3.7B). Marine transgression and deposition of the Early Pliocene is responsible for the deposition of the Varswater Formation on which 2ABb, 2Bkmb1 and 2Bkmb2 palaeosols formed (Fig. 3.7C).

Like modern day soil profiles, the pedogenically modified horizons invariably must have developed during periods of minimum erosional and depositional activities, i.e. periods of relative geomorphic stability. The Mid-Miocene palaeosols are well developed with at least three distinct horizons. This indicates that there was a prolonged period of minimum deposition and erosion before the overlying Late Miocene higher energy marine phosphates were deposited. Similarly, the Early Pliocene palaeosols of the pedocomplex have undergone good development and display evidence of advanced pedogenesis. The 2Bkmb1 and 2Bkmb2 horizons have

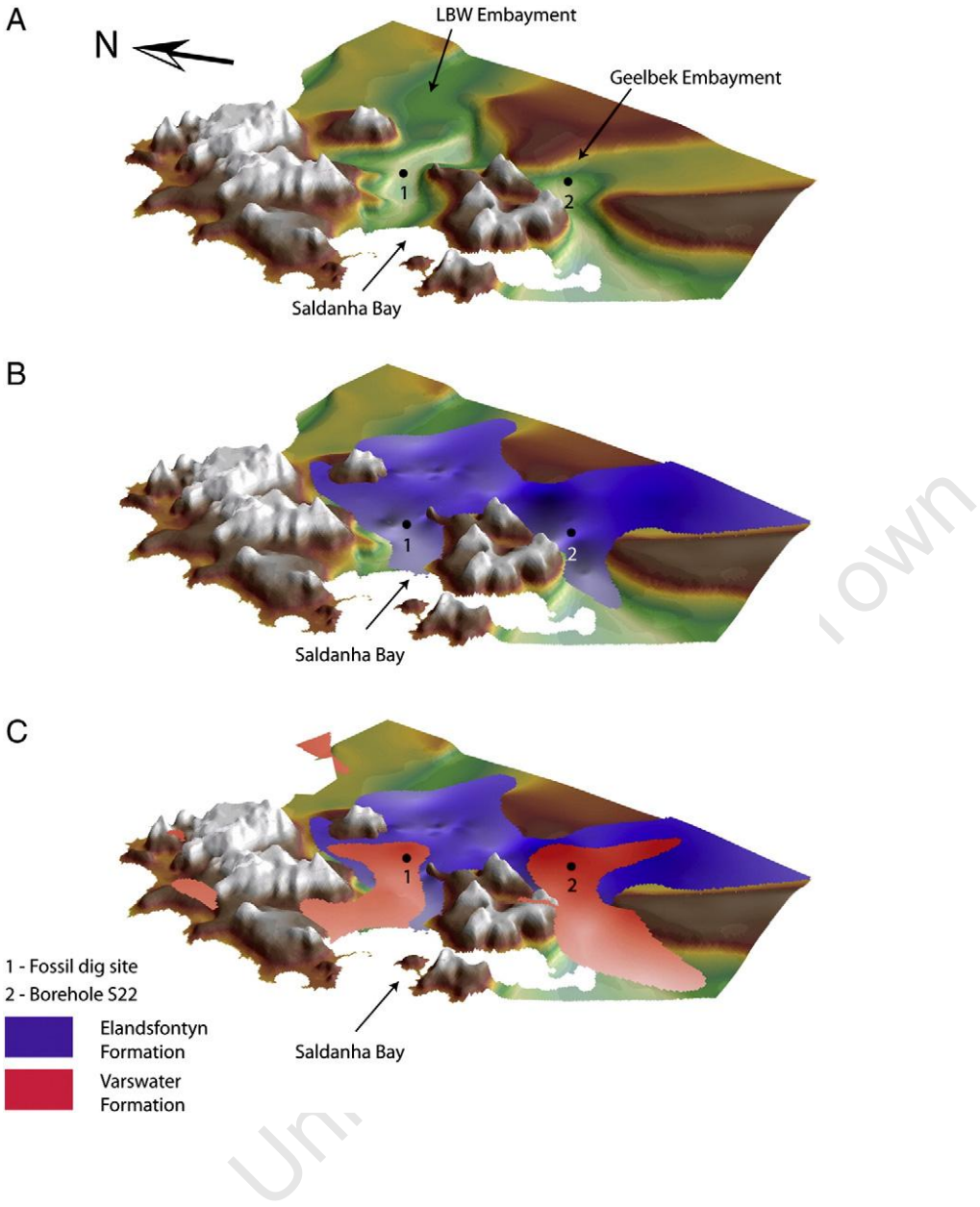

Fig. 3.7. Sequence of major Neogene erosional and depositional events in the LBW environs: A, Fluvial incision during Oligocene lowstands; B, Early–Middle Miocene sea level (base level) rise and deposition of the fluvial Elandsfontyn Formation; C, Major Early Pliocene transgression and deposition of the Varswater Formation (Roberts et al, 2011)

illuvial materials from the '2ABb' horizon and the vertic properties (from field observation) of the horizons possibly attest to hydro- and faunal pedoturbation during the globally recorded Early Pliocene highstand (Haq et al., 1987; Zachos et al., 2001). Invariably, the poor alteration

of the mineral components of the pedosediments interbedding the palaeosols suggests either or both a very slow rate of weathering and a short exposure time for pedogenic processes.

Tubular rhizoliths or rootcastes are prolific in the Plio-Pleistocene sediments. Rhizoliths are faithful indicators of palaeodrainage (Liutkus, 2009) and are formed from low nutrient but cation-rich sand where there is transpiration-driven water flux mass flow to roots in excess of what is required by the plant (Cramer and Hawkins, 2009). Working on a Palaeogene sedimentary environment in the Bighorn basin, USA, Kraus and Hasiotis (2006) reported that calcareous rhizocretions—either calcareous, tubular concretions or micro-accumulations of carbonate within gray rhizotubules—are common in moderately well-drained red palaeosols. The palaeoenvironmental implication of these rhizoliths is standing shallow water table and possibly a palaeosol.

The redness rating of a soil is strongly correlated with hematite content in soils (Torrent et al., 1983). Scarciglia et al. (2006) associated redness of a soil to indicate it's formation under a warm, sub-tropical climate with well-drained conditions. In the present study, the Early Pliocene 2Bkmb1 has the highest redness rating in the pedocomplex and may be an indication of formation of soil under a warm subtropical climate with/ without presence of well-drained geomorphic conditions.

The Middle Miocene palaeosols have mixed clay mineralogy of halloysite, chlorite, muscovite mica, and kaolinite. This can be attributed to clay sources coming from different parent materials during transportation. Chlorite is known for its high water retention properties that promote hydromorphism in soils from ground water (Lee et al., 2003). Even though the kaolinite found here could have been transported, Allen and Hajeck, (1989) opined that most kaolinite in soils originate from weathering of soil parent materials in near surface environments

and are likely to have been subjected to one or more sedimentary cycles subsequent to its original formation. In this sequence, redistribution of calcite throughout the overlying Plio-Pleistocene palaeosols and sediments is evident, possibly due to the high solubility of carbonates in soil environments. Allophane and imogolite peaks are noted here in the Early Pliocene palaeosols. These amorphous and short-range order minerals are of non-tephric origin since there is no history of Late Cenozoic volcanic activity in the region (Roberts et al., 2011). The origin of these minerals can therefore be interpreted as fluvial, i.e. deposited by a stream (Parfitt, 2009). On the mechanism of the formation of imogolite and of allophanes with imogolite-like structures in B horizons. Farmer (1982) explained it only by their deposition from hydroxyaluminium silicate (proto-imogolite) soils, which are known to have the necessary chemical and colloidal stability to act as the agent of transport of Al and, in part, Fe. The presence of sepiolite in the Bk horizon indicates aridity. This fibrous clay mineral is climatically sensitive and highly unstable in the soil environments and is weathered to smectite at mean annual precipitation in excess of 300 mm (Paquet and Millot, 1973).

From the micromorphology observations, it is apparent that both the Mid Miocene and Early Pliocene palaeosols are affected by *in situ* reworking and mass transportation which have undergone certain degrees of pedogenesis. The evidence for this is clearly shown in their massive microstructure with variable abundance of closed polyconcave vughs, often grading to vesicles; and a granular microstructure with rounded to subrounded aggregates that are excremental in origin; and the presence of fragmented pedofeatures. Thin section observations indicate that the major cause of disruption or deformation of the parent sediments is strong seasonal palaeo water saturation. Fine particle size distribution and fluctuating seasonal humid

palaeoenvironments are responsible for the high water retention properties and low permeability of the palaeosols and consequently for the reduction and mobilization of Fe and Mn, resulting in

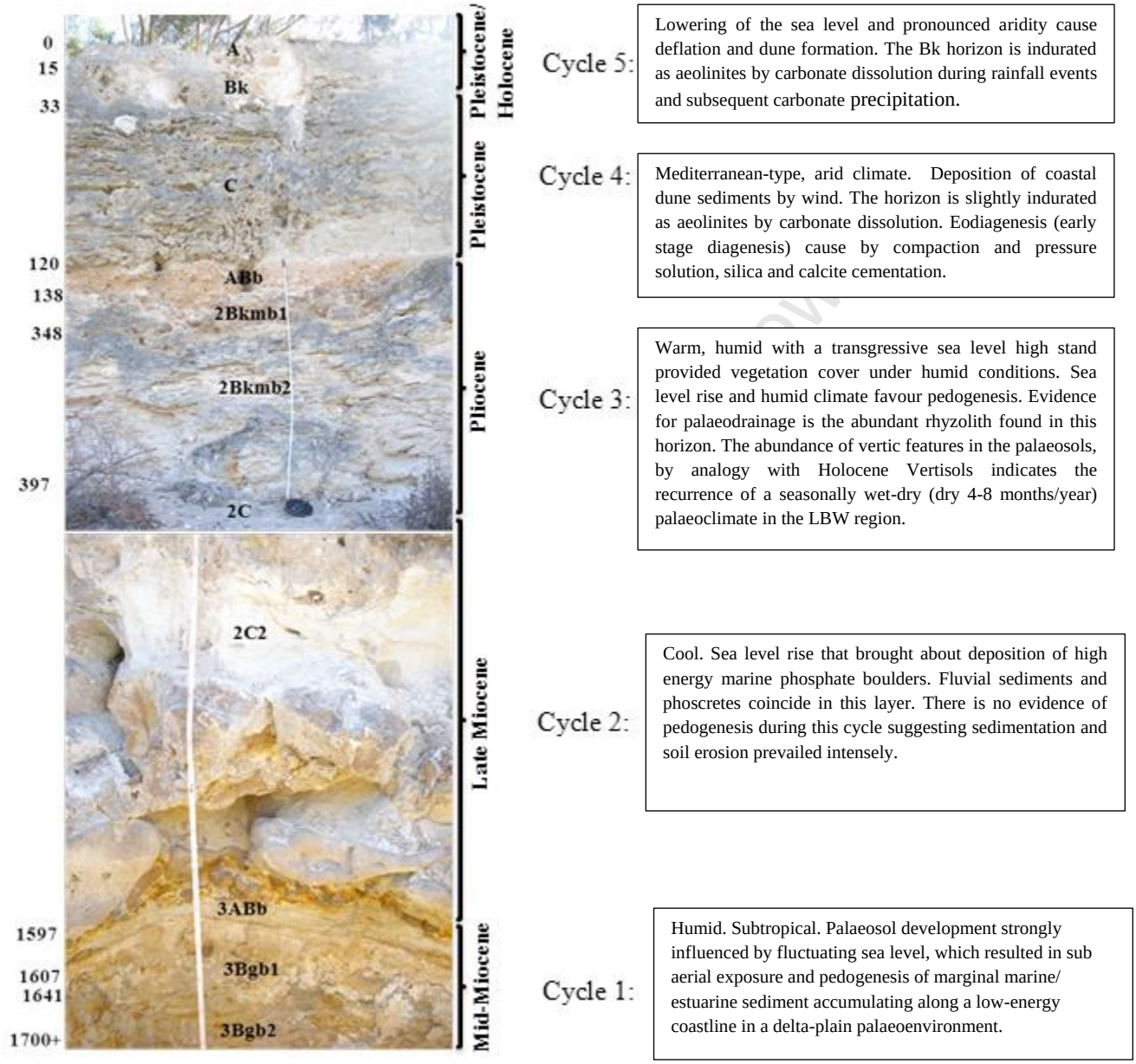

Fig 3.8. Model of climatic cycling of pedogenesis and sedimentation

in the formation of Fe and Mn oxide pedofeatures. In thin sections, the Bkmb1 and Bkmb2 have open porphyric c/f-related distribution, a blocky microstructure and grano-striated b-fabrics. These features are typical of vertic properties in palaeosols (Kovda and Mermut, 2010). The vertic property results from shrink-swell processes, pedoturbation and lateral shearing due to the fluctuating water table in the clayey components. Similar processes may accounts for the micritic/microsparitic calcite coatings and hypocoatings in the voids of the Bkmb2 horizon.

A schematic presentation of the reconstructed palaeoenvironments from this study (Fig. 3.8) gotten from a combination of the above discussed proxies support earlier environmental and climate changes as reported for LBW (Hendy, 1982; Roberts 2011). The Late Cenozoic pedogenesis and sedimentation cycle of LBW depositional environment generally reflect the global trend as reported by Haq et al. (1987) and glacio-eustacy trend of Zachos et al., (2001). The Quaternary sequences depict (semi) aridity in the environment. According to deMenocal (1995) marine records of African climate variability document a shift toward more arid conditions after 2.8 million years ago (Ma), evidently resulting from remote forcing by cold North Atlantic sea-surface temperatures associated with the onset of Northern Hemisphere glacial cycles.

3.6. Conclusions

The mineralogical assemblages of palaeosols and pedosediments from the West Coast Fossil Park of South Africa and pedofeature evidences from their micromorphology indicates repeated rythmic changes of climate during the Late Cenozoic. Warming and increased humidity in the periods of soil formation prompted changes in clay mineralogy, with the formation of

kaolinite and halloysite during the Mid-Miocene and suggest conditions consistent with a subtropical climate. The more advanced weathered nature of this palaeosol is further shown in its higher clay content. While the overlying Plio-Pleistocene palaeosols and sediments contain, none is evident in the underlying palaeosols which may suggest inflow and sedimentation of marine sediments containing shells only after Mid-Miocene in the locality. There presence of non-tephric short-range order minerals- allophane and imogolite - in the Pliocene palaeosols may originate from palaeo stream beds as this locality was subsequently submerged under high palaeowater table during the global Late Pliocene highstand. The 2Bkmb1 horizon is comparatively sandier than 2Bkmb2, hence the minimal amount of iron oxides appear to be sufficient for more intense reddening; the finer the particle sizes, the larger the surface area and the more iron oxide pigment needed to achieve same degree of colouration. In the Late Neogene section, surface erosion and sedimentary fossilization are followed secondary carbonitization and subsequent induration at varying intensities. Both Mid Miocene and Early Pliocene palaeosols are affected by *in situ* reworking and mass transportation. Quartz exoscopy of the Holocene surficial sediments indicate strong aeolian processes. A model of the climatic cycling of pedogenesis and sedimentations in the LBW environment shows five cycles ranging from arid to warm humid palaeoclimate. This study further supports earlier studies which suggest that LBW has been under recurrent sea level oscillations. In times of geomorphodynamic stability, erosion and sedimentation are limited and pedogenesis progressed.

References

Allen, B.L., Hajek, B.F., 1989. Mineral occurrence in soil environments. In: Dixon, J.B., Weed, S.B. (Eds.), Minerals in Soil Environments, (second Ed.). Soil Science Society of America, vol. 1. Soil Science Society of America, Madison, WI, pp. 199 – 264.

Barrón, V., Torrent, J., 1986. Use of the Kubelka-Munk theory to study the influence of iron oxides on soil colour. Journal of Soil Science 37, 499-510.

Birkeland, P. W., 1984. Soils and Geomorphology. Oxford University Press, New York.

Blaise, B., 1989. Clay-mineral assemblages from Late Quaternary deposits on Vancouver Island, southwestern British Columbia, Canada. Quaternary Research 31, 41–56.

Blum, W., 2005. Soils and climate change. Journal of Soils and Sediments 117, 1–7.

Bouyoucos, G.J., 1962. Hydrometer method improved for making particle size analyses of soils. Agron. J. 53, 464–465.

Bullock, P., Fedoroff, N., Jongerius, A., Stoops, G., Tursina, T., 1985. Handbook for soil thin section description. Waine Research. England.

Chase, B. M. and Meadows, M. E., 2007. Late Quaternary dynamics of southern Africa's winter rainfall zone. Earth-Science Reviews 84(3-4), 103-138.

Cramer, M. D., Hawkins, H. J., 2009. A physiological mechanism for the formation of root casts. Palaeogeography, Palaeoclimatology, Palaeoecology 74, 125-133.

deMenocal, P. B., 1995. Plio-Pleistocene African Climate. Science , 270 (5233), 53–59.

Du, J., Hong, H., Zhang, K., 2010. Clay mineralogy and its palaeoclimatic indicative significance of Miocene-Pliocene sediments in Qimugan of Xinjiang. Chinese Journal of Ecology 29, 923–932.

Farmer, V. C., 1982. Significance of the presence of allophane and imogolite in podzol Bs horizons for podzolization mechanisms: A review, Soil Science and Plant Nutrition 28(4), 571-578.

Fedoroff, N., Courty, M., Guo, Z., 2010. Palaeosoils and Relict Soils. In:Stoops, G., Marcelino, V., & Mees, F. (Eds.). (2010). Interpretation of micromorphological features of soils and regoliths. Elsevier Science. 623-654.

Feng, Z. D and Wang, H. B., 2005. Pedostratigraphy and carbonate accumulation in the last interglacial pedocomplex of the Chinese loess plateau. Soil Science Society of America Journal 69, 1094-1101.

Food and Agricultural Organisation (FAO), 2006. Guideline for Soil Description, 4th edition. FAO, Rome, Italy (109 pp.).

Halkett, D., Hart, T., Yates, R., Volman, T.P., Parkington, J.E., Klein, R.J., CruzUribe, K., Avery, G., 2003. First excavation of intact Middle Stone Age layers at Ysterfontein, western Cape province, South Africa: implications for Middle Stone Age ecology. Journal of Archaeological Science 30, 955-971.

Haq, B.U., Hardenbol, J., Vail, P.R., 1987. Chronology of fluctuating sea levels since the Triassic. Science 235, 1156–1167.

Hendey, Q.B., 1982. Langebaanweg: A Record of Past Life. South African Museum, Cape Town. 71 pp.

Hopley, P. J., Latham, A. G., Marshall, J. D., 2006. Palaeoenvironments and palaeodiets of mid-Pliocene micromammals from Makapansgat Limeworks, South Africa: A stable isotope and dental microwear approach, Palaeogeography, Palaeoclimatology, Palaeoecology, 233, (3–4) 235-251.

Hong, H., 2012. Clay Mineralogy of the Zhada Sediments: Evidence for Climatic and Tectonic Evolution Since ~9 Ma in Zhada, Southwestern Tibet. Clays and Clay Minerals 60, 240–253.

Hurst, V. J., 1977. Visual estimated of iron in saprolite. Geol. Soc. Am. Bull., 88:174-176.

Kemp, R.A., 1999. Micromorphology of loess-paleosol sequences: a record of palaeoenvironmental change. Catena 35, 179–196.

Kemp, R., 1998. Role of micromorphology in paleopedological research. Quaternary International 51/52,133–141.

Khormali, F., Kehl, M., 2011. Micromorphology and development of loess-derived surface and buried soils along a precipitation gradient in Northern Iran. Quaternary International 234, (1-2), 109–123.

Kovda, I., Mermut, A. R., 2010. Vertic Feature. In: Stoops, G., Marcelino, V., & Mees, F. (Eds.). (2010). Interpretation of micromorphological features of soils and regoliths. Elsevier Science. 109-127 pp.

Kraus, M. J., Hasiotis, S. T., 2006. Significance of Different Modes of Rhizolith Preservation to Interpreting Paleoenvironmental and Paleohydrologic Settings: Examples from Paleogene Paleosols, Bighorn Basin, Wyoming, U.S.A. Journal of Sedimentary Research 76, 633-646.

Lee, B.D., Sears, S.K., Graham, R.C., Amrhein, C., Vali, H. 2003. Secondary mineral genesis from chlorite and serpentine in an ultramafic soil toposequence. Soil Science Society of America Journal 67, 1309-1317.

Liutkus, C. M., 2009. Using Petrography and Geochemistry to Determine the Origin and Formation Mechanism of Calcitic Plant Molds; Rhizolith or Tufa? Journal of Sedimentary Research, 79, 906-917.

Mack, G., James, W., 1994. Paleoclimate and the global distribution of paleosols. The Journal of Geology 102, 360–366.

Mahaney, W.C., Vortisch, W., 1989. Scanning electron microscopy of feldspar and volcanic glass weathering and neoformation of clay minerals in a quaternary paleosol sequence, Mount Kenya, East Africa. Journal of African Earth Sciences (and the Middle East) 9, 729–737.

Mahaney, W.C., Vortisch, W.B., Spence, J.R., 1988. Pollen study and scanning electron microscopy of Aeolian grains in a compound paleosol in the mutonga drainage, Mount Kenya. Journal of African Earth Sciences (and the Middle East) 7 (7-8), 895–902.

Manegold, A., 2010. First evidence for a nightjar (Caprimulgidae, Aves) in the early Pliocene of Langebaanweg, South Africa. Palaeobiodiversity and Palaeoenvironments 90, 163–168.

May, J.-H., Zech, R., Veit, H., 2008. Late Quaternary paleosol–sediment-sequences and landscape evolution along the Andean piedmont, Bolivian Chaco. Geomorphology 98, 34–54.

Mücher, H., van Steijn, H., Kwaad, F., 2010. Colluvial and mass wasting deposits. In Stoops, G., Marcelino, V., Mees, F. (eds.), Interpretation of Micromorphological Features of Soils and Regoliths. Elsevier, Amsterdam, pp. 37–48.

Munsell Color Co., 2000. Munsell Soil Color Charts. Gretag Macberth, New York

Nedachi, Y., Nedachi, M., Bennett, G., Ohmoto, H., 2005. Geochemistry and mineralogy of the 2.45 Ga Pronto paleosols, Ontario, Canada. Chemical Geology 214 (1-2), 21–44.

Olson, S.L., 1984. A hamerkop from the early Pliocene of South Africa (Aves: Scopidae). Proceedings of the Biological Society Washinghton 97, 736–740.

Panagiotaras, D., Papoulis, D., Kontopoulos, N., Avramidis, P., 2012. Geochemical processes and sedimentological characteristics of Holocene lagoon deposits, Alikes Lagoon, Zakynthos Island, western Greece. Geological Journal 47, 372–387.

Paquet, H., Millot, G., 1973. Geochemical evolution of clay minerals in the weathered products in soils of Mediterranean climate. In: Serratosa, J.M. (Ed.), Proceedings of International Clay Conference 1972. Madrid, pp. 199–206.

Parfitt, R. L., 2009. Allophane and imogolite: role in soil biogeochemical processes. Clay Minerals. 44, 135–155.

Parkinson, Randall, W., Huggins, Eve, Taylor, D., S., 2012. Sedimentary environments, karstification, and the preservation of a late Pleistocene coastal bone bed: pine island conservation area, brevard county, Florida, USA. Florida Scientist 75, 25–40.

Presley, D.R., Hartley, P.E., Ransom, M.D., 2010. Mineralogy and morphological properties of buried polygenetic paleosols formed in late quaternary sediments on upland landscapes of the central plains, USA. Geoderma 154 (3-4), 508–517.

Reeuwijk, LP van (2002) – Editor. Procedures for Soil Analysis. 6th edition. – Technical Paper/International Soil Reference and Information Centre,Wageningen, The Netherlands.

Retallack, G.J., Krinsley, D.H., 1993. Metamorphic alteration of a Precambrian (2.2 Ga) paleosol from South Africa revealed by backscattered electron imaging. Precambrian Research 63(1-2), 27–41.

Roberts, D.L., Matthews, T., Herries, A.I.R., Boulter, C., Scott, L., Dondo, C., Mtembi, P., Browning, C., Smith, R.M.H., Haarhoff, P., Bateman, M.D., 2011. Regional and global context of the Late Cenozoic Langebaanweg (LBW) palaeontological site: West Coast of South Africa. Earth-Science Reviews 106, 191–214

Roberts, D. L., Bateman, M. D., Murray-Wallace, C. V., Carr, A. S., Holmes, P. J. (2009). West coast dune plumes: Climate driven contrasts in dune field morphogenesis along the western and southern South African coasts. Palaeogeography, Palaeoclimatology, Palaeoecology, 271(1-2), 24–38.

Roberts, D.L., 2006. Lithostratigraphy of the Sandveld Group. S. Afr. Committee Stratigr. Lithostratigraphic Ser. 9, 25–26.

Roberts, D.L., Berger, L., 1997. Last interglacial c.117 kyr human footprints, South Africa. South African Journal of Science 93, 349–350.

Roberts, D.L., Matthews, T., Herries, A.I.R., Boulter, C., Scott, L., Dondo, C., Mtembi, P., Browning, C., Smith, R.M.H., Haarhoff, P., Bateman, M.D., 2011. Regional and global context of the Late Cenozoic Langebaanweg (LBW) palaeontological site: West Coast of South Africa. Earth-Science Reviews 106, 191–214.

Rostási, Á., Raucsik, B., Varga, A., 2011. Palaeoenvironmental controls on the clay mineralogy of Carnian sections from the Transdanubian Range (Hungary). Palaeogeography Palaeoclimatology Palaeoecology 300, 101–112.

Roy, M.K., Ahmed, S.S., Bhattacharjee, T.K., Mahmud, S., Moniruzzaman, M., Masidul Haque, M., Saha, S., Ismail Molla, M., Roy, P.C., 2012. Paleoenvironment of deposition of the Dupi Tila Formation, Lalmai Hills, Comilla, Bangladesh. Journal of the Geological Society of India 80, 409–419.

Scarciglia, F., Pulice, I., Robustelli, G., Vecchio, G., 2006. Soil chronosequences on Quaternary marine terraces along the northwestern coast of Calabria (Southern Italy). Quaternary International 156-157, 133–155.

Scott, J R., Stynder, Deano, D., Schubert, W., 2011. Dental microwear texture analysis of fossil carnivores from Langebaanweg, South Africa. American Journal of Physical Anthropology 144, 268–268.

Sheldon, N.D., Tabor, N.J., 2009. Quantitative paleoenvironmental and paleoclimatic reconstruction using paleosols. Earth-Science Reviews 95, 1–52.

Singer, A., 1984. The paleoclimatic interpretation of clay minerals in sediments — a review, Earth-Science Reviews 21,251-293.

Singer, R., Wymer, J., 1968. Archaeological investigations at the Saldanha skull site in South Africa. South African Archaeology Bulletin 23, 63-74.

Srivastava, P., Parkash, B., 2002. Polygenetic soils of the north-central part of the Gangetic Plains: A micromorphologica approach. Catena 46, 43-259.

Srivastava, P., Rajak, M.K., Singh, L.P., 2009. Late Quaternary alluvial fans and paleosols of the Kangra basin, NW Himalaya: Tectonic and paleoclimatic implications. CATENA 76, 135–154.

Stoops, G., Marcelino, V., Mees, F., 2010. Interpretation of micromorphological features of soils and regoliths. Elsevier Science. 707 pp.

Thiry, M., 2000. Palaeoclimatic interpretation of clay minerals in marine deposits: an outlook from the continental origin. Earth-Science Reviews 49 (1-4), 201–221.

Todisco, D., Bhiry, N., 2008. Micromorphology of periglacial sediments from the Tayara site, Qikirtaq Island, Nunavik (Canada). Catena 76, 1–21.

Torrent J., Schwertmann, U., Fechter, H., 1983. Quantitative relationships between soil colour and hematite content. Soil Science 136, 354-358.

Torrent, J., Schwertmann, U., Schulze D. G.,1980. Iron oxide mineralogy of some soils of two river terrace sequences in Spain. Geoderma 23, 191-208.

U.S. Salinity Lab. Staff., 1954. Methods for soil characterization. In: Diagnosis and improvement of saline and alkali soils. Agr. Handbook 60, USDA, Washington, D.C. pp 83-147.

Velde, B., 1995. Origin and mineralogy of clays: clays and the environment. Berlin, Springer-Verlag, 334 pp

Von Suchodoletz, H., Kühn, P., Hambach, U., Dietze, M., Zöller, L., Faust, D., 2009. Loess-like and palaeosol sediments from Lanzarote (Canary Islands/Spain) — Indicators of palaeoenvironmental change during the Late Quaternary. Palaeogeography, Palaeoclimatology, Palaeoecology 278, 71–87.

Watanabe, T., Minoura, K., Nara, F.W., Shichi, K., Horiuchi, K., Kakegawa, T., Kawai, T., 2012. Last glacial to post glacial climate changes in continental Asia inferred from multi-proxy records (geochemistry, clay mineralogy, and paleontology) from Lake Hovsgol, northwest Mongolia. Global and Planetary Change 88-89, 53–63.

Xie, Q., Chen, T., Zhou, H., Xu, X., Xu, H., Ji, J., Lu, H., Balsam, W., 2013. Mechanism of palygorskite formation in the Red Clay Formation on the Chinese Loess Plateau, northwest China. Geoderma 192, 39–49.

Zachos, J., Pagani, M., Sloan, L., Thomas, E., Billups, K., 2001. Trends, rhythms, and aberrations in global climate 65 Ma to Present. Science 292, 686–693.

CHAPTER FOUR

MULTI-PROXY PALAEOSOL EVIDENCE FOR LATE QUATERNARY (MIS 4) ENVIRONMENTAL AND CLIMATE CHANGES ON THE COASTS OF SOUTH AFRICA

Abstract

Palaeosols are common along the coastline of southern South Africa as stacked aeolian dune deposits but have rarely been studied. We selected two late Quaternary palaeosols exposed in a marine cliff-face at Koeberg and coastal barrier dune at Goukamma, South Africa in order to improve our understanding of their pedogenesis and palaeoclimate dynamics. Palaeosol-based proxies explored include: elemental geochemistry by X-ray fluorescence spectrophotometry, $\delta^{13}C$ and $\delta^{18}O$ isotopes, micromorphology and clay mineralogy by x-ray diffraction. Selected physico-chemical soil properties were analyzed by routine laboratory procedures. The palaeosols comprise predominantly loamy sand to sandy clay loam textures, have a high pH (>6.5), and very low electrical conductivity (<0.89 mS cm^{-1}). SiO_2 and CaO are the most abundant of all the elements in the cambic and calcic horizons respectively. The low levels of Al in the parent materials most likely invalidated the applicability of chemical weathering indices (CIA) to assess weathering intensity. In the case of chemical index of weathering (CIW), the age and sedimentary settings of the palaeosols overruled the possibility for K metasomatism and illitization by metamorphism. The indices WI-1 and W1-2 developed by Darmody et al. (2005) appear more consistent with depth. The palaeo MAT computed from palaeosol carbonate oxygen isotope is 14 and 11^{o}C for Koeberg and Goukamma respectively, while the maximum MAP obtained from the cambic horizon (Bw) of the Goukamma coastal barrier is 653 mm yr^{-1}. The layering seen in the thin section of the calcic layer at Goukamma indicates deposition, possibly by sedimentary differentiation across a palaeo-slope. Clastic calcite and muscovite mica are the dominant minerals in these palaeosols indicating impeded chemical weathering. Similar to many other parts of the world, the coastlines of South Africa has experienced environmental and climate oscillations in the Quaternary. We conclude that along the southern South Africa coasts, a palaeosol based approach to palaeoenvironmental and palaeoclimate reconstruction in combination with other proxies such as pollen and marine based isotopes can provide insights into the environmental oscillations of the late Quaternary.

Key words: geochemistry, micromorphology, pedogenesis, Quaternary, stable isotopes, weathering

4.1. Introduction

Aeolian sand dunes and coastal barriers are common along the southern African coastline. Previous studies have documented their distribution, chronology, provenance, and geomorphology (e. g. Marker and Holmes, 2002; Roberts et al., 2008; Bateman et al., 2004; Dunajko and Bateman, 2010). Such coastal formations represent the largest Southern Hemisphere continental deposits of this nature outside Australia (Brooke, 2001; Bateman et al., 2004). Palaeosols (fossil soils) are sporadically exposed at sea cliffs at a depth beneath the coastal aeolian deposits and sand dunes. Given that palaeosols, like modern soils, formed as a result of the complex interplay between parent material, climate, organism, topography and time (Schaetzl and Anderson, 2005), they have the potential to yield an archive of palaeoenvironmental and palaeoclimatic signatures.

In interpreting the palaeoenvironmental implication of palaeosols, several inherent proxies may be applicable. Scientists have applied both qualitative and quantitative methods, such as micromorphology, clay mineralogy, stable isotope geochemistry and chemical weathering indices. In identifying and describing certain pedogenic features and the relative spatial architecture of undisturbed samples, interpretation of micromorphology may reveal the prevailing environmental conditions under which the soils formed (e. g. Todisco and Bhiry, 2008; Tsatskin et al., 2008). In addition to topographic position, soil clay minerals are correlated with climate parameters such as temperature and moisture, the prevailing climate conditions could be ascertained from qualitative mineralogy (e. g. Rostási et al., 2011). It is generally understood that the $\delta^{18}O$ values of pedogenic calcite are directly related to the $\delta^{18}O$ of value of the water from which it formed, indicating the temperature of mineral crystallization (O'Neil et al., 1969) and so the potential of stable isotope geochemistry of pedogenic carbonates as a

palaeotemperature proxy is realizable (e. g. Liutkus et al., 2005; Maher and Thompson, 2012). Chemical weathering indices based on elemental oxide composition ratios are also potential palaeoenvironmental proxies since, by comparing ratios of elements that are likely to remain stable under surface weathering conditions with those of the protolith, provenance and degree of pedogenesis may be established (e. g. Adams et al., 2011; Yang et al., 2004). Combinations of these proxies are particularly useful (e. g. Prochnow et al., 2006; Watanabe et al., 2012).

A number of geochemical climofunctions have also been developed over the years based on a combination of the above mentioned proxies in order to develop more quantitative palaeoenvironmental and palaeoclimate reconstructions. Sheldon and Tabor (2009) provide an extensive review of available geochemical climofunctions. Models of this type have limited applicability but are continuously modified as our understanding of pedogenesis improves (e. g. Cotton and Sheldon, 2012). The overarching principles upon which climofunction models were developed are based on the fact that many geologic and pedogenic processes can readily be quantified *vis-à-vis* geochemical elements abundance and redistribution changes as the soil develops from the protolith (parent material) over a given depth (Sheldon and Tabor, 2009). Soils vary both in space and time and, since most of these models were largely developed with dataset from the temperate climate situations the application to, say, semi-arid or tropical situations is untested thus far. It becomes expedient to validate these models in other regions and climates of the world.

The coastal margins of South Africa have proved responsive to Quaternary climate change ocean current dynamics (e.g. Baxter and Meadows, 1999; Bateman et al., 2004; Roberts et al., 2011). These environments are also of special interest to archaeologists exploring the origin of anatomically and behaviourally modern humans (*Homo s. sapiens*) (Brown et al., 2009). It is

therefore important to combine multiple proxies such as marine, palynological and palaeosol-based evidence to improve our knowledge of the associated palaeoenvironments. Previous AAR/OSL dating of the palaeosols and sand dunes in palaeosols exposed at sea cliffs at Koeberg and a coastal barrier at Goukamma nature reserve confirms that these facies are of late Quaternary in age (Roberts et al., 2008; Bateman et al., 2011). We hypothesize here that the palaeosols would probably have formed under glacial conditions when the seal level must have retrogressed to give way for pedogenesis under an aerobic soil environment and geomorphic stable landscape. In this study, we carried out preliminary investigations on palaeosols exposed in coastal cliffs in two localities in order to characterise their clay mineralogy, micromorphological and geochemical properties with the view of providing a quantitative and qualitative reconstruction of the Koeberg and Goukamma palaeoenvironments and palaeoclimate during the late Quaternary.

4.2. Geographical and geological setting

The exposed surface sampled at Koeberg coastal cliff lies north of Cape Town on the west coast at 33°37′15.0″S and 18°23′27.0″ E, some 200 meters northwest of the Koeberg nuclear power plant, while the palaeosol section at Goukamma is exposed on the seaward side of a dune barrier a few kilometres east of Sedgefield between 34°02′48″ S, 22°50′20″ E and 34°02′53″ S, 22°50′43″ E (Fig. 4.1). Koeberg lies within the so-called winter rainfall zone (Chase and Meadows 2007) and today receives around 372 mm precipitation annually. Goukamma receives precipitation all year round from a combination of both winter cyclonic and tropical easterly flow activity (South African Weather Bureau, 1986). The nature and distribution of rainfall across South Africa reflects the combined influence of 1) the seasonal intensification and northward

expansion of the westerlies and the associated frontal depressions that transport moisture during winter, 2) disturbances in tropical easterly flow, which transport moisture from the Indian Ocean

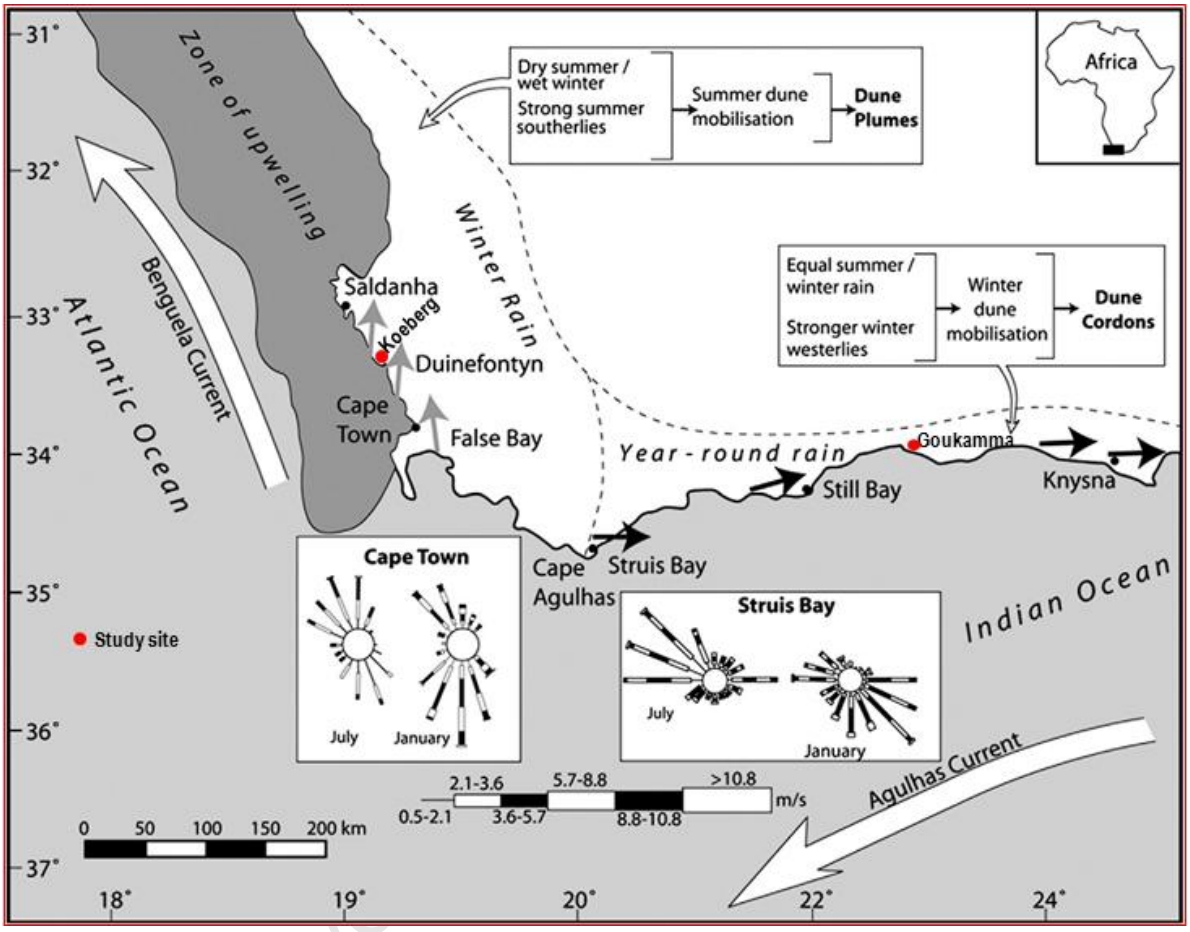

Fig. 4.1. Geographical location of the study sites in relation to major rainfall regions (adapted from Roberts et al., 2009).

during the summer, and 3) a range of disturbances associated with the interaction of temperate and tropical systems, such as ridging anticyclones and southerly meridional flow, which promote the advection of moisture from the Indian Ocean to the southern margin of the subcontinent (Tyson, 1986; Tyson and Preston-Whyte, 2000; Chase et al., (in press). There is evidence for intermittent contraction and expansion of faunal and floral distributions in the region during the Pliocene due to the above discussed climate fluctuations (e.g. Irving, 1998; Carr et al., 2006).

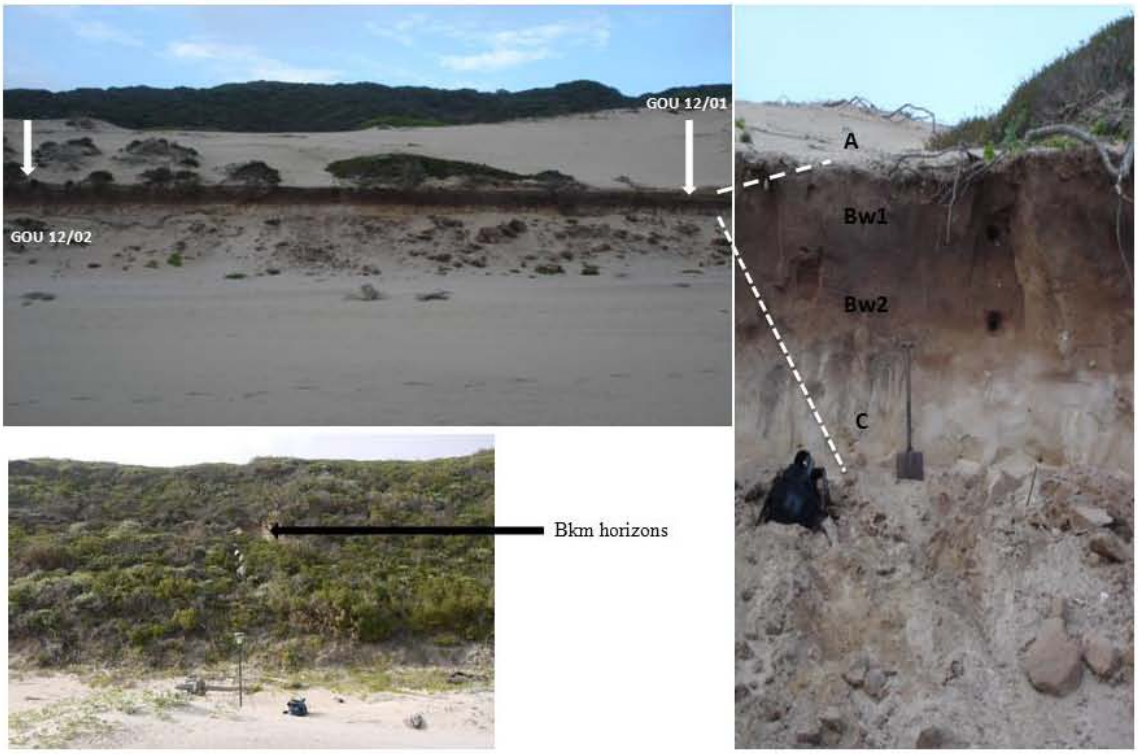

a.

b.

Fig. 4.2. Views of a. Goukamma coastal barrier; b. Koeberg showing the sampled locations. (b is after Roberts et al., 2009).

Both localities are underlain by strata of established aeolian sedimentary patterns which were established in the Late Neogene and persisted into the Quaternary (Roberts et al., 2009, Bateman et al, 2011). Recurring Cenozoic marine transgressions are largely accountable for the bevelled seaward-dipping landforms as seen at Koeberg (Roberts et al., 2008). The Wankoe Formation of the Bredasdorp Group forms a parallel series of dune cordons at Koeberg (Roberts et al., 2008). The seaward coastal barrier at Goukamma (Fig. 4.2) is currently undergoing marine erosion forming high, laterally extensive cliffs exposing the studied palaeosol-sediment sequences. Samples from both sites were underlain and overlain by sedimentary aeolinites with varying degrees of cementation, depending on their carbonate contents (Figs. 4.2 and 4.3).

4.3. Materials and methods

4.3.1. Field sampling

Exposed surfaces at Koeberg and Goukamma were cleaned in such a way as to avoid the possibility of contamination of soil horizons with overlying soils (Figs. 4.2, 4.3). Undisturbed hand samples were then removed from each horizon of the palaeosol sequences, specifically marked and bagged for thin section preparation. Ten representative samples were collected from both sites for further laboratory investigations. In the field, colour was described using the Munsel soil colour system (Munsel Colour Company, 2000), while the general macromorphological properties were described and designated in accordance with the guidelines for soil profile description (FAO, 2006) and Soil Survey Staff (2010).

4.3.2. Laboratory methods

Pretreatment of samples included gently grinding to break up clods and subsequently passing it through a 2mm sieve to separate gravel and roots/rhizomes from the 2mm soil fraction. Particle size distribution was determined by hydrometer method (Bouyoucos, 1962). Both soil pH and electrical conductivity were measured with digital FieldScout SoilStik pH meter and electrical conductivity meter respectively in a 1:2.5 (soil to solution) ratio. Calcium carbonate content of samples was determined by the gravimetric method as described by the U.S. Salinity Laboratory Staff (1954). Total elemental oxides compositions of the samples were determined using XRF spectroscopy (X-Lab 2000) and intensity data were collected using the Philips X40 software. Standard pellets of 5g were made out of homogeneised samples for total elemental oxide compositions by X-ray fluorescence spectrophotometry at the Department of Geological Sciences at the University of Cape Town. Matrix corrections were made on all elements using the de Jongh model in the X40 software. Theoretical alpha coefficients, calculated using the Philips on-line ALPHAS programme, are used in the de Jongh model. For micromorphology description and interpretation, samples from representative horizons at both sites were collected for thin section preparation and subsequent study under a petrographic light microscope. Oriented samples were impregnated with resin under vacuum before sectioning. Slides were viewed with polarizing petrographic microscope (Nikon) and images captured with Olympus ALTRA 20 camera. Clay mineral analyses was conducted using a Phillips PW 3830/40 Generator with a PW 3710 mpd control X-ray diffraction system supported by the Xpert data collector/identify software. Reported values are the average of measurements taken in triplicates. Weight percentages given by XRF were recalculated to molar ratios, following Sheldon et al. (2002), for use in chemical weathering analyses. New Gasbench II method was used to analyze

for stable isotopes ($\delta^{18}O$ and $\delta^{13}C$) composition of carbonate palaeosols at the Archaeometry Research Laboratory, University of Cape Town. Samples were weighed into 12 mL borosilicate tubes and screw top lids containing a septum were used to close the tubes. The tubes were placed in a temperature controlled sampler tray set to 72^{o}C. Using the CTC Analytics A200S autosampler the tubes were flushed with helium to remove the atmospheric air present in them. 5 to 7 drops (according to sample size) of warm (72^{o}C) acid (85% orthophosphoric acid and phosphorus pentoxide, SG of solution = 1.92) were then manually added to each sample tube through the septum using a 1mL syringe. The samples were left to react for three hours before starting the run. Standards used are: Cavendish Marble: crushed marble from Cavendish Square in Claremont. It was calibrated in our lab against a commercial reference gas. Mike Hall of Cambridge University also calibrated this marble. Discrepancy between the two measurements was 0.35 for the oxygen (-8.95 us, -8.60 them) and 0.05 (0.34 us, 0.39 them) for carbon. NBS 18, NBS 19, NBS 20 are from the US Department of Commerce, Bureau of Standards samples. Carrara marble and Lincoln Limestone are commercial product, CarraraZ was calibrated at Cambridge by Mike Hall; the new Carrara marble value has been determined against CarraraZ. Reported values are the average of measurements taken in triplicates.

4.3.3 Weathering indices and geochemical climofunctions

Soil geochemical indices such as Rb/Sr, Sr/Ba, Na/K, CaO/Al_2O_3 have been adjudged to be more sensitive to palaeoclimatic changes than magnetic susceptibility and grain size (Chen et al., 1998, 1999; Yang et al., 2004). To evaluate pedogenic processes quantitatively across the pedocomplex, we used a range of parameters including the following: ΣBases/Al, for hydrolysis; the rationale behind this ratio is that common rock-forming alkaline and alkaline earth metals are lost relative to Al during pedogenesis and thus it is a measure of chemical weathering intensity

(e.g. Retallack, 1999; Sayyed and Hundekari, 2006). The ratio of Al/Si is a measure of clayeyness: the higher the value of this ratio, the more weathered or clayey the soil is because Al accumulates as clay minerals form in soils by hydrolysis. The Ti/Al ratio measures provenance by acidification process and rests on the fact that Ti is most readily lost by physical weathering, whereas Al is lost preferentially by chemical weathering (see Nesbitt and Young 1984, Sawyer, 1986). The K+Na/Al ratio is a proxy for salinization, while Ba/Sr is used to infer trace element leaching/hydrolysis because alkali elements that accumulate as soluble salts are not removed (Sheldon and Tabor, 2009). The Chemical Index of Alteration (CIA) as proposed by Nesbit and Young (1982), the Chemical Index of Weathering (CIW or CIA-K), which is a modified version of CIA takes care of post-burial addition of K by metasomatism and/ or illitization of clay minerals soils by removing K in the equation, and two weathering indices (WI-1 and WI-2) employed by Darmody et al. (2005) were used quantitatively to evaluate the intensity of chemical weathering in the soils and pedosediments. WI-1 and WI-2 were developed from dataset of modern soils with granitic parent materials, although their wider application to soils developed on other parent materials is yet to be demonstrated (Sheldon and Tabor, 2009).

Palaeoprecipitation was calculated using the model of Sheldon et al. (2002), who developed this using Marbut's (1935) soil database and modern measurements of MAP. From the model,

MAP = -259Ln (total exchangeable bases/Al) + 759 …Equation 1

Sheldon et al. (2002) reported this is applied most appropriately to Bw or Bt horizons since the dataset used to derive the model were obtained from such horizons.

Also palaeotemperature was calculated from the Cerling and Quade (1993) model:

$\delta^{18}O_{cc}$ (‰, PDB) = 0.49T−12.65 …Equation 2

This is derived from the empirical relationship measured between pedogenic calcite and $\delta^{18}O$ values ($\delta^{18}O_{cc}$) and measured mean annual surface air temperature from soils in interior continental sites.

4.4. Results

4.4.1. Macromorphological and selected physico-chemical properties

In an independent study, Roberts et al., 2009 reported that the Koeberg carbonate palaeosol (Bkm horizon) (their D1 palaeosol) formed during the MIS 4/ Holocene transition. On the other hand, based on stratigraphic chronology, Goukamma palaeosols (Bw horizons) formed post ~79 ka and the overlying sediments during the mid-late Holocene (6.9 to 3.3 ka) (Bateman et al., 2011). At Koeberg, a calcrete palaeosol profile was sampled at a single locality (Fig. 3) location due to the difficulty of access, while at Goukamma; the overlying A horizon was sampled in one place while the B horizons (which represent the palaeosols) were sampled at three different points (Fig. 2). There are many similarities in the macromorphological properties of the two late Quaternary palaeosols, while there are differences in the depth of pedogenesis and colour (Table 4.1). At each site, the surface materials (A-horizons) have higher hues, thereby making them lighter in colour than the underlying horizons. Both palaeosol sites are characterised by single grained sediment structure at the surface horizons, while the underlying B horizons have moderate to strong subangular blocky structure. Where present, the roots are few (subsurface horizons) to common (A horizons) in abundance. At Koeberg, both the sediments and the palaeosol horizons reacted positively with diluted HCl indicating the presence of carbonates, while the cambic (Bw) horizons at Goukamma did not. Molluscan shells both whole and fragmented are prominent in the surface horizons at both sites. Percentage clay content of the

horizons increases with depth at both locations, with sandy texture being typical of the surface horizons and loamy texture for the subsurface horizons (Table 4.2). Generally, the soil pH is high (alkaline) with a pH (H_2O) ranging from 6.2 to 9.7 while electrical conductivity (EC) is very low, ranging between just 0.08 to 0.88 mS cm^{-1}. The Bkm horizons have $CaCO_3$ equivalent

Table 4.1. Profile description of the macromorphological properties of the late Quaternary palaeosols from Koeberg and Goukamma

Horizon	Height (cm)	Facies	Colour[1] (moist)	>2mm fragments	Structure[2]	Root	Boundary[3]	Consistency (moist)	Field texture	Cementation	React HCl	other features
Profile KGB 12/01												
A	27	aeolian	7.5YR 6/2	absent	1gr	common	as	loose	sand	none	occasional	marine shells
Bkm	36	calcrete	7.5Y 8/1	absent	3sbk	few	cw	firm	loamy sand	carbonate	strong	rhizoliths
Profile GOU 12/01												
A	13	aeolian	7.5YR 6/2	absent	1gr	common	cs	loose	sand	none	occasional	marine shells
Bw1	52	marine	7.5YR 2.5/2	absent	2mgr	common	cw	friable	loam	none	none	-
Bw2	67	marine	7.5YR 3/4	occasional	2mgr	few	cw	friable	loam	none	none	-
C	138+	silcrete	2.5Y 8/1	occasional	blk	none	-	firm	sand	none	none	-
Profile GOU 12/02												
Bw1	34	marine	7.5YR 2.5/2	absent	2mgr	common	cw	friable	loam	none	none	-
Bw2	51	marine	10YR 3/2	occasional	2mgr	few	cw	friable	loam	none	none	-
Profile GOU 12/03												
Bkm1	15	calcrete	5Y 7/1	absent	3sbk	few	b	firm	sandy loam	carbonate	strong	-
Bkm2	48	calcrete	2.5Y 5/4	absent	3sbk	few	b	firm	sandy loam	carbonate	strong	-

[1]nd – not determined

[2] 1– weak; 2 – medium; 3 – strong; gr – granular; sbk – subangular blocky; abk – angular blocky, blk – blocky; Gr. S – gravelly sand

[3] a – abrupt; c – clear; s – smooth; g – gradual; w – wavy; b – discontinuous

Table 4.2. Selected physico-chemical properties of late Quaternary palaeosols from Koeberg and Goukamma

Horizon	Colour (moist)	colour notation	Sand	Silt (IUSS)	Clay	Texture‡	pH (H_2O)	EC mS cm^{-1}	$CaCO_3$* g kg^{-1}
Profile KGB 12/01(33°37'15.0"S, 18°23'27.0" E)									
A	7.5YR 6/2	pinkish gray	898	27	75	Sa	8.1	0.08	191
Bkm	2.5Y 5/4	light olive brown	638	137	225	SaClLo	8.9	0.11	537
Profile GOU 12/01(34°02'47.8"S, 22°50'20.2" E)									
A	7.5YR 6/2	pinkish gray	789	121	91	LoSa	7.3	0.17	nd
Bw1	7.5YR 2.5/2	very dark brown	588	163	250	SaClLo	6.7	0.52	nd
Bw2	7.5YR 3/4	dark brown	450	200	350	ClLo	6.8	0.88	nd
C	2.5Y 8/2	pale yellow	925	53	22	Sa	6.5	0.49	nd
Profile GOU 12/02(34°02'49.2"S, 22°50'29.5" E)									
Bw1	7.5YR 2.5/2	very dark brown	613	100	288	SaClLo	6.8	0.79	nd
Bw2	10YR 3/2	very dark grayish brown	488	188	375	ClLo	6.8	0.53	nd
Profile GOU 12/03 (34°02'53.0"S, 22°50'42.6" E)									
Bkm1	5Y 7/1	light gray	679	41	280	SaClLo	9.2	0.17	512
Bkm2	2.5Y 5/4	light olive brown	479	181	340	SaClLo	8.9	0.48	443

‡Sa – sand; ClLo – clay loam; LoSa – loamy sand; SaClLo – sandy clay loam

*nd – not determined

contents ranging from 443 to 537 g kg^{-1} while there is no indication of carbonate in the Bw horizons.

4.4.2. Geochemistry

Silica is the dominant elemental oxide in all horizons (Table 4.3) with the exception of Bkm1 at Goukamma, which is dominated by CaO. It ranged in values from 54.91 to 94.56%. In order of abundance, SiO_2 > CaO > Al_2O_3 > Fe_2O_3 occur in all the A and B horizons. Where present, MnO, Cr_2O_3 and NiO are found in only trace quantities. The carbonate palaeosols (Bkm) horizons at both sites had the highest loss on ignition (LOI). Zirconium (Zr), strontium (Sr) and sulphur (S) are the most abundant minor elements in the palaeosols and sediments (Table 4.4). Molybdenum (Mo), cobalt, nickel, scandium, copper and uranium are the least abundant minor elements. At both locations, lead (Pb) is the most abundant heavy metal in the palaeosols and sediments, with values ranging from 3.1 to 8.5 ppm.

4.4.3. Weathering indices and geochemical climofunctions

Quantitative evaluation of the three pedogenic processes (hydrolysis, acidification and salinization) supports the observed qualitative properties (Table 4.5). Although generally low at both locations Al/Si ratios, a measure of clayeyness, were indeed observed to be slightly higher in horizons with corresponding relatively higher clay contents. Ascertaining the provenance of pedogenesis from either physical or chemical weathering by acidification (which is pH-dependent) is very difficult as there proved to be only minor variations (<0.1) in Ti/Al ratios across the profiles. The four weathering indices used in the quantification weathering process (CIA and CIW also referred to as CIA-K) and weathering intensity (WI-1 and WI-2), yield

Table 4.3. Major oxides composition of late Quaternary palaeosols from Koeberg and Goukamma

Horizon	SiO_2	TiO_2	Al_2O_3	Fe_2O_3	MnO	MgO	CaO	Na_2O	K_2O	P_2O_5	SO_3	Cr_2O_3	NiO	LOI
	----------(%)----------													
Profile KGB 12/01														
A	69.26	0.07	0.58	0.16	0.01	0.15	15.24	0.15	0.21	0.14	0.12	0.00	0.00	13.90
Bkm	18.11	0.02	0.27	0.05	0.00	1.03	35.22	0.09	0.03	0.28	0.52	0.00	0.00	43.31
Profile GOU 12/01														
A	90.26	0.07	0.58	0.16	0.01	0.15	4.24	0.15	0.21	0.14	0.12	0.00	0.00	2.85
Bw1	86.27	0.43	3.19	1.78	0.03	0.27	2.27	0.35	0.60	0.09	0.02	0.00	0.00	3.52
Bw2	70.53	0.33	1.97	1.23	0.02	0.27	12.35	0.23	0.31	0.10	0.02	0.01	0.00	11.27
C	94.56	0.33	2.78	0.64	0.01	0.00	0.10	0.04	0.09	0.06	0.00	0.00	0.00	1.43
Profile GOU 12/02														
Bw1	74.02	0.35	2.27	1.41	0.02	0.36	10.35	0.30	0.48	0.13	0.04	0.04	0.00	9.38
Bw2	70.45	0.24	2.38	1.25	0.01	0.30	11.85	0.25	0.46	0.09	0.03	0.00	0.00	11.20
Profile GOU 12/03														
Bkm1	25.68	0.04	0.55	0.36	0.01	0.50	37.04	0.10	0.05	0.04	0.17	0.00	0.01	33.03
Bkm2	54.91	0.09	1.10	0.67	0.01	0.28	21.61	0.18	0.16	0.07	0.05	0.00	0.00	19.21

LOI – Loss on Ignition in a furnace at 950 ^oC (= chemically bound H_2O and CO_2)
Fe_2O_3 is expressed as total Fe

Table 4.4. Minor Element composition of late Quaternary palaeosols from Koeberg and Goukamma

	Mo	Nb	Zr	Y	Sr	Rb	U	Th	Pb	Zn	Cu	Ni	Co	Mn	Cr	V	Sc	Ba	S
	---------- (ppm) ----------																		
Profile KGB 12/01																			
A	<0.4	5.2	167.3	11.0	647.9	7.3	<0.9	<0.9	3.1	4.8	<1.4	<1.8	<2.2	32.7	17.2	10.5	<2.1	96.9	1257.6
Bkm	<0.4	1.8	58.2	4.7	576.9	3.9	<0.9	<0.9	3.6	4.8	3.5	<1.8	<2.2	6.8	10.7	<2.4	<2.1	94.0	669.4
Profile GOU 12/01																			
A	<0.4	5.4	244.9	13.5	433.1	6.0	<0.9	<0.9	2.9	4.1	<1.4	<1.8	<2.2	55.7	16.9	13.2	<2.1	85.3	768.5
Bw1	<0.4	11.7	580.6	24.5	102.2	30.9	<0.9	4.1	8.5	13.3	<1.4	3.7	<2.2	256.1	57.6	36.6	5.4	148.7	121.8
Bw2	<0.4	9.9	523.4	18.7	125.1	17.8	<0.9	2.8	7.0	10.4	<1.4	<1.8	<2.2	101.4	38.5	25.8	<2.1	123.6	232.3
C	<0.4	5.6	314.8	19.0	7.6	5.2	<0.9	5.5	6.2	4.4	<1.4	<1.8	<2.2	44.3	20.5	26.2	4.2	89.8	101.3
Profile GOU 12/02																			
Bw1	<0.4	11.9	534.9	18.7	323.8	21.9	<0.9	1.9	6.5	12.7	<1.4	4.3	<2.2	156.6	427.0	24.2	<2.1	123.4	310.7
Bw2	<0.4	6.1	329.6	18.4	192.3	24.2	<0.9	1.8	6.5	11.9	<1.4	<1.8	<2.2	94.6	45.5	26.4	<2.1	132.8	274.2
Profile GOU 12/03																			
Bkm1	<0.4	<0.3	71.1	12.4	337.6	6.3	<0.9	<0.9	3.7	5.8	<1.4	<1.8	<2.2	29.2	22.0	9.1	<2.1	130.0	1078.1
Bkm2	<0.4	1.5	126.9	11.3	267.5	11.8	<0.9	<0.9	4.9	7.3	<1.4	<1.8	<2.2	56.6	21.9	16.1	<2.1	112.0	536.2

Table 4.5. Geochemical weathering indices and climofunctions results of the late Quaternary palaeosols from Koeberg and Goukamma

Horizon	Al/Si	Ti/Al	K+Na/Al	CIA	CIW	WI-1	WI-2	$\delta^{13}C$	$\delta^{18}O$	$\delta^{18}H_2O$	MAT (^oC)	MAP (mm yr^{-1})
Profile KGB 12/01												
A	0.01	0.14	0.93	2.67	2.72	283.97	94.16	-	-	-	-	-
Bkm	0.02	0.10	0.63	0.56	0.56	720.35	177.58	-1.43	-5.97	-7.06	14[a]	-
Profile GOU 12/01												
A	0.01	0.14	0.93	8.47	8.90	293.91	98.12	-	-	-	-	-
Bw1	0.04	0.15	0.45	41.51	47.29	27.84	13.13	-	-	-	-	653[b]
Bw2	0.03	0.19	0.41	10.12	10.38	39.63	19.94	-	-	-	-	188[b]
C	0.03	0.13	0.07	89.33	93.57	68.60	20.91	-	-	-	-	-
Profile GOU 12/02												
Bw1	0.04	0.17	0.52	13.03	13.62	35.14	17.53	-	-	-	-	260[b]
Bw2	0.04	0.12	0.45	12.23	12.70	40.73	18.19	-	-	-	-	243[b]
Profile GOU 12/03												
Bkm1	0.01	0.09	0.40	1.07	1.08	140.03	68.29	-2.89	-7.57	-8.59	10[a]	-
Bkm2	0.01	0.10	0.46	3.57	3.60	78.14	37.13	-2.44	-6.83	-7.88	12[a]	-

[a]: Cerling and Quade, 1993; [b]: Sheldon et al., 2002

inconsistent results down the profile sections. The chemical index of alteration (CIA) values were remarkably low (<15 on the average) and similarly the chemical index of weathering (CIW) values. The results of $\delta^{18}O$ values of the carbonate palaeosols are used to calculate the palaeotemperature indicate an average of 22 and 14 ^{o}C and then 18 and 11^{o}C for Koeberg and Goukamma respectively (Table 4.5). Palaeosols from Koeberg did not satisfy the conditions for MAP calculation using any of the evaluated climofunctions. However, the "Bw" horizons at Goukamma met the requirements for the use of Sheldon et al. (2002) model and the maximum MAP value obtained is 653 mm yr^{-1}.

4.4.4. Micromorphology

The thin sections are described on the basis of groundmass, void, microstructure and pedofeatures (Table 4.6) while the photomicrographs of thin sections and scanning electron microscopy is presented in Fig. 4.3. The overlying sediments in the A horizons were predominantly single grained in structure and as such could not be sampled for thin section preparation. All the palaeosols are dominated by coarse components, usually > 69% of the total thin section area (t.t.s.a), with the fine components ranging from 15 – 30% of the t.t.s.a. and voids taking up 5%. While the Bkm palaeosols showed impregnative, depletion and crystalline pedofeatures (Table 4.6, Fig. 4.4a, c), the Bw palaeosols has a characteristic textural pedofeatures (Fig. 4.4e, f). Scanning electron microscopy of the clay sized carbonate palaeosol at Koeberg shows the white fluffy traces of calcite mineral (Fig. 4.4b), while at Goukamma, small traces of sepiolite fibres coating an irregular void wall composed of calcite (Fig. 4.4d) is conspicuous.

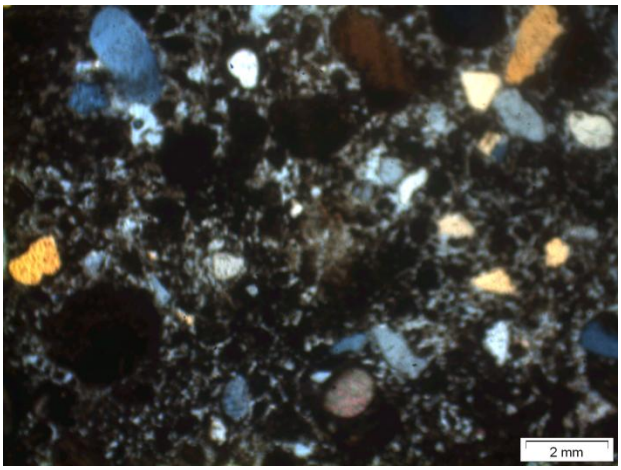

A. Koeberg Bkm horizon

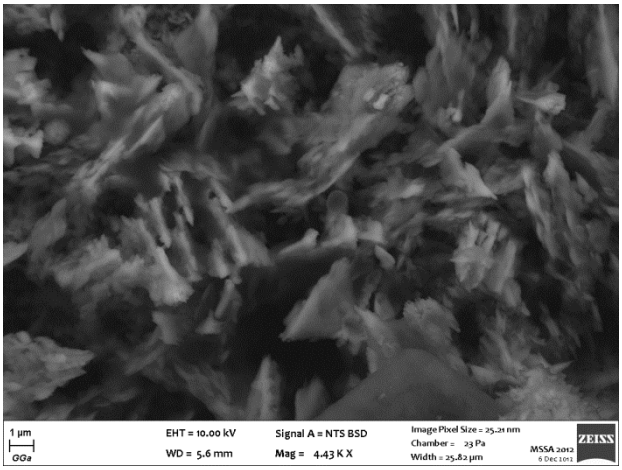

B. SEM of Fig. A.

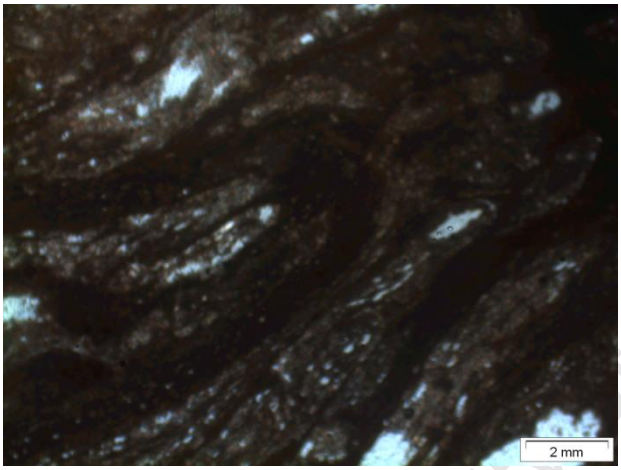

C. Goukamma "Bkm1"

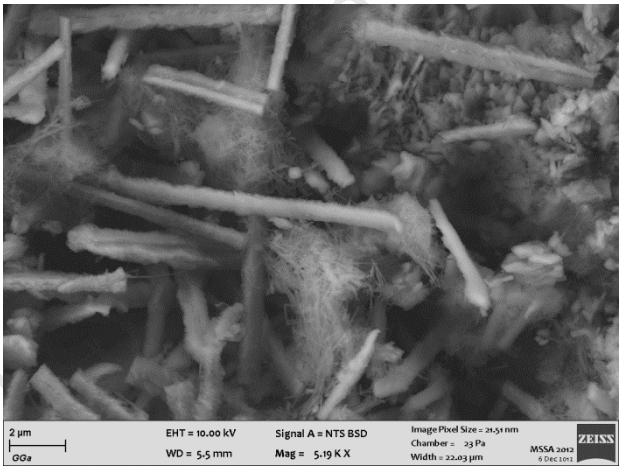

D. SEM of Fig. C

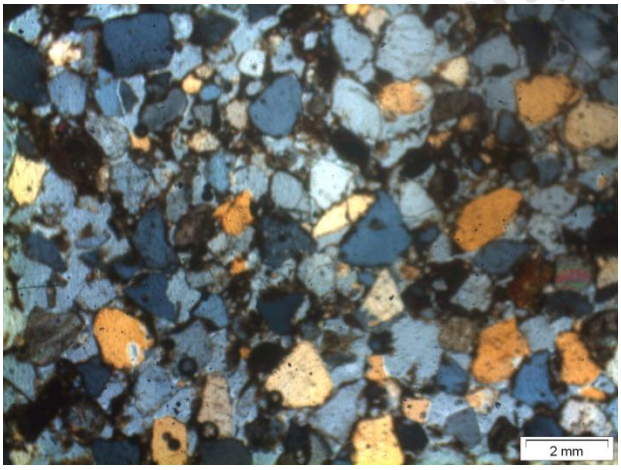

E. Bw1

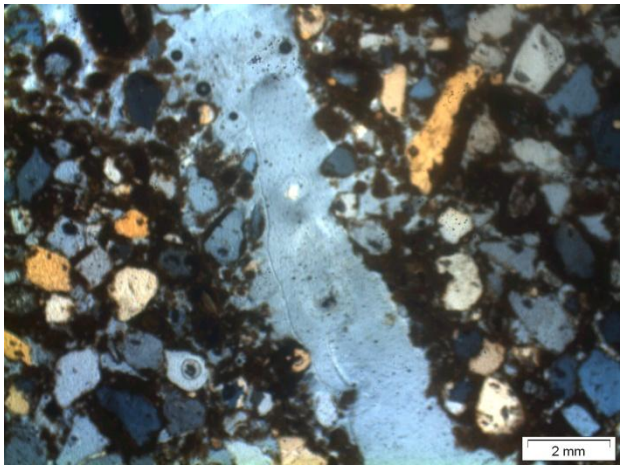

F. Bw2

Fig. 4.3. Photomicrographs of selected palaeosols and pedosediments. (A) Carbonate coatings and Fe/Mn oxide coating pedofeatures around sand grains (cross polar). (B) High resolution electron scan of the palaeosols showing flakes of muscovite on carbonates. (C) Evidence of layering in the "Bkm" horizon suggesting water could be responsible for the accumulation of fine materials. (D) High resolution SEM "C" palaeosol showing a loose mat of interwoven calcite fibres on an irregular void wall (E) Compound packing voids of the "Bw1" showing the dominance of sandy textural pedofeatures. (F) Chambers voids of the "Bw2" palaeosol showing infilling of carbonates in the void.

Table 4.6. Summary of the micromorphological description of the late Quaternary palaeosols from Koeberg and Goukamma

Horizon	Groundmass	Void and microstructure	Pedofeatures
Profile KGB 12/01			
2Bkmb	**C/F distribution**: porphyric; **C/F limit**: clay/sand; **coarse component**: 70% of the t.t.s.a., silt and fine to coarse sand, smooth and spheroidal fracture, shape subrounded to subangular high variability within random fabric associated with shape, elongated grains are randomly distributed; **fine component**: fabric: crystallitic b-fabric; 25% t.t.s.a.,	5% of the t.t.s.a.; channel, dominant voids are chambers; **microstructure:** massive	impregnative pedofeatures associated with illuviation and impure clay with hypo coatings around peds; iron oxide coatings on walls of peds, plant residues
Profile GOU 12/01			
Bw1	**C/F distribution**: porphyric; **C/F limit**: clay/sand; **coarse component**: 90% of the t.t.s.a., silt and fine to coarse sand, smooth and spheroidal fracture, shape rounded to subrounded variability within random fabric associated with shape, elongated grains are randomly distributed;	5-10% of the t.t.s.a.; few simple to frequent compound packing voids; **microstructure**: single grain structure	Textural sandy pedofeatures associated with aeolian transportation; plant . residues
Bw2	**C/F distribution**: porphyric; **C/F limit**: clay/sand; **coarse component**: 70% of the t.t.s.a., silt and fine to coarse sand, smooth and spheroidal fracture, shape subrounded to subangular high variability within random fabric associated with shape, elongated grains are randomly distributed; **fine component**: fabric: 30% t.t.s.a..	5% of the t.t.s.a.; channel, dominant voids are chambers; **microstructure**: massive	Textural pedofeatures associated with calcium carbonate coatings around peds; calcium carbonate coating on walls of peds, plant residues
Bkmb1	**C/F distribution**: enaulic; **C/F limit**: clay/sand; **coarse component**: 80% of the t.t.s.a., silt and fine to coarse sand, smooth and spheroidal fracture, shape subrounded to subangular high variability within random fabric associated with shape; **fine component**: fabric: crystallitic b-fabric, 15% t.t.s.a.	5% of the t.t.s.a.; few simple packing voids; microstructure: single to bridged grain	Depletion and crystalline pedofeatures associated with iron oxide eluviation and translocation within the soil fabric; iron oxide quasi- and hypo-coatings on walls of peds; organic residues

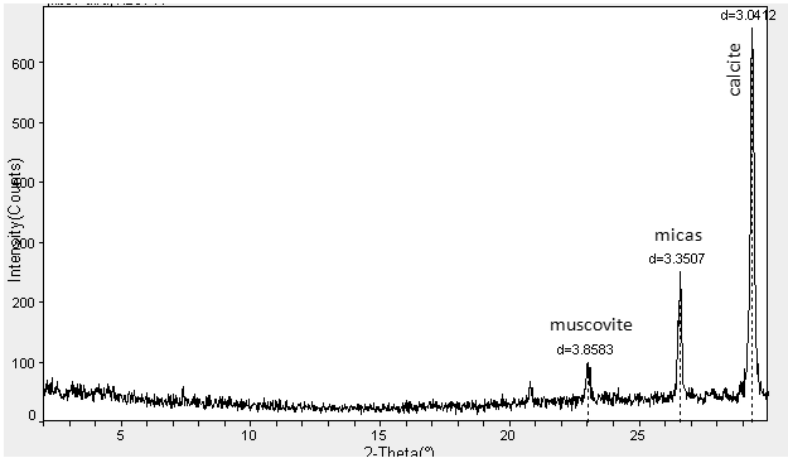

Koeberg A horizon

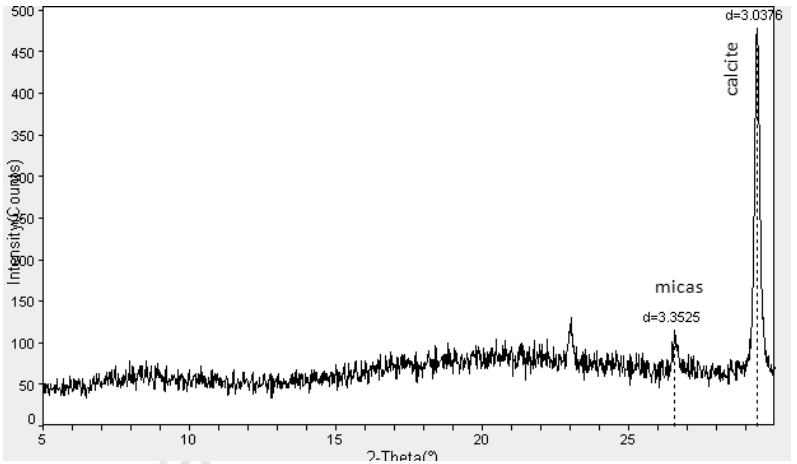

Koeberg Bkm palaeosol

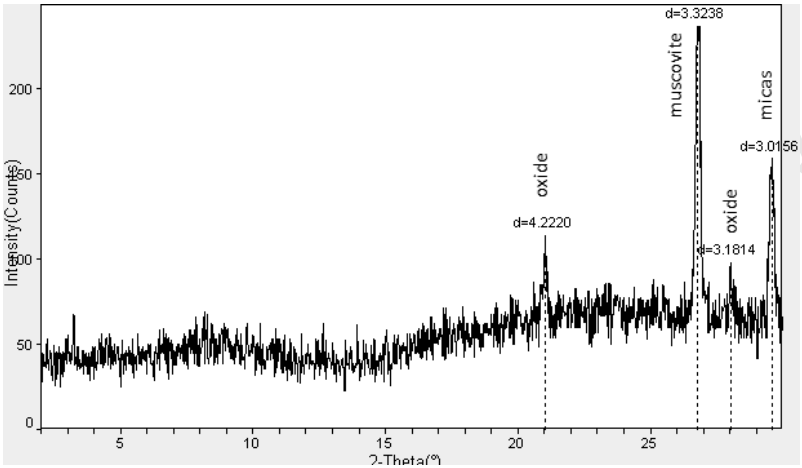

Goukamma Bw1 horizon

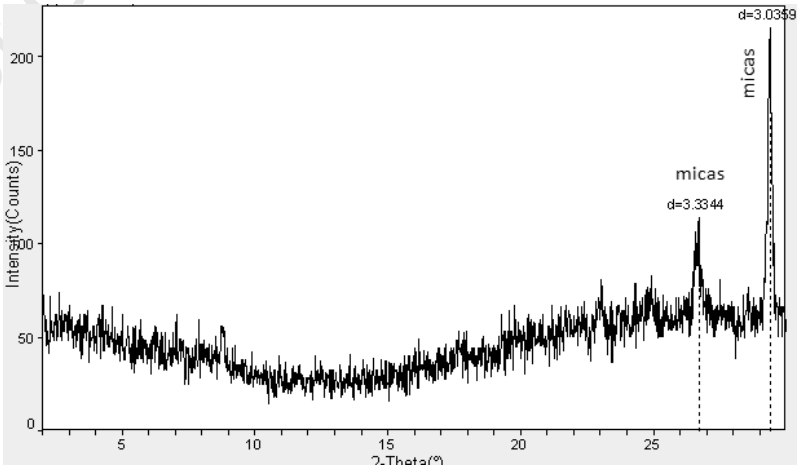

Goukamma Bw2 horison

Fig. 4.4. Clay mineralogy PXRD plots of selected samples from Koeberg and Goukamma palaeosol sequences.

4.4.5. Clay mineralogy

Qualitatively, the palaeosols had similar mineral composition: micas and calcite (Fig. 4.5), with the dominant form of micas being muscovite. Traces of oxide minerals were additionally detected in the "Bw" palaeosols. Flakes of muscovite are visibly evident from the SEM of the Bkm palaeosols (Fig. 4.4b, d). And calcite infers on them the characteristic fluffy and tangential needle shaped fibrous nature.

4.5. Discussion

Inferences from all the palaeosol based proxies support moderate pedogenesis at Koeberg most likely prompted by low precipitation, and a moderately developed profile with cambic horizons at Goukamma. For soil development to progress there should suitable environmental and climatic conditions and either the rate of accumulation of new materials should be less than the removal rate (i.e. minimal erosion) or the rate of accumulation of new material not excessive (Minasny et al., 2008). Marine mollusca found on the surface horizons originate from the Atlantic and Indian Oceans that are adjacent to Koeberg and Goukamma sites respectively. The palaeosols therefore react with dilute acid, confirming the presence of carbonates, which has its origin from marine lives. These marine shells would in time be dissolved and leached through the subsurface horizons and provide a cementing property to the carbonate palaeosols. The low quantity of roots at the surface horizons arguably could be due to continuous sedimentation and erosion of coastal and aeolian materials, which makes the soilscape unstable for the growth of plant species.

It is also self-evident that the coarse nature of the parent material (marine sand) played a fundamental role in the palaeosol texture. The dominantly sandy to loamy texture and friable to

loose consistency of the palaeosols would usually promote excessive water drainage through soil profiles (Bosch et al., 2012) thereby enhancing hydroturbation. At the Goukamma coastal barrier dune, the two profiles (GOU 12/01 and GOU 12/02) (Fig. 4.2) has very similar physicochemical properties. The palaeosols are well drained and had no evidence of any illuvial accumulation at the B horizons probably due to their texture. The distribution of carbonate palaeosols found at Goukamma (GOU 12/03) (Fig. 4.2) is arguably because the dune where it is has been stabilized by vegetation, thereby reducing speed of infiltration and erosion. Accumulation of calcium carbonates with very limited loss through leaching is accountable for the high soil pH recorded in the area. Scientists have long shown there is a strong correlation between soils carbonate content and pH (Rogovska et al., 2007). The abundance of calcretes at Koeberg particular points that evapotranspiration has been in excess of precipitation in the locality. Where present, calcium carbonate from marine shells also clearly influences geochemistry of the palaeosols. Silica is the most dominant element in the palaeosols and sediments with the exception of the Bkm1 palaeosol at Goukamma which is dominated by CaO. The dominance of silica is clearly from the parent material, which is marine sand.

CIA applicability in the palaeosols and sediments is highly constrained due to its relatively higher carbonate contents than silicate rocks for which the index was developed from. Sheldon and Tabor (2009) reported that CIA is least useful for limestone because they have low Al levels from the outset and thus, very low CIA values that may not change appreciably during pedogenesis. Inconsistencies in the CIW values would suggest this index is not ideal for the late Quaternary palaeosols since there is no evidence of K metasomatism or illitization in the soils. Developed to account for the post-burial addition of K by metasomatism and illitization of clay minerals in sub-metamorphic burial conditions, CIW have been reported to mainly suitable in

metamorphosed environments or very old palaeosols, for example those of the Precambrian (Sheldon and Tabor, 2009). Data is not sufficient to support or refute the applicability of WI-1 and WI-2 to the palaeosols. This perhaps could be attributed to the insignificant differences in the values of Al/Si (clayeyness) ratios of the palaeosol sequences with depth. It should be recalled that a positive correlation of WI-1 and WI-2 with Si/Al (1/"clayeyness", section 4.4.3.3) was reported by Darmody et al. (2005) which proves that it measured weathering intensity in the studied modern soil formation with granitic parent materials.

The clay-sized fraction mineralogy of the palaeosols comprises clastic calcite and micas. One would expect a manifold clay minerals composition in a well-developed modern soil, but this is not obtainable in these localities, which supports a young soil model for the profiles. Calcite, found in the Koeberg carbonate palaeosols is known to occur over a wide range of climates. It been widely reported to be present in sub-humid to arid soils (Dixon et al., 1989). Muscovite, which occurs at both sites, is more resistant in pedogenic environments than any other mica such as biotite and this explains why it is also very present in the palaeosols since they formed from marine sands which are parent materials mostly resistant to weathering.

Pedogenesis at both localities started most likely during the MIS 4-2 regressive phase, which coincides with the period sedimentation on the coastal barrier dunes of Goukamma began (Carr et al., 2007). Periods of sea low stand provided a good environment for the interaction climate and organisms on the parent material (marine sand). Holocene palaeoenvironments have been characterised by high climate variability occurring at intervals of thousands to hundreds of thousands of years (Williams et al., 2008) and the values to the palaeoprecipitation and temperature obtained from this study supports the believe. The present day Koeberg has a MAT of 17^{o}C (Potgieter and Fick, 2007) whereas the $\delta^{18}O$ isotope palaeotemperature from the

palaeosol is 14^{o}C, suggesting a cooler palaeoclimate during the MIS 4-2 standstill at Koeberg. MAP was not obtained for Koeberg since the palaeosols did not fit the criteria for application of the MAP models used in this study. At Goukamma, which falls within the all-year-round rainfall zone, the calculated palaeotemperature from the pedogenic carbonate at GOU/12/03 is 11^{o}C while the present day location has a MAT of 17^{o}C suggesting a cooler palaeoclimate. The maximum value for palaeoprecipitation obtained a Goukamma is 653 mm yr^{-1}. The modern MAP nearby Knysna is 800-100 mm yr^{-1}, suggesting a lower palaeoprecipitation. Working on the MIS 4 palaeoenvironments of South Africa, Chase (2010), reported it was a period of relatively cool, moist climates, the ubiquity of which transcends the modern regional climate boundaries. Great care is, however, required when using geochemical data in obtaining palaeoclimatic information from palaeosols sequences in a coastal settings because these weathering indices are not only sensitive to climate but also to soil age. Moreover, the degree of weathering decreases with soil depth; in an eroded palaeosol profile, the most strongly weathered upper part may have been removed so that only the weathering index of the lower part is available. Hence, both soil age and erosion need to be considered in order to obtain reasonable palaeoclimatic information.

6. Conclusions

The following conclusions about Koeberg and Goukamma palaeosol sequences are made:

1. The MIS 4/ Holocene boundary at Koeberg were predominantly cool and dry while that of Goukamma was cool, but moist. The present day climatic forcing which affects the overall climate of Southern Africa most likely would have been accountable for the palaeoclimate trend.
2. We confirm the use of CIA and CIW to evaluate weathering intensity is greatly constrained for carbonate palaeosols probably due the low level of aluminum oxide in the protolith

(parent material). The WI-1 and WI-2 weathering indices of Darmody et al. (2005) seem more consistent, but certainly calls for further evaluation due to the few data points used in this study.

3. Higher resolution chronology of palaeosols from South Africa and further sampling are needed to develop a database for Southern Africa palaeoenvironmental studies and correlation and comparison with evidences available from the Northern Hemisphere.

References

Adams, J.S., Kraus, M.J., Wing, S.L., 2011. Evaluating the use of weathering indices for determining mean annual precipitation in the ancient stratigraphic record. Palaeogeography, Palaeoclimatology Palaeoecology 309, 358–366.

Bateman, M.D., Carr, A.S., Dunajko, A.C., Holmes, P.J., Roberts, D.L., McLaren, S.J., Bryant, R.G., Marker, M.E., Murray-Wallace, C. V., 2011. The evolution of coastal barrier systems: a case study of the Middle-Late Pleistocene Wilderness barriers, South Africa. Quaternary Science Reviews 30, 63–81.

Bateman, M.D., Holmes, P.J., Carr, A.S., Horton, B.P., Jaiswal, M.K., 2004. Aeolianite and barrier dune construction spanning the last two glacial–interglacial cycles from the southern Cape coast, South Africa. Quaternary Science Reviews 23, 1681–1698.

Baxter, A.J., Meadows, M.E., 1999. Evidence for Holocene sea level change at Verlorenvlei, Western Cape, South Africa. Quaternary International 56, 65–79.

Bosch, D.D., Truman, C.C., Potter, T.L., West, L.T., Strickland, T.C., Hubbard, R.K., 2012. Tillage and slope position impact on field-scale hydrologic processes in the South Atlantic Coastal Plain. Agricultural Water Management 111, 40–52.

Bouyoucos, G.J., 1962. Hydrometer method improved for making particle size analyses of soils. Agronomy Journal 53, 464–465.

Brooke, B., 2001. The distribution of carbonate eolianite. Earth Science Reviews 55, 135 - 164.

Brown, K. S., Marean, C. W., Herries, A. I. R., Jacobs, Z., Tribolo, C., Braun, D., Bernatchez, J., 2009. Fire as an engineering tool of early modern humans. Science 325, 859–862.

Carr, A.S., Thomas, D.S.G., Bateman, M.D., Meadows, M.E., Chase, B., 2006. Late Quaternary palaeoenvironments of the winter- rainfall zone of southern Africa: palynological and sedimentological evidence from the Agulhas Plain. Palaeogeography Palaeoclimatology Palaeoecology 239, 147–165.

Cerling, T.E., Quade, J., 1993. Stable carbon and oxygen isotopes in soil carbonates. In: McKenzie, J.A., Savin, S. (Eds.), Climate Change in Continental Isotopic Records. Geophysics Monograph, vol. 78. American Geophysical Union, Washington (DC), pp. 217–231

Chase, B.M., Boom, A., Carr, A.S., Meadows, M.E., Reimer, P.J. (in press). Holocene climate change in the southernmost South Africa: rock hyrax middens records shifts in southern westerlies. Quaternary Science Reviews.

Chase, B. M., 2010. South African palaeoenvironments during marine oxygen isotope stage 4: a context for the Howiesons Poort and Still Bay industries. Journal of Archaeological Science 37, 1359–1366.

Chase, B.M., Meadows, M.E., 2007. Late Quaternary dynamics of southern Africa's winter rainfall zone. Earth-Science Reviews 84, 103-138.

Chen, J., Ji, J.F., Qiu, G., Lu, H., 1998. Geochemical studies on the intensity of chemical weathering in Luochuan loess–paleosol sequence, China. Science in China 41, 235–241.

Chen, J., An, Z.S., Head, J., 1999. Variation of Rb/Sr ratios in the loess–paleosol sequences of central China during the last 130,000 years and their implications for monsoon paleoclimatology. Quaternary Research 51, 215–219.

Cotton, J.M., Sheldon, N.D., 2012. New constraints on using paleosols to reconstruct atmospheric pCO2. Geological Society of America Bulletin 124 , 1411–1423.

Darmody, R.G., Thorn, C.E., Allen, C.E., 2005. Chemical weather and boulder mantles, Kärkevagge, Swedish Lapland. Geomorphology 67, 159–170.

Day, P. R., 1965. Particle Fractionation and Particle-Size Analysis. In: C. A. Black (ed) Methods of Soil Analysis. Part I. Soil Science Society of America, Madison.

Dixon, J.B., 1989. Kaolin and serpentine group minerals, In: Dixon, J.B.,Weed, S.B. (Eds.), Minerals in Soil Environments, 2nd Ed. Soil Science Society of America Book Series, vol. 1, pp. 467–526.

Dunajko, A.C., Bateman, M.D., 2010. Sediment provenance of the Wilderness barrier dunes, southern Cape coast, South Africa. Terra Nova 22, 417–423.

Irving, S.J., 1998. Late Quaternary Palaeoenvironments at Vanker- velsvlei, near Kynsna, South Africa. Unpublished MSc thesis, University of Cape Town.

Liutkus, C.M., Wright, J.D., Ashley, G.M., Sikes, N.E., 2005. Paleoenvironmental interpretation of lake-margin deposits using δ13C and δ18O results from early Pleistocene carbonate rhizoliths, Olduvai Gorge, Tanzania. Geology 33, 377-380.

Food and Agricultural Organisation (FAO), 2006. Guideline for Soil Description, 4th edition. FAO, Rome, Italy (109 pp.).

Maher, B. A., Thompson, R., 2012. Oxygen isotopes from Chinese caves: records not of monsoon rainfall but of circulation regime. Journal of Quaternary Science 27, 615–624.

Marbut, C.F. 1935. Soils of the United States. U.S. Department of Agriculture, Washington DC.

Marker, M.E., Holmes, P.J., 2002. The distribution and environmental implications of coversand deposits in the Southern Cape, South Africa. South African Journal of Geology 105 , 135–146.

Minasny, B., McBratney, A.B., Salvador-Blanes, S., 2008. Quantitative models for pedogenesis — A review. Geoderma 144, 140–157.

Munsell Colour Co. 2000. Munsell soil color charts. Baltimore: Munsell Color Company.

Nesbitt, H.W., Young, G.M., 1984. Prediction of some weathering trends of plutonic and volcanic rocks based on thermodynamic and kinetic considerations. Geochimica et Cosmochimica Acta. 48, 1523–1534.

O'Neil, J.R., Clayton, R.N., Mayeda, T.K., 1969. Oxygen isotope fractionation in divalent metal carbonates. Journal of Chemical Physics 51, 5547–5558.

Potgieter, F., Fick, G., 2007. Meteorological analysis for proposed pebble bed modular reactor demonstration power plant. SHE Cape and Cape Weatherwise international (cc). 11 pp.

Prochnow, S.J., Nordt, L.C., Atchley, S.C., Hudec, M.R., 2006. Multi-proxy paleosol evidence for middle and late Triassic climate trends in eastern Utah. Palaeogeography, Palaeoclimatology, Palaeoecology 232, 53–72.

Retallack, G.J., 1999. Post-apocalyptic greenhouse paleoclimate revealed by earliest Triassic paleosols in the Sydney Basin, Australia. Geological Society of America Bulletin 111, 52–70.

Roberts, D. L., Bateman, M. D., Murray-Wallace, C. V., Carr, A. S., Holmes, P. J. (2009). West coast dune plumes: Climate driven contrasts in dunefield morphogenesis along the western and

southern South African coasts. Palaeogeography, Palaeoclimatology Palaeoecology 271(1-2), 24–38.

Roberts, D.L., Bateman, M.D., Murray-Wallace, C. V., Carr, A.S., Holmes, P.J., 2008. Last Interglacial fossil elephant trackways dated by OSL/AAR in coastal aeolianites, Still Bay, South Africa. Palaeogeography, Palaeoclimatology, Palaeoecology 257, 261–279.

Roberts, D.L., Matthews, T., Herries, A.I.R., Boulter, C., Scott, L., Dondo, C., Mtembi, P., Browning, C., Smith, R.M.H., Haarhoff, P., Bateman, M.D., 2011. Regional and global context of the Late Cenozoic Langebaanweg (LBW) palaeontological site: West Coast of South Africa. Earth-Science Reviews 106, 191–214.

Rogovska, N.P., Blackmer, A.M., Mallarino, A.P., 2007. Relationships between Soybean Yield, Soil pH, and Soil Carbonate Concentration. Soil Science Society of America Journal 71, 1251–1256.

Rostási, Á., Raucsik, B., Varga, A., 2011. Palaeoenvironmental controls on the clay mineralogy of Carnian sections from the Transdanubian Range (Hungary). Palaeogeography, Palaeoclimatology, Palaeoecology 300, 101–112.

Sayyed, M.R., Hundekari, S.M., 2006. Preliminary comparison of ancient bole beds and modern soils developed upon the Deccan volcanic basalts around Pune (India): potential for paleoenvironmental reconstruction. Quaternary International 156– 157, 189–199.

Sawyer, E.W., 1986. The influence of source rock type, chemical weathering and sorting on the geochemistry of clastic sediments from the Quetico metasedimentary belt, Superior Province, Canada. Chemical Geology 55, 77–95.

Schaetzl, R.J., Anderson, S., 2005. Soils. Genesis and Geomorphology. Cambridge University Press, Cambridge 817 pp.

Sheldon, N.D., Tabor, N.J., 2009. Quantitative paleoenvironmental and paleoclimatic reconstruction using paleosols. Earth-Science Reviews 95, 1–52.

Sheldon, N.D., Retallack, G.J., Tanaka, S., 2002. Geochemical climofunctions from North America soils and application to paleosols across the Eocene–Oligocene boundary in Oregon. Journal of Geology 110, 687–696.

Soil Survey Staff, 2010. Keys to Soil Taxonomy, 11th ed. USDA-Natural Resources Conservation Service, Washington, DC.

Todisco, D., Bhiry, N., 2008. Micromorphology of periglacial sediments from the Tayara site, Qikirtaq Island, Nunavik (Canada). Catena 76, 1–21.

Tsatskin, A., Gendler, T., Heller, F., 2008. Improved Paleopedological Reconstruction of Vertic Paleosols at Novaya Etuliya, Moldova Via Integration of Soil Micromorphology and Environmental Magnetism. New Trends in Soil Micromorphology. pp 91-110.

Tyson, P.D., 1999. Late-Quaternary and Holocene palaeoclimates of southern Africa: a synthesis. South African Journal of Geology 102, 335–349. Tyson, P.D., 1986. Climatic Change and Variability in Southern Africa. Oxford University Press, Cape Town.

Tyson, P.D., Preston-Whyte, R.A., 2000. The Weather and Climate of Southern Africa. Oxford University Press, Cape Town. 396 pp.

United States Salinity Lab. Staff., 1954. Methods for soil characterization. In: Diagnosis and improvement of saline and alkali soils. Agricultural Handbook 60, USDA, Washington, D.C. pp 83-147.

Watanabe, T., Minoura, K., Nara, F.W., Shichi, K., Horiuchi, K., Kakegawa, T., Kawai, T., 2012. Last glacial to post glacial climate changes in continental Asia inferred from multi-proxy records (geochemistry, clay mineralogy, and paleontology) from Lake Hovsgol, northwest Mongolia. Global and Planetary Change 88-89, 53–63.

Williams, J.W., Webb, T.I., Richard, P. H., Newby, P., 2000. Late Quaternary biomes of Canada and the eastern United States. Journal of Biogeography 27, 585–607.

Weather Bureau, 1986. Climate of South Africa – Climate Statistics up to 1984 (WB40). Weather Bureau, Department of Environment Affairs, Government Printer, Pretoria.

Yang, S.Y., Li, C.X., Yang, D.Y., Li, X.S., 2004. Chemical weathering of the loess deposits in the lower Changjiang Valley, China, and paleoclimatic implications. Quaternary International 117, 27–34.

CHAPTER FIVE
EVALUATION OF PEDOGENESIS AND PALAEOENVIRONMENTAL CONDITIONS OF A PALAEOSOL ASSOCIATED WITH STONE LINE IN THE CAPE PENINSULA, SOUTH AFRICA

Abstract

The soil-geomorphic unit at the base of the southeastern slope of the Devil's Peak Mountain in the Cape Peninsula, South Africa has a duplex morphology; soils developed from quartz arenite facies over buried palaeosols formed on deeply weathered Neoproterozoic metasediments. The soils, for which there is no previous documented research, are separated by a stonelayer. Here we present the results of the macro- and micromorphological investigations, in addition to selected physico-chemical, geochemical and mineralogical properties for a section up to the depth of 4 metres in thickness. The main objectives are to characterise the soils and draw inferences regarding their pedogenesis and palaeoenvironment aspects. The results of the study suggests that two major regional climate cycles are in evidence: a relatively warm and humid subtropical climate which gave rise to the formation of the buried red vertic palaeosol and a drier, more seasonal semi-arid Mediterranean climate under which the soils overlying the stone line are currently forming, as inferred from poor horizonation and translocation of colluvial materials. The stone layer appears to have been deposited as a lag by a palaeoriver as the energy decreased and the material was later mixed with the soil matrix by pedoturbation. The major pedogenic processes in the older horizon include plinthization, and it has few roots and high clay content (>32%); and in the younger overlying soil, podzolization, and roots are common with low clay content (<9%). Total element abundance followed $SiO_2 > Al_2O_3 > Fe_2O_3 > TiO_2$ order with other major elements being in relatively smaller amounts. The presence of smectitic clay could possibly be responsible for the formation of slickensides in the vertic palaeosol. Variations in climate and parent material are the principal causes of differences in the soil properties. WI-2 proposed by Darmody et al., (2005) is the most suitable for evaluating pedogenesis in the soils.

Keywords: geochemistry, paleoclimate, stonelayer, Table Mountain, weathering.

5.1. Introduction

Soils with stone lines are frequent in tropical and subtropical environments. In South Africa, they are widely present and usually demarcate the transition from A or E and B horizons (Fey, 2009). One of the early researchers, Sharpe (1938), defined a "stone line" as a three dimensional subsurface soil horizon dominated by larger particles (>2mm) which generally parallels the surface topography of a landscape. In most cases, stone lines are found at the basal layer of two-layered soil biomantles (Schaetzl and Anderson 2005; Fey 2009). Stone lines which are more than one stone thick are referred to as "stonelayers" or "stone zones" (Johnson, 1989).

The lithological content of a stonelayer may be variable; while many are dominantly lithic clasts of quartzose, others may be of metallic nodules and concretions of iron and manganese oxides, anthropogenic remnants and shells in the case of calcareous soils with marine origin, precious stones or some combinations thereof (Johnson, 2002). Even though soils with stone lines are common, their genesis is often poorly understood and the interpretation of their genesis has generated major controversy amongst earth scientists (Morrás et al., 2009).

Existing models on the mode of formation of stone line in soils may be summarized as: (a) pediplanation processes associated with climate change resulting in erosion of quartzite and vein quartz, and subsequent transport of the fragments; (b) transport of fragments along steep slopes by colluvial processes; (c) *in situ* sinking of hardened coarse fragments previously broken down by chemical weathering; and (d) bioturbation which may cause downward movement of the gravel-sized particles (Ségalen, 1994).

An autochthonous origin for soils with stone lines was proposed by Laporte (1962) contrary to the allochthonous origin which some earlier authors had reported. He interpreted the occurrence of stone lines in soils as a product of bioturbation or physical processes which

involves the translocation of materials from the upper horizons to the subsurface. The three notable bioturbation sub-processes through which this would be possible are: biomixing, biotransfer and biosorting. Stoops (1989) also proposed an *in situ* origin for stone lines in Central Africa. He noted that, while the stonelayers could have formed from the parent materials or selective hardening of component parts, the materials on the surface could be attributed to an admixture of allochthonous materials and fine materials from the deeper horizons by bioturbation.

A "dynamic denudation model" has been proposed by Johnson et al. (1985a, b) for the evolution of stonelayers in soils. In this model, the expression of dynamic denudation is that bioturbation, considered dominant in soil biomantles, combined with other biological and traditional pedogenic processes (e.g. eluviations-illuviations, organic matter mineralization, weathering-biochemical transformations, wind and water erosion-deposition, geochemical capillary surface-wickings and precipitations, freeze-thaw, dilations-contractions, etc.) being subsidiary. The lower horizon of the profile would have the stonelayer results from biosorting, while soil fauna would develop the surface layer by translocation of materials from the deeper to the surface mantle. Lastly, some other authors have proposed that stonelayers form in soils and sediments as a result of weathering and mineralogical transformations (cf. Morrás et al., 2009).

Conceptual models also exist for the mode of formation of surface materials overlying stonelayers. Kellog and Devol's (1949) work led to the development of the erosion-pedimentation-pedisedimentation model of Ruhe et al. (e.g. Ruhe and Cady 1954; Ruhe, 1959). A major problem with this model is that it is not applicable in all instances (Ségalen, 1994; Morrás et al., 2009) because the transport of oxic (sediment-water interface) materials during

landscape formation is generally believed to have occurred over a short period of time as opposed to fluvial and aeolian deposits (van Wanbeke et al., 1983).

One major problem associated with genetic interpretation of soil and palaeosol profiles with stonelayers is horizon designation. Generally, stonelayer profiles follow a mineral soil (MS)-stonelayer (SL)-underlying weathered or saprolite (W) convention from surface downwards. In the older versions of soil classification (e. g. Soil Survey Staff, 1975 and FAO-UNESCO, 1988), soils with stonelayers were considered to be geological in origin rather than pedogenic (Ségalen, 1994). Researchers have over the years used various different notations in describing stonelayer soils. While some used the traditional A-B-C notation, others simply described their morphology without attaching any alphabetical symbols (Ségalen, 1994). In tropical soils with intensive activity of bioturbation by ants and termites, the 'M-SL-W' notation was used (Watson, 1961; Williams, 1968; Johnson, 1995). However, in the most recent editions of Soil Taxonomy (Soil Survey Staff, 1999 and 2006), stonelayers are included among lithological discontinuities and as an indication that the soil may have developed from more than one parent material.

Stonelayers occur widely in South African soils and the Cape Peninsula appears to be no exception. An excavation due to a building development on the southeastern toeslope of the Devil's Peak part of Table Mountain revealed a conspicuous stonelayer at a depth of 140cm. The stonelayer runs parallel to the topography of the contemporary landscape and demarcates two morphologically distinctive soils, viz. predominantly sandy soil horizons overlying deeply weathered red palaeosols. Considering the modern climate of the region, which is 'Mediterranean-type', we hypothesize that the buried palaeosols formed under environmental and climatic condition different from what obtains today. The overarching aim of this paper is to

provide an improved palaeoenvironmental reconstruction and interpretation of the operational geomorphological-pedological processes in the area through time. Thus, the specific objectives are to examine: i) the macro- and micromorphology, physico-chemical, geochemical and mineralogical properties of the soils and palaeosols and ii) use these data to calculate MAP and MAT using geochemical climofunctions and chemical weathering intensities.

5.2. Geographical and geological setting

The Cape Peninsula, a 470 km^2 area of pronounced topography and varied climate, forms the southwestern tip of the Cape Floristic Region, South Africa (Cowling et al., 1996) (Fig. 5.1). The studied profile represents a soil-geomorphic unit and is located near the foot of iconic Devil's Peak, formed of Palaeozoic Cape Supergroup rocks (Fig. 5.2). While the lower slopes of the mountain have been extensively used for residential purposes, the upper slopes are still largely conserved as the habitat (Table Mountain National Park) for indigenous afro-montane plant communities of mountain fynbos. The area has a climate characterized by cool, wet winters and warm, dry, windy summers. The amount and spatial distribution of rainfall in the region is strongly variable and strongly influenced by topography, although the mean annual precipitation and temperature for the location are 1300mm and 17.3 ^{o}C respectively (Harris et al., 2010).

Based on published geological data and geotechnical investigations previously undertaken by Kantey & Templer (2008), the site is known to be underlain at depth by deeply weathered meta-sedimentary strata of the Neoproterozoic Tygerberg Formation of the Malmesbury Group. The meta-sedimentary strata originally comprised deep water marine mudrock and are mantled by relatively thin deposits composed of alluvial river terrace material (Kantey and Templer, 2008).

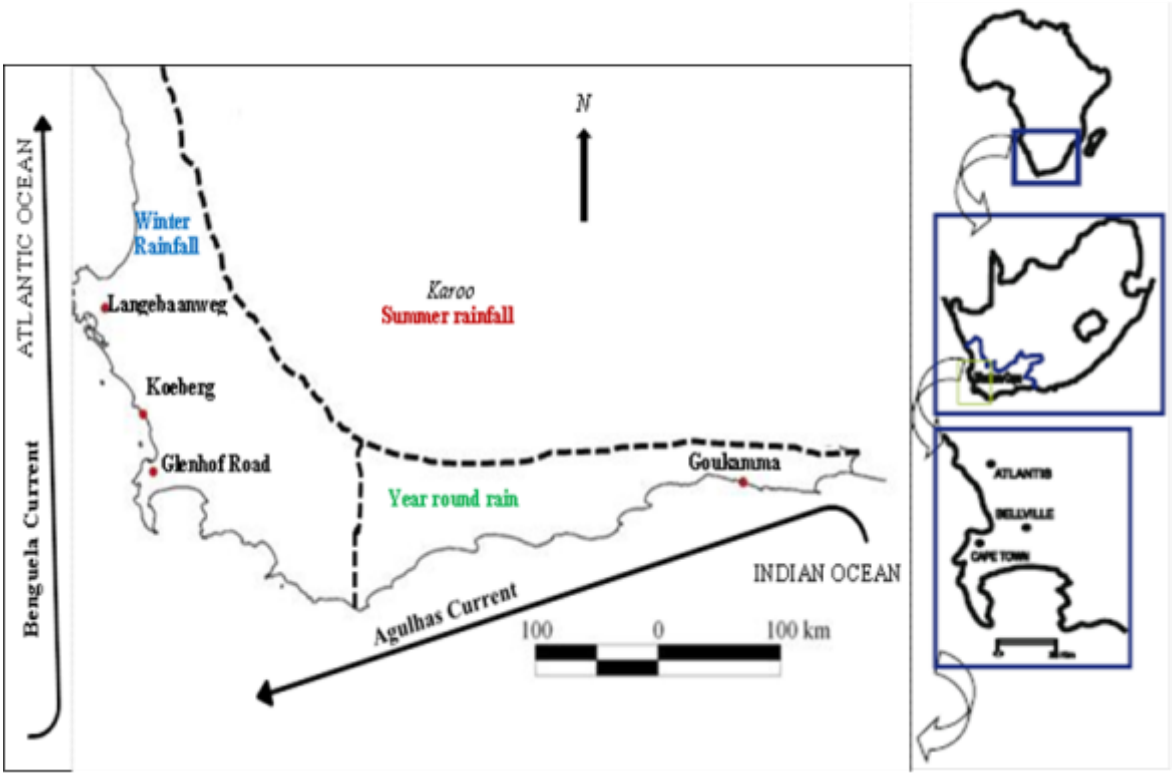

Fig. 5.1. Map of Western Cape showing the location of the studied pit at Glenhof Road.

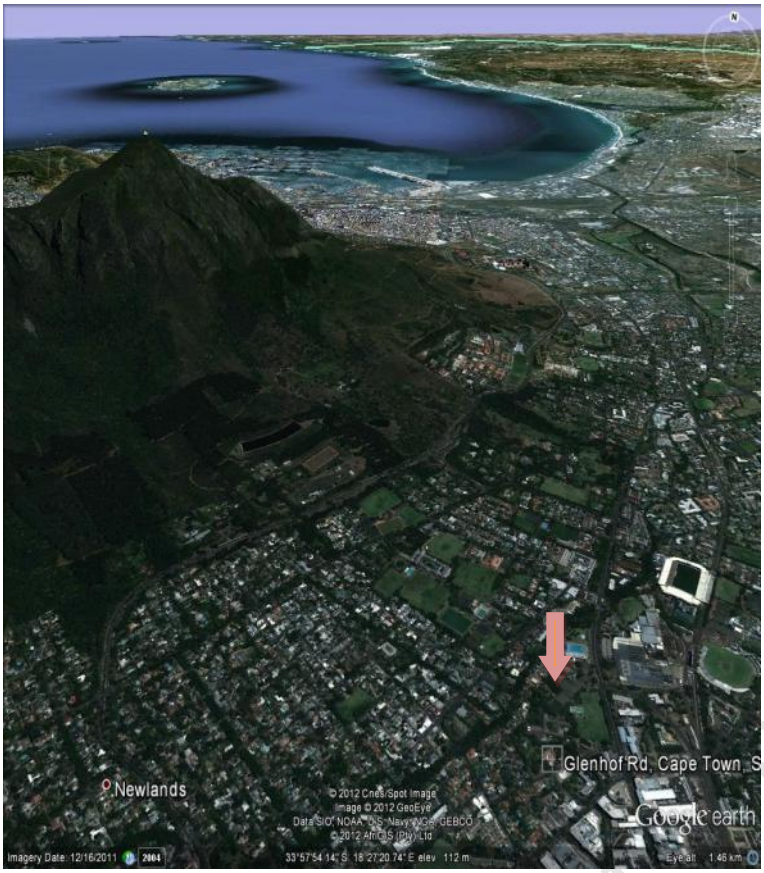

Fig. 5.2. An aeriel photo showing the geomorphic context of the pedon

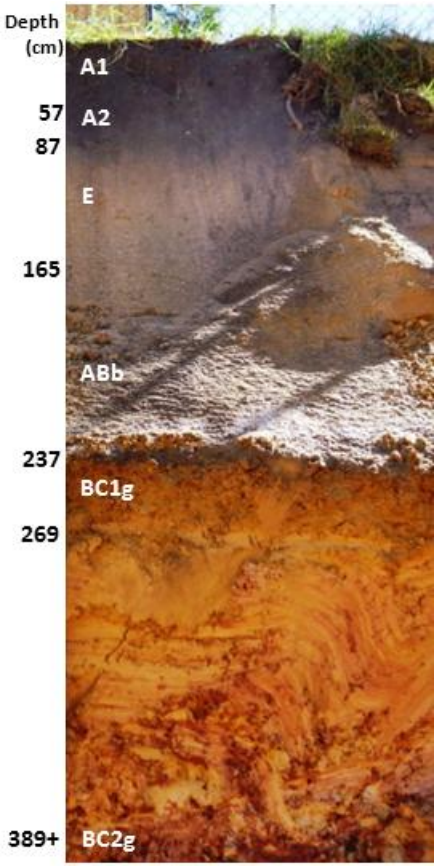

Fig 5.3. Lithostratiphy of the pedon

5. 3. Materials and methods

5.3.1 Field sampling

Undisturbed hand samples were then taken from each horizon of the duplex pedon. These samples were specifically marked for thin section preparation. A total of six representative samples were also collected and bagged for further laboratory investigations. In the field, colour was described using the Munsel soil colour system (Munsel Color Company, 2000), while the general macromorphological properties were described in accordance with the guidelines for soil profile description (FAO, 2006).

5.3.2. Laboratory methods

Pretreatment of samples included gently grinding to break up clods and subsequently passing it through a 2mm sieve to separate gravel and roots/rhizomes from the 2mm soil fraction. Dry and moist colours were determined using Munsell color chart. Dry and moist colours were measured using a Munsell color chart. The Soil Redness Rating (Hurst, 1977) was calculated using the formula RR= H.C/V, where C = chroma, V = value and H = hue (12.5 for hue 7.5R; 10 for hue 10R; 7.5 for 2.5YR; 5 for 5YR, 2.5 for 7.5YR; and 0 for 10YR of the Munsell colour nomenclature) after Torrent et al., (1980) and Barrón and Torrent (1986). Particle size distribution was determined by hydrometer method (Bouyoucos, 1962). Both soil pH and electrical conductivity were measured with pH and electrical conductivity meters respectively in a 1:2.5 (soil to solution) ratio. For micromorphological analyses, cores and undisturbed samples were collected from each representative horizon of the profile for thin sectioning and subsequent study under a petrographic microscope. Oriented samples were impregnated with resins under vacuum before sectioning. Slides were viewed with a polarizing petrographic microscope (Nikon) and images captured with an Olympus ALTRA 20 camera. Total elemental oxide composition of the samples was determined using XRF spectroscopy (X-Lab 2000) and intensity data were collected using the Philips X40 software. Matrix corrections are made on all elements using the de Jongh model in the X40 software. Theoretical alpha coefficients, calculated using the Philips on-line ALPHAS programme, are used in the de Jongh model. Clay mineral analyses was conducted with a Phillips PW 3830/40 Generator with a PW 3710 mpd control X-ray diffraction system using the Xpert data collector/identify software. Reported values are the average of measurements taken in triplicates.

5.3.3 Geochemical mass balance, weathering indices and geochemical climofunctions

A geochemical mass balance calculation was used to quantify the net result of pedogenic weathering. The formula, equation (1), assumes that an immobile element behaves conservatively and corrects mobile element concentrations for volumetric strain during weathering and pedogenesis (Chadwick et al., 1990; Du et al., 2010)

$$\tau i,j = \frac{Ci,p}{Ci,w} \frac{Cj,w}{Cj,p} - 1 \qquad \text{…equation (1)}$$

where C is the concentration (weight percentage or molar mass), with "*i*" for immobile element, "*j"* for element in question, *w* for weathered material and *p* for parent material. If τi, j = −1, then the element "*i"* is completely depleted during chemical weathering. In most cases, this equation provides a tool for estimating elemental loss or gain within a profile, although the mass-balance equations have several critical assumptions. Firstly, there should be a genetic relationship between regolith and its parent material. Second, since the calculations are highly dependent on immobile elemental concentrations, the reference element should be conservative in its real sense. Zirconium is the chosen immobile element for this study because Zr primarily resides in zircon, which is highly resistant to chemical weathering and inter-sample variations in Zr are less than for Ti.

To evaluate pedogenic processes quantitatively across the pedocomplex, we used a range of parameters including the following: ΣBases/Al, for hydrolysis; the rationale behind this ratio is that common rock-forming alkaline and alkaline earth metals are lost relative to Al during pedogenesis and thus it is a measure of chemical weathering intensity (e.g. Retallack, 1999; Sayyed and Hundekari, 2006). Sericitization is a process whereby plagioclases and other minerals are replaced by sericite through the effect on rocks of low temperature thermo-geochemistry and is computed using the K_2O/Al_2O_3 ratio (Nesbitt and Young, 1984). The ratio

of Al/Si is a measure of clayeyness: the higher the value of this ratio, the more weathered or clayey the soil is because Al accumulates as clay minerals form in soils by hydrolysis. The Ti/Al ratio measures provenance by acidification process and relies on the fact that Ti is most readily lost by physical weathering, whereas Al is lost through chemical weathering (see Nesbitt and Young 1984, Sawyer, 1986). The K+Na/Al ratio is a proxy for salinization, while Ba/Sr is used infer trace element leaching/hydrolysis because alkali elements accumulate as soluble salts are not removed (Sheldon and Tabor, 2009). To quantify the totality of weathering processes, we used four geochemical indices:

(i) chemical index of alteration ($CIA = 100 \times \frac{Al}{Al+Ca+K+Na}$) …equation 2

as proposed by Nesbit and Young (1982);

(ii) chemical index of weathering ($CIW = 100 \times \frac{Al}{Al+Ca+Na}$) …equation 3

by Harnois (1988), this in principle is the same with CIA-K of Maynard, (1992) although developed for different purposes;

(iii) weathering indices ($WI - 1 = \frac{Si+Ca}{Fe+Ti}$) …equation 4

iv) ($WI - 2 = \frac{Si+Ca}{Fe+Ti+Al}$) …equation 4

both of which were proposed by Darmody et al., (2005). In all four index calculations, each elemental oxide is first converted to moles. CIA is the oldest established of all the tested indices and has been adjudged most suitable for application in silicate rocks. To account for post-burial K metasomatism, CIW was developed by (Harnois, 1988) removing K parameter from CIA. CIW was primarily proposed to account for illitization, which is primarily of interest in metamorphosed rocks or in very old palaeosols, e.g. Precambrian. The first two indices have

been used extensively for soils and palaeosols while the last two indices developed from granitic parent materials; have not been widely applied to palaeosols (Sheldon and tabor, 2009).

5.4. Results and discussion

5.4.1 Lithostratigraphy and field observations

The horizon designation of the pedon follows the traditional A-B-C convention. Six genetic horizons were identified: A1-A2-E-2ABb-BC1g-BCg2 (Fig. 5.3). This is typical of the "A-E-B-C" general horizonation of most soils found in midlatitudes and subtropics (Johnson, 1995). The two deepest and oldest, strongly contrasting, horizons with redoximorphic features developed from strongly weathered residual late Precambrian meta-sedimentary mudrock (Rozendaal et al., 1999). A stonelayer, which defines a clear boundary between the units which are clearly derived from completely different parent materials, is mixed in a fabric of coarse sandy materials and occurs as the third horizon (from below), while the uppermost three horizons are made up of transported fluvial/ colluvial weakly developed soils which formed from detrital quartz arenite. Ages of the Malmesbury Supergroup are poorly constrained, and few absolute ages are available. It was deposited on the Kibaran basement and intruded by the Cape granite suite. Therefore, deposition, deformation and metamorphism of the Malmesbury group occurred between 1.2 Ga and 510 Ma (Belcher and Kisters, 2003). However, an available isotopic Rb-Sr age for Malmesbury shale yields 595 ± 45 mya (Allsopp and Kolbe, 1965).

5.4.2. Macromorphology

The colluvial/fluvial nature of the A1, A2 and E horizons is reflected in the heterogeneity of its components which is predominantly sand. Colour is another markedly distinguishing

feature of the pedon. The lower and older palaeoregolith and palaeosol horizons are distinctively reddish with mottles of plinthite in varying shades of red and yellow (Table 5.1). The other horizons above the stonelayer are yellowish with varying Values and Chroma while the A1 horizon is black (5YR 2.5/1). The boundary between the stonelayer which marks the base of the biomantle of the pedon is abrupt, marking a transition to depositional discontinuity. There is a strongly contrasting difference in the macromorphology of the duplex pedon. While the underlying older material was composed of metamorphosed mudrock (with very little imprint of pedogenesis) the upper horizons were unconsolidated sand. The differences in both consistency and structure (Table 5.1) may be attributed to variation in the parent materials (e.g. Simon et al., 1990).

More roots were seen in the upper soils than the underlying red palaeosol. Organic matter may be responsible for the dark colour of the A1 and A2 horizons as it is the zone of maximum soil organic matter mineralization. According to Schulze et al., (1993), humic acid, which mask the yellowish brown color of fulvic acid, are usually responsible for the darker colors of soil organic matter. It has been widely reported that, under an oxygen rich environment, iron oxides impart reddish colour to soils (e.g. Torrent et al., 1983; Schwertmann, 1993; Yaalon, 1997) and this accounts for the yellowish to reddish colours of the underlying horizons and the buried palaeosols.

Table 5.1. Profile descriptions of the macromorphological properties of the pedon

Horizon	Depth (cm)	Facies	Colour[1] (moist)	>2mm fragments	Structure[2]	Root	Boundary[3]	Consistency (moist)	Field texture	Gravel (>2 mm)	React HCl	other features
A1	0-57	colluvial	10YR 2/1	absent	1gr	frequent	gs	loose	sand	absent	none	plastic rubbles
A2	57-87	ditto	10YR 5/6	absent	2gr	common	ac	loose	loamy sand	absent	none	-
E	87-165	fluvial	2.5 Y 5/6	absent	2gr	few	ac	loose	sand	absent	none	-
2ABb	165-237	fluvial	2.5YR 6/8	frequent	1gr	few	gs	loose	loamy sand	absent	none	stones, gravels
2BCg1	237-269	residual	10R 7/8	absent	massive	few	gs	very firm	clay	absent	none	slickenside
2BCg2	269-389+	residual	10R 5/8	absent	massive	few	-	very firm	clay	absent	none	slickenside

[1]nd – not determined
[2] 1– weak; 2 – medium; 3 – strong; gr – granular; sbk – subangular blocky; abk – angular blocky, blk – blocky; Gr. S – gravelly sand
[3] a – abrupt; c – clear; s – smooth; g – gradual; w – wavy

5.4.3 Laboratory analyses

5.4.3.1 Physico-chemical properties

Disparities in the duplex soils are further evident in some of their selected physical and chemical properties (Table 5.2). The upper horizons above the stonelayer, derived from quartz arenite have a significantly lower redness rating (0) than the underlying horizons which have a redness rating of 16. This suggests advanced rubification in the palaeoregolith and palaeosols. Typically, redness rating strongly correlates positively with haematite content in soils (e.g. Torrent et al., 1980). The surface horizon showed a dominance of sand over silt and clay in the particle size distribution – typical of what should be expected of transported sandstone with minimal influence of organic matter. The palaeoregolith is characterized by sandy clay loam to clay textures, which is to be expected if derived from highly weathered metamorphosed shales, as is the case. The soil reaction (pH) of the BCbg1 and BCbg2 horizons is strongly acidic, while the A1, A2 and E horizons is mildly acidic. Slight differences in the pH once again could be attributed to the chemical nature of the respective parent materials. Another reason could also be due to geomorphic position of the profile. Soluble salts from the adjacent uplands are more likely to be leached by lateral soil water movement (Sariyildiz et al., 2005). The addition of fine aerosols from numerous pans in the interior of the region could also be an additional reason for the slightly higher pH. Dust has been reported to have the ability to change soil properties including pH (Pagotto et al., 2001) and is certainly a significant factor in supplementing nutrients within fynbos soils.

Table 5.2. Selected physico-chemical properties of the pedon

Horizon	Colour (dry)	RR[◊] dry	RR[◊] moist	Sand (<2mm) (g kg^{-1})	Silt (<2mm) (g kg^{-1})	Clay (<2mm) (g kg^{-1})	Texture[╬] (IUSS)	pH (H_2O)	EC mS cm^{-1}
A1	5YR 4/1	1.25	0.0	789	121	90	LoSa	6.3	0.07
A2	10YR 7/6	0.0	0.0	908	22	70	Sa	6.2	0.02
E	10YR 7/8	0.0	nd	908	21	70	Sa	5.7	0.02
2ABb	10YR 7/8	0.0	8.6	899	11	90	LoSa	5.1	0.07
2BCg1	10YR 8/6	0.0	11.4	263	113	625	Clay	4.9	0.07
2BCg2	10YR 8/8	0.0	16.0	563	113	325	SaClLo	5.0	0.06

[◊] Redness rating

[╬] Sa – sand; ClLo – clay loam; LoSa – loamy sand; SaClLo – sandy clay loam; Cl – clay

[*] nd – not determined

5.4.3.2 Geochemistry

In the entire pedon, results of the total elemental analyses show that major oxides (Table 5.3) occur in the following order: $SiO_2 > Al_2O_3 > Fe_2O_3 > TiO_2$ with other major elements being in relatively smaller amounts. Silica is the most abundant oxide. Aluminium oxide and Fe_2O_3 showed remarkable differences in composition between horizons. While the mean Al_2O_3 content of the 2BCg1 and 2BCg2 is 20.53% that of the overlying soil is only 2.87%. Total Fe oxide contained in the buried palaeosol horizons has a mean value of 13.89% while the overlying soils derived from the sandstone have just 1.15%. Differences in parent material properties clearly account for the disparity in the geochemistry, as has been reported elsewhere (e.g. Brimhall et al., 1991; Strawn et al., 2002; Rawlins et al., 2003). The minor element oxides results (Table 5.4) show Zirconium is predominant within in the profile. Molybdenum and Zirconium are the only minor elements whose distribution across the pedon appeared uniform and seemingly independent of the differences in parent materials. Heavy metals such as Pb, Zn, Cu, Ni and Co were in higher concentrations in the palaeosols (Table 5.4). In general, the pattern of occurrence of minor elements illustrates marked differences between the overlying Quaternary soils and the underlying older palaeosol.

Table 5.3. Major elemental oxide composition of the pedon

	SiO_2	TiO_2	Al_2O_3	Fe_2O_3	MnO	MgO	CaO	Na_2O	K_2O	P_2O_5	SO_3	Cr_2O_3	NiO	LOI
	----------(%)----------													
A1	89.394	0.287	2.942	2.106	0.021	0.064	0.451	0.090	0.215	0.199	0.009	0.002	0.001	3.28
A2	93.557	0.333	2.777	0.637	0.012	0.001	0.096	0.039	0.094	0.063	0.001	0.002	0.001	1.63
E	93.340	0.258	2.908	0.717	0.012	0.001	0.080	0.027	0.081	0.039	0.001	0.002	0.001	1.76
2ABb	90.404	0.227	4.020	1.692	0.010	0.001	0.107	0.024	0.089	0.039	0.001	0.001	0.001	2.32
2BCg1	54.044	0.621	17.115	17.075	0.012	0.095	0.078	0.026	0.544	0.057	0.003	0.017	0.001	8.33
2BCg2	48.592	1.023	23.958	10.706	0.020	0.116	0.194	0.037	1.193	0.111	0.017	0.015	0.002	9.27

LOI – Loss on Ignition in a furnace at 950 ^oC (= chemically bound H_2O and CO_2)
Fe_2O_3 is expressed as total Fe

Table 5.4. Minor elemental composition of the pedon

	Mo	Nb	Zr	Y	Sr	Rb	U	Th	Pb	Zn	Cu	Ni	Co	Mn	Cr	V	Sc	Ba	S
	---------- (ppm) ----------																		
A1	<0.4	6.5	307.5	21.2	34.7	15.2	<0.9	6.3	59.2	86.1	10.2	4.1	<2.2	134.8	43.0	32.0	4.3	145.7	363.7
A2	<0.4	8.2	428.1	22.0	7.7	5.5	<0.9	5.7	5.6	4.7	<1.4	<1.8	<2.2	42.4	21.5	25.4	2.5	44.0	66.9
E	<0.4	5.6	324.3	19.0	7.6	5.2	<0.9	6.3	6.2	4.4	<1.4	<1.8	<2.2	32.3	20.5	26.2	4.2	37.8	70.3
2ABb	<0.4	3.0	230.8	19.5	7.0	5.6	<0.9	6.8	6.8	4.7	<1.4	<1.8	<2.2	28.6	36.9	44.8	3.3	43.0	153.4
2BCg1	<0.4	10.0	243.3	26.1	18.0	29.0	5.4	32.1	21.7	12.3	5.9	13.5	12.6	43.2	155.8	199.7	21.1	120.3	638.9
2BCg2	<0.4	19.9	262.0	26.4	36.0	61.9	7.4	27.7	26.6	17.2	7.1	17.6	4.9	112.6	118.8	155.3	18.9	194.7	581.1

5.4.3.3. Geochemical mass balance

Further data analysis shows the redistribution of the elemental oxides down the profile has been influence by pedogenic processes and this is seen in the geochemical mass balance plots (Fig 5.4a - e). Both silica and TiO_2 have clearly been lost across the profile (fig 5.4a). The loss of silica (desilication) results from chemical weathering, a breakdown of parent material preceding soil formation. Magnesium oxide showed neither increase nor decrease across the profile (Fig. 5.4b), and may indicate that this is in equilibrium in the soil. Also, manganese oxide was neither lost nor gained in the upper soils above the stonelayer (Fig 5.4b), but there was a gain in the palaeosols beneath the stonelayer. The pattern is somewhat different pattern for Fe and Al oxides. Iron and Aluminium oxides are depleted only in the upper horizons of the younger soil (fig 5.4c). Loss of K_2O and P_2O_5 is evident throughout the profile (fig 5.4d) and, given their, high solubility, leaching would most likely be the process involved. Calcium oxide was also lost down the profile (Fig 4e and high solubility of this mineral is the most likely cause of this trend as well. Sodium oxide, which is also very soluble in soils, reveals a 10% relative increase in the surface horizon and gradually becomes depleted down the profile. In the buried palaeosol, both Fe and Al are observed to have been gained and led to relatively high concentrations of iron oxide in the palaeosol. This is consistent with the fact that they have developed from highly weathered parent material, metasediments which are primarily rich in iron oxide minerals.

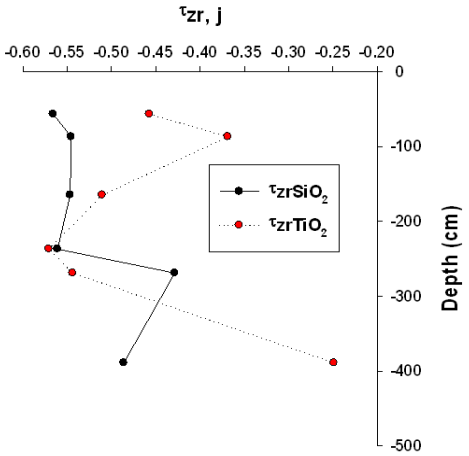

a

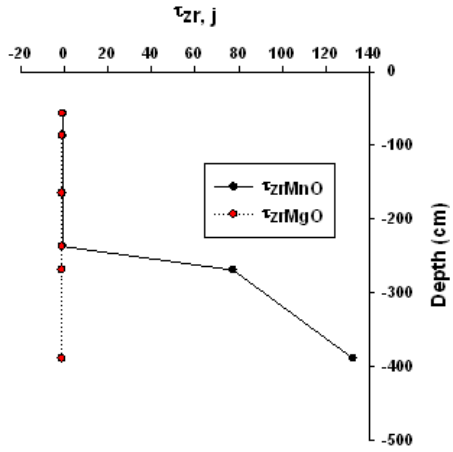

b

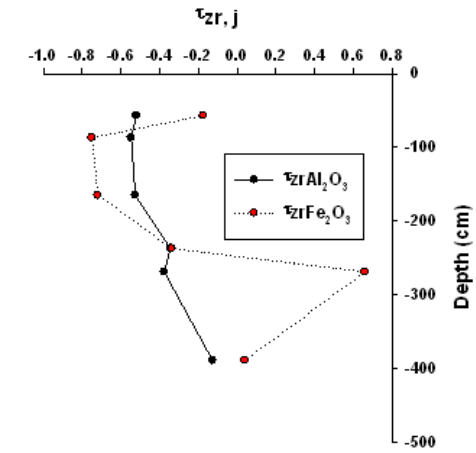

c

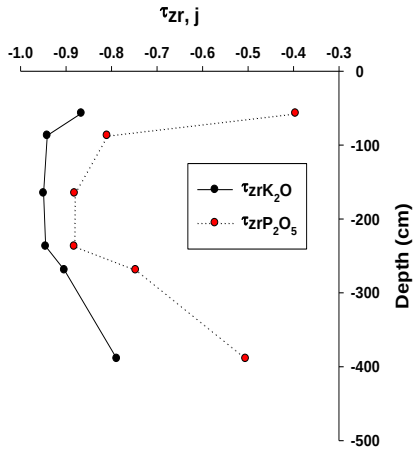

d

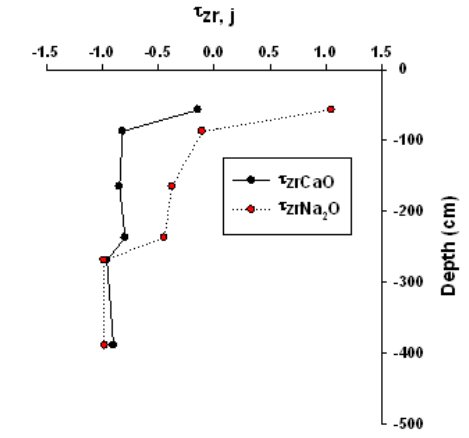

e

Fig. 5.4. Geochemical mass balance plots, (237cm is the abrupt boundary of the duplex pedon).

5.4.3.4. Chemical weathering indices

The higher leaching rate in the upper horizons is quite possibly as result of their texture as they indicate the highest percentage sand composition in the entire pedon. Sandy soils undergo higher leaching due to increased pore and macro-aggregate pore space. . The underlying palaeosols show the highest degree of hydrolysis. The result shows that the upper soil has higher Ti/Al values than the older buried palaeosol. In soils, Ti is more readily removed by physical weathering, whereas Al by chemical weathering (Sheldon and Tabor, 2009).

Table 5.5. Geochemical weathering indices of the duplex pedon

Horizon	ΣBases/Al	Al/Si	Ti/Al	K+Na/Al	Ba/Sr	CIA	CIW	WI-1	WI-2
A1	0.39	0.04	0.11	0.16	1.95	73.30	80.02	25.60	13.15
A2	0.18	0.03	0.14	0.07	3.28	89.31	93.77	67.86	20.70
E	0.15	0.04	0.10	0.06	3.35	91.38	95.15	66.58	19.90
2ABb	0.17	0.05	0.06	0.04	2.61	92.68	95.75	32.09	12.28
2BCg1	0.58	0.36	0.04	0.05	1.74	94.51	99.18	2.06	1.18
2BCg2	1.23	0.56	0.05	0.08	2.57	91.64	98.70	2.82	1.10

In this case the index confirms a much more advanced weathering stage of the buried soils than those at the surface. Values obtained in this study are comparable with those obtained by Sheldon (2006a) and Sheldon et al. (2009) while studying the Ti/Al ratios of moderately developed sandstone-parented and mudstone-parented palaeosols respectively. Degree of salinization, which was estimated using the (K+Na)/Al ratio, is consistently negligible throughout the pedon and suggests minimal soluble salt presence and activity within the profile. Hydrolysis and leaching were further evaluated using the Ba/Sr ratio. Strontium has higher solubility in soils than Barium (Sheldon and Tabor, 2009). Therefore the higher the ratio, the greater the activity of these pedogenic processes in the horizon. From the result, the two horizons (A2 and E) have undergone more leaching and hydrolysis than the other horizons. The high sand content of these horizons is consistent with this trend.

5.4.3.5 Micromorphology

Thin sections of the samples were studied with a petrographic microscope. The procedures of Bullock et al. (1985) and Stoopes (2003) were used in the interpretation of the thin sections. Groundmass, microstructure, void and pedofeatures were described for each sample from a specified horizon. A detailed summary of the properties is presented in Table 6. The micromorphological interpretation of the palaeoenvironment was based on the fact that some palaeosol features developed from the same process acting on modern soils (e.g Liu et al., 1987, Kemp et al., 1995).

5.4.3.5.1 Mineral components

The coarse mineral particles (>100 µm) of the A1, A2, E and ABb, developed from quartz arenite are dorminated by randomly scattered quartz and plagioclase, with some orthoclase feldspar. Other minerals include a few biotite micas (Fig. 5.5A-D). These samples also contain more coarse mineral fragments; they were well to moderately sorted medium to coarse sand (250-2000 µm). They are poorly-washed sands (Fig. 5A-D). Characteristically, most mineral grains in the "A1" and "A2" thin sections are loosely arranged with a single grain structure, simple packing voids and a monic related distribution (Fig. 5A, B) and constitute over 70% of the total thin section area (t.t.s.a). An intergrain microaggragete structure and complex packing voids with enaulic to chitonic related distribution is present in the poorly washed sand in alluvial/colluvial laid E and ABb horizons (Fig. 5.5C, D). Fines (<63 µm) mainly occur in soliflucted and silty to sandy clayey loam highly weathered meta sediment from which the BCbg1 and BCbg2 horizons developed. They are dense and abundant, and provide aggregation up to a porphyric related distribution (Fig. 5.5E, F).

In the stonelayer, which as noted marks a transition from one geological/ geomorphological event to the other, there is a heterogeneous mixture of imbricated, rounded to subrounded pebbles/ gravels of different sizes in a matrix of medium to coarse sandy soil fabric . Such deposition occurs as a result of the gradual waning of a debris-laden water current depositing finer materials as its velocity decreased and bioturbation.

5.4.3.5.2. Terrestrial humus characterisation

Low organic matter accumulation and high degree of bioturbation in sandy soils due to moles, molerats and ants would best describe current faunal and floral activities in the Cape

Peninsula. Organic matter traces were mostly evident in the surface horizons A1, A2 and ABb thin sections albeit in a very low amount. Dark patches on the sections are indicative of organic matter (Fig 5.5A, B, and D). Fresh roots and rootlets were mainly found throughout the pedon with the exception of the A1 horizon which showed few decaying organic matter. Compaction and post-burial alteration may likely be responsible for the virtually absence of organic matter in the buried palaeosols.

Table 5.6. Summary of the micromorphological description of the pedon

Horizon	Groundmass	Void and microstructure	Pedofeatures
A1	**C/F distribution**: porphyric to gefuric; **C/F limit**: clay/sand; **coarse component**: 70% of the t.t.s.a., silt and fine to coarse sand, smooth and spheroidal fracture, shape subrounded to high variability within random fabric associated with shape, elongated grains are randomly distributed; **fine component**: fabric: crystallitic b-fabric, 20% t.t.s.a	granular with simple to complex packing voids	Typic and hypo-coatings of iron oxides around sand grains; textural, fabric pedofeatures weakly separated; orientation of crumbs is parallel to the bottom of the horizon; size is variable within matrix; quasi clay coating on walls of peds; organic pigments.
A2	Groundmass is not prominent; **C/F limit**: clay/sand; **coarse component**: 70% of the t.t.s.a., fine to coarse sand, shape subrounded to subangular, high variability within random fabric associated with shape; fine component.	Single grain structure of quartz arenite loosely arranged with very little fine materials to provide aggregation	Textural, fabric pedofeatures weakly separated, is parallel to the bottom of the horizon; variable within the matrix; plant residues; 10% clay coatings.
E	Groundmass is not prominent; **C/F limit**: clay/sand; **coarse component**: 70% of the t.t.s.a., fine to coarse sand, shape subrounded to subangular, high variability within random fabric associated with shape; fine component.	Single grain structure of quartz arenite loosely arranged with very little fine materials to provide aggregation	Textural, fabric pedofeatures weakly separated, is parallel to the bottom of the horizon; variable within the matrix
2ABb	Groundmass is not prominent; **C/F limit**: clay/sand; **coarse component**: 80% of the t.t.s.a., fine to coarse sand, shape subrounded to subangular, high variability within random fabric associated with shape; fine component.	5% of the t.t.s.a granular structure of loosely arranged with very little fine materials to provide aggregation	Textural, fabric pedofeatures weakly separated, is parallel to the bottom of the horizon; variable within the matrix; coating of calcium carbonate

Table 5.6. continued.

Horizon	Groundmass	Voids and microstructure	Pedofeatures
2BCg1	**C/F distribution**: fine monic to chitonic; **C/F limit**: clay/sand; **coarse component**: 10% of the t.t.s.a., silt and fine sand, shape rounded to subrounded, moderate variability within random fabric associated with shape; **fine component**: 80% t.t.s.a., fabric: stipple-speckled b-fabric.	Abundance very variable within thin; section, about 5% of the t.t.s.a.; channels, chambers, and vughs; **channels and chambers**: walls covered by dusty hypo-coatings; random vesicles and vughs distribution, cloudy aspect of clay in all voids; **microstructure**: massive	Textural, fabric pedofeatures; pedality is strongly developed; compound iron oxide nodules; clay coatings; dense infillings; illuvial clay concentrations
2BCg2	**C/F distribution**: fine monic to chitonic; **C/F limit**: clay/sand; **coarse component**: 10% of the t.t.s.a., silt and fine sand, shape rounded to subrounded, moderate variability within random fabric associated with shape; **fine component**: 80% t.t.s.a., fabric: stipple-speckled b-fabric.	Abundance very variable within thin; section, about 5% of the t.t.s.a.; channels, chambers, and vughs; **channels and chambers**: walls covered by dusty hypo-coatings; random vesicles and vughs distribution, cloudy aspect of clay in all voids; **microstructure**: massive	Textural, fabric pedofeatures; pedality is strongly developed; compound nodules; coatings of iron oxides; dense infillings; illuvial clay concentrations

5.4.3.5.3 Pedological processes

5.4.3.5.3.1 Mineral component alteration

All horizons from the stonelayer and above showed poor mineral alteration and minimal chemical weathering. This is further supported by data on geochemical weathering intensity. Mineral components are generally fresh, subrounded to subangular (Fig 5.5A-D). Occasional reddish-brown Fe oxide and/or Fe hydroxide staining occurs along cleavage lines and fractures in some grains (Fig. 5.5C, D). Very few mineral components of the overlying horizons reveal evidence of mechanical cracking fissures indicating that they are disturbed and transported over short distance and not *in situ*. The low alteration of the mineral components suggests a very slow rate of weathering and most likely a short exposure time for pedogenic processes. On the other hand, the buried palaeosol displays a high degree of mineral component alteration. This is reflected in its high content of dense fine materials (Fig 5.5E, F). Advanced sericitization of mostly plagioclase feldspars is also observed.

5.4.3.5.3.2. Redoximorphic features (redox concentrations)

Conspicous redoximorphism is apparent in the deeply weathered buried palaeosols (Fig. 5.5E, F), with abundant reddish, brown-reddish, dark brown to black (PPL) Fe or ferromanganse. oxide and/or hydroxide segregations with sharp boundaries, aggregate to compound impregnative subrounded nodules. Simple, composite or nucleic nodules are also common.

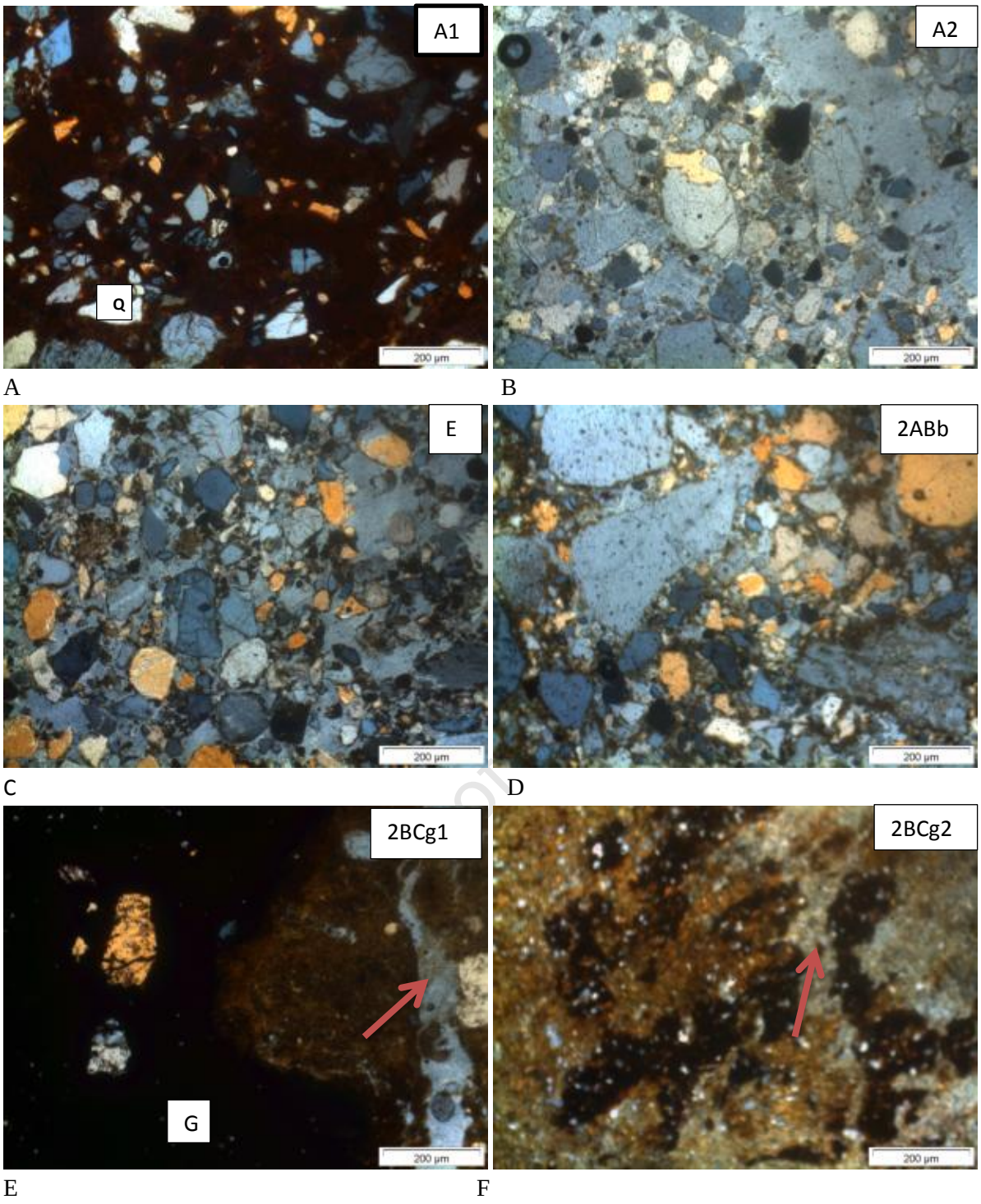

Fig. 5.5. Photomicrographs of the thin sections viewed under cross polarized light. Arrows shows the direction of the channel voids; Q is quartz grain; G is the redoximorphic iron rich groundmass.

Redoximorphism is associated with aquic conditions in the horizons with seasonal waterlogging and a fluctuating water table. One important pedogenic consequence of water table fluctuation is plinthization – the formation of plinthites in soils. Vepraskas et al. (1994) reported that nodules form when air penetrated slowsly into a wet matrix containing Fe (II) and Mn (II). Pore linings are also common (Fig 5.5F) along some ped surfaces. In wet soils, pore linings form when reduced Fe and Mn ions diffuse towards aerated macropores followed by susbsequent oxidation and precipitation (Vepraskas et al., 1994).

5.4.3.5.3.3. Translocation of fine particles

Few observable features are present in the thin sections to indicate translocation of fine materials (mostly silt and and clay coatings) which moderatly occurred in the moderately to poorly-washed sandy A1, A2 and E horizons. Infilling of packing voids in the sandy surface layers including the stonelayer bestows on them sandy textural pedofeature. Illuvial features occur as a result of textural variations and drainage conditions and are most likely associated with the present-day water seepage through the soil vadose layers. Evidence of prolonged translocation of organic to organo-iron coatings is generally rare in the mineral components of the alluvial/colluvial horizons. This therefore, signifies limited translocation and deposition of mobile substances in the unsaturated flow zones. The translocation of fine particles is however more pronounced in the buried palaeosols, as reflected in the redistribution of the chemical components leading the formation of Fe and Mn oxides/ hydroxides nodules within the soil fabrics.

5.4.3.5.3.4. Aggregates and matrix coatings

Surface horizons of the recent deposits show varying degrees of granular microstructures with weakly subrounded aggregates (Fig. 5.5C, D). Coatings are also abundantly evident in the redoximorphic buried palaeosols. Granular microstructures are associated with mechanical stresses and internal modifications in the alluvial/colluvial

sediments. Encircling coatings around grains and redoximorphic nodules are associated with a granostriated b-fabric (Todisco and Bhiry, 2008).

5.4.3.5.3.5. Geomorphological processes and anthropenic features

Throughout the pedon, the effect of processes associated with pedogenesis and weatheringare more pronounced than anthropogenic factors at the micromorphology level. In other words there is no conclusive evidence of sedimentation induced by human activities in particular at the footslope. Human influence, however, is evident in to the topmost "A1" horizon. Signs of human trampling and use of heavy machineries for road and house construction are locally shown by grains colliding with each other (Fig. 5.5A). This is further substantiated by the presence of plastic remnants seen in the surface horizon during field studies.

5.4.3.6 Clay mineralogy

Depending on age, soils show varying stages of minerological weathering due to rock-water interactions (Mareschal et al., 2011). The clay mineralogy of both the recent, overlying soil and the underlying palaeosol show a combination of different minerals. The soils and palaeosol are composed of mica, vermiculite, smectite, chlorite, kaolinite, paragonite, quartz, goethite gypsum, and interstratified minerals in varying quantities (Table 5.7). However, there is a contrast in the pattern of ditribution of these minerals above and below the stonelayer. Whereas micas, gypsum and halloysite are conspicoulsy absent in the buried palaeosol, smectite and goethite are obviously absent in the soils above the stonelayer. In soils and palaeosols, clay sized minerals rarely occur in isolation; rather they are typically composed of different mineral species (Wilson, 1999; Sheldon and Tabor, 2009).

Table 5.7. Clay mineralogy of the pedon

Horizon	Minerals
Ap	Halloysite, gypsum, micas, paragonite, smectite
Bw	chlorite, gypsum, vermiculite, mica
E	vermiculite, kaolinite, gibbsite, quartz
2ABb	Chlorite, Halloysite, kaolinite, mica
2Btssb1	Chlorite, paragonite, goethite, vermiculite-kaolinite
2Btssb2	chlorite-smectite, chlorite, kaolinite, paragonite, goethite, quartz

5.5. Discussion

Apparently, there has been translocation of colloidal soil materials across the duplex soil and this mixing is mostly evident in the stonelayer (2ABb1) (Fig. 5.3). The entire toeslope of the Devils peak appears to be covered by the same type of detrital quartz arenite as encountered in the pit. Although no absolute age is available for the arenite, the weak horizonation of the soils formed on it suggests they may be Quaternary. The soils are similar in degree of horizon development as Quaternary soils found elsewhere in the Western Cape (Department of Public Works, 2007).

Results of the macromorphological observations show dissimilarities among the horizons in some parameters (Table 5.1). This is basically due to the differences in parent materials and their age/ degree of weathering. The observations support the idea that the parent materials from which the upper soil developed were transported by either and/ or both water and gravity from the slope of the Devils peak mountain (Fig 5.2) and deposited at the footslope by sedimentary differentiation. The stonelayer, (ABb horizon) marks a transition of the pedon from an eluvial E horizon to buried BC horizons. The most likely situation is that this layer represents a palaeoerosion surface, an observation that is supported by the presence

of common plant roots and rootlets within the layer as imprints. In addition to having very smooth rounded to subrounded shapes, the stones are imbricated (overlapping one another, Fig. 5.3) in a manner that suggests they were transported and lean in the downslope ward direction of water flow. Most reported stonelayers associated with soils and palaeosols and are usually assumed to be of pedogenic origin. In South Africa, as in other midlatitude regions, soils with relatively thin biomantles and minimal bioturbation (Brink, 1985; Johnson 1990; Fey 2009) are regarded as formed from a combination of geological and geomorphological processes and this is assumed to be the case for the stonelayer in this pedon.

The environmental chemistry of Mn is largely governed by pH and redox conditions (LaZerte and Burling, 1990). Many factors could have accounted for the relatively increased MnO oxide in the subsoil. Anaerobic conditions are important in affecting dissolved Mn, for example, under waterlogged conditions, particulate manganese oxides are reduced (Stokes et al., 1988). The elevated Mn in the subsoil could have also come from the wash off from the upper slopes of the Devils peak mountain by hill-wash during the geological period when the stonelayer was deposited and subsequent leaching. Sources of the Mn pool in soils include bedrock, direct deposition from particulate manganese in the atmosphere, surface runoff and leaching (Stokes et al., 1988). Weathering of the parent sandstone and chelation with organic matter may have been responsible for the loss of Fe and Al on the uppermost soils (Wagai and Meyer, 2007). The waterlogged pedoenvironment of the palaeosol may have also contributed to increase Fe and Al oxides as elements are crystallized through dissolution. Anthropogenic inputs (sources from domestic homes) are the likely source of elevated Na_2O in the surface horizon.

The results (Table 5.6) support the conclusion that the 2BCg1 and 2BCg2 horizons are the most strongly weathered. The consistency of the results between different indices

suggests that they can be a reliable indicator of weathering. However, there are some inconsistencies in the values of CIA and CIW in relation to the younger soil horizons; while these two indices suggest that the eluvial "E" horizon has undergone more weathering than "A" horizons, both WI-1 and WI-2 indicate the opposite. CIA and CIW and WI-2 results imply a slightly higher weathering intensity for the stony horizon (stonelayer) than the overlying horizons, while the WI-1 results imply that the stonelayer is more strongly weathered than the "A2" and "E" horizons but less strongly weathered than the A horizon. The WI-1 and WI-2 indices are positively correlated with Si/Al (1/"clayeness"), suggesting they reflect weathering intensity. While both WI-1 and WI- 2 may be acceptable, the results of this study confirm that WI-2 is the most suitable index out of the four as a reliable indicator of weathering intensity.

The presence of smectite in the buried palaeosols is consistent with the conclusion of Borchardt (1989) who reported that the pedoenvironmental conditions needed for the formation of smectites include poor drainge condition, high soil pH and high chemical activity of silica and basic cations. These conditions are also accountable for the presence of goethite, an oxide of iron, in the clay mineral fraction of the soils through advanced weathereing of feldspar contained in the shale parent material. Kaolinite which occurs in association with the oxide and oxihydroxide of iron - goethite and gibbsite - in the subsurface horizons. According to Dixon (1989), pedogenic kaolinites form under well drained acidic soil condition with moderate silicate activity and is characteristic of warm humid climates. Kaolinite has also been reported as an abundant mineral in palaeosols that formed under palaeotropical climates (e.g. Gill and Yemane, 1996; Tabor and Montañez, 2004; Jacobs et al., 2005). Gypsum, on the other is a sedimentary evaporite deposit and this could only be seen in the two uppermost horizons of the pedon. This evaporite would most likely come from the ocean brine of the atlantic ocean which flows not far from this location. Gypsum has

been reported to form from saline lakes and salt pans (e.g. Last and Schweyen, 1983; Schreiber and Tabakh, 2000). Micas in the soils were dominated by the species paragonite. Paragonite is present in both the soil and palaeosols. This further supports that there is a wide variety of micas occurrence in soil environment. The origin of micas in these soil samples could be attributed to deposition by fluids circulating during both contact and regional metamorphism as the Cape Peninsula was once submerged under water ~560 millions of years ago (Compton, 2004). Micas occur in a large range of rocks and over 28 species are known

Regional climate or local geomorphic controls on palaeoenvironment

From the results of the samples collected from the soils and palaeosols at the foot slope of the Devils peak mountain, it is very obvious that the the Cape Peninsula has witnessed significant palaeoenvironmental and climatic oscillations. Al though absolute ages are not available for these samples, some inferences are possible about their formational environments deduced from the range of parameters analysed and discussed above.

Soils developed under Mediterranean climate generally contains small amounts of iron oxides (Torrent and Barron, 1993). The impacts of iron oxides on soil properties are diverse, of which colour is the most marked under mediterranean-climate conditions. Soil reddening (rubifaction) is prompted by pedogenic hematite formation. The strongly contrasting colours of the duplex pedon obviously suggests a major shift in the pedoenvironmental and climatic conditions that lead to their formation and their age. We argue that the underlying red palaeosol formed under a humid tropical to subtropical climate, which favoured the formation of hematite. Hematite forms by a dehydration-recrystallisation process under an elevated temperature regime. We also report that the temperature at the time of their formation should ideally be warm. Smectite as observed in the mineralogy studies

further supports this. Micas, kaolinite and quartz in the underlying palaeosols clearly indicate advanced chemical weathering and regional metamorphism of the parent rock.

The formation of interstratified clay minerals (in the palaeosol) is generally associated with soils developed in humid climates, where it forms an important ephemeral stage during the transformation of smectite to kaolinite (Srivastava and Parkash, 1998). The presence of these minerals also suggests a more advanced weathering stage than is observed in the overlying soils.

Clay illuviation was operational during both arid and humid climates hence the presence of clay micas across the pedon. A more intense illuviation of clays durring the wetter and warmer climate may have also resulted in the argillic horizon of the palaeosols increasing in thickness with the age of the soil. This trend has also been reported by Srivastava et al. (1994). Thus the major operational pedogenic processes in the recent overlying soils include illuviation, slow organic matter mineralization, podzolization and cumulization. Such processes have been reported in the Quaternary deposits of the Western Cape during the Holocene (Roberts and Brink 2003). In contrast, major pedogenic processes in the buried late Precambrian palaeosols have included rubefaction, gleization, plinthization.

5.6. Conclusions

Soils and sediments are the largely undiscovered books of the past. The soils at the base of the southern slope of Devils Peak Mountain have a duplex morphology – a pedologically younger soil horizons overlying a buried red palaeosol with vertic properties. Variation in parent material emerges therefore as the major reason for textural differences shown in the pedon. These soils have strongly contrasting properties which points to the fact that there have been climatic oscillations since the inception of their pedogenesis. This claim is strongly supported by the evidence from the macro- and micromorphology of the soils,

their geochemical weathering indices and climofunctions, and clay mineralogy. This implies that the temperature at the time was a little lower and precipitation was higher. We advice that caution is required when using geochemical weathering indices for obtaining palaeoclimatic information from palaeosols because these weathering indices are not only sensitive to climate but also to soil age. Moreover, the degree of weathering decreases with soil depth; in an eroded palaeosol the most strongly weathered upper part may have been removed so that only the weathering index of the lower part is available. Hence, both soil age and erosion need to be considered in order to obtain reasonable palaeoclimatic information.

Reference

Allsopp, H. L, Kolbe, P., 1965. Isotopic age determinations on the Cape Granite and intruded Malmesbury sediments, Cape Peninsula, South Africa, Geochimica et Cosmochimica Acta 29 (10), 1115-1130.

Barrón, V., Torrent, J., 1987. Origin of red-yellow mottling in a Ferric Acrisol of southern Spain. Zeitschrift für Pflanzenernährung und Bodenkunde 150, 308–313.

Barron, V., Torrent, J., 1986. Use of the Kubelka–Munk theory to study the influence of iron oxides on soil colour. Journal of Soil Science 37, 499–510.

Belcher, R.W., Kisters, A. F. M., 2003. Lithostratigraphic correlations in the western branch of the Pan-African Saldania belt, South Africa: the Malmesbury Group revisited. South African Journal of Geology 106, 327-342.

Borchardt, G., 1989. Smectites. In: Dixon, J.B., Weed, S.B. (Eds.), Minerals in Soil Environments. Soil Science Society of America, Madison, pp. 675–727.

Bouyoucos, J. B., 1962. Hydrometer method for making particle-size analysis of soils. Agronomy Journal 54, 464–465.

Bullock, P., Fedoroff, N., Jongerius, A., Stoops, Tursina, G., Babel, U., 1985. Handbook for Soil Thin Section Description. Waine Research Publications - Wolverhampton (U.K.), 152 p.

Brimhall, G. H., Lewis, C. J., Ford, C., Bratt, J., Taylor, G., Warin, O., 1991 Quantitative geochemical approach to pedogenesis: importance of parent material reduction, volumetric expansion, and eolian influx in lateritization, Geoderma 51 (1–4), 51-91.

Brink, A. B.A., 1985. Engineering Geology of Southern Africa 4: Post-Gondwana Deposits. Building Publications, Pretoria, S. Africa.

Chadwick, O.A., Brimhall, G.H., Hendricks, D.M., 1990. From a black to a gray box — a mass balance interpretation of pedogenesis. Geomorphology 3, 369–390.

Compton, J.S., 2004. The Rocks and Mountains of Cape Town. Juta and Co Ltd., Cape Town 114pp.

Cowling, R. M., MacDonald, I. A. W., Simmons, M. T., 1996. The Cape Peninsula, South Africa: physiographical, biological and historical background to an extraordinary hot-spot of biodiversity. Biodiversity & Conservation 5, (5) 527-550

Darmody, R. G., Thorn, C. E., Allen, C. E., 2005. Chemical weather and boulder mantles, Kärkevagge, Swedish Lapland. Geomorphology 67, 159–170.

Department of Public Works, 2007. Identification of Problematic Soils in Southern Africa. Technical notes for Civil and Structural Engineer. 75 pp.

Dixon, J.B., 1989. Kaolin and serpentine group minerals, In: Dixon, J.B., Weed, S.B. (Eds.), Minerals in Soil Environments, 2nd edition. Soil Science Society of America, Madison, pp. 467–525.

Du, X., Rate, A.W., Gee, M., 2010. Geochemical mass-balance in intensely weathered soils, Darling Range, Western Australia. 19th World Congress of Soil Science, Soil Solutions for a Changing World 1 – 6 August 2010, Brisbane, Australia. Published on DVD.

Driese, S. G., Nordt, L. C., Lynn, W.C., Stiles, C. A., Mora, C. I., Wilding, L. P., 2005. Distinguishing climate in the soil record using chemical trends in a Vertisol climosequence from the Texas coast prairie, and application to interpreting Paleozoic paleosols in the Appalachian Basin, U.S.A. Journal of Sedimentary Research 75(3), 339-349.

FAO-UNESCO, 1998. World reference base for soil resources. World Soil Resource Reports, Vol. 84, UNESCO, Rome, p. 88.

FAO (Food and Agricultural Organisation of the United Nations), 1977. Guideline for Soil Profile Description, 2nd ed., p. 3-49, SRDCS, Land and Water Development Division, Rome.

Fey, M.V. 2009. Soils of South Africa. Stellenbosch University, Stellenbosch, South Africa. Craft Printing International, Ltd, Singapore

Gill, S., Yemane, K., 1996. Implications of a Lower Pennsylvanian Ultisol for equatorial Pangean climates and early, oligotrophic, forest ecosystems. Geology 24, 905-908.

Harnois, L., 1988. The CIW index: a new chemical index of weathering. Sedimentary Geology 55, 319–322.

Harris C., Burgers, C., Miller J., Rawoot F., 2010. O- and h-isotope record of Cape Town rainfall From 1996 to 2008, and its application to recharge Studies of table mountain groundwater, south Africa. South African Journal of Geology 113.1 33-56.

Heal, K. V. 2001. Manganese and land-use in upland catchments in Scotland. Science of the Total Environment 265 (1 –3), 169–179.

Hurst, V.J., 1977. Visual estimation of iron in saprolite. Geol. Soc. Amer. Bull. 88, 174–176.

Jacob, D. J., Field, B. D., Li, Q., Blake, D. R., de Gouw, J., Warneke, C., Hansel, A., Wisthaler, A., Singh, H. B., Guenther, A., 2005. Global budget of methanol: Constraints from atmospheric observations, Journal of Geophysical Research 110, D08303, doi:10.1029/2004JD005172.

Johnson, D. L., 1989. Subsurface stone lines, stone zones, artifact-manuport layers, and biomantles produced by bioturbation via pocket gophers (Thomomys bottae). American Antiquity 54, 292-326.

Johnson, D.L., 1990. Biomantle evolution and the redistribution of Earth materials and artifacts. Soil Science 149, 84–102.

Johnson, D.L., 1995. Reassessment of early and modern soil horizon designation frameworks and associated pedogenetic processes: Are midlatitude A E B-C horizons equivalent to tropical M S W horizons? Soil Science (Trends in Agricultural Science) 2, 77–91.

Johnson, D. L., 2002. Darwin would be proud: Bioturbation, dynamic denudation, and the power of theory in science. Geoarchaeology 17 (1–2), 7–40 and 631–632.

Johnson, D.L., Domier, J. E. J., Johnson, D. N., 2005a. Reflections on the nature of soil and its biomantle. Annals, Association of American Geographers95 (1), 11–31.

Johnson, D.L., Domier, J. E. J., Johnson, D. N., 2005b. Animating the biodynamics of soil thickness using process vector analysis: A dynamic denudation approach to soil formation. Geomorphology 67 (1–4), 23–46.

Kemp. R. A., Derbyshire, E., Meng X. M., Chen, F. H., Pan, B. T., 1995. Pedosedimentary reconstruction of a thick loess-paleosol sequence near Lanzhou in north central China. Quaternary Research 43, 30–45.

Laporte, G.,1962. Reconnaissancepe´dologique le long De La voie ferre´e COMILOG. Officedela Recherche Scientifique et Techniqued'Outre- Mer (ORSTOM-IRSC), Paris,149 pp.

Last, W. M., Scheweyen, T. H., 1990. Sedimentology and geochemistry of saline lakes of the Great Plains. Hydrobiologia 105(1), 245-263.

LaZerte, B. D., Burling, K. 1990. Manganese speciation in dilute waters of the Precambrian Shield, Canada. Water Research, 24, 1097–1101.

Lowenstein, T. K., Hardie, L. A., 1985. Criteria for the recognition of salt-pan evaporates. Sedimentology 32 (5), 627–644 DOI: 10.1111/j.1365-3091.1985.tb00478.x

Liu, T.S., Zhang, S. X., and Han, J. M., 1987. Stratigraphy and palaeoenvironmental changes in the loess of central China. Quaternary Science Reviews 6, 489-501.

Mareschal, L., Nzila, J. D. D., Turpault, M. P., M'Bou, A. T., Mazoumbou, J. C., Bouillet, J. P., Ranger, J., Laclau, J. P., 2011. Mineralogical and physico-chemical properties of Ferralic Arenosols derived from unconsolidated Plio-Pleistocenic deposits in the coastal plains of Congo. Geoderma 162, 159–170.

Maynard, J.B., 1992. Chemistry of modern soils as a guide to interpreting Precambrian paleosols. Journal of Geology 100, 279–289.

Morrás, H., Moretti, L., Píccolo, G., Zech., W., 2009. Genesis of subtropical soils with stony horizons in NE Argentina: Autochthony and polygenesis. Quaternary International, 196 (1-2), 137–159.

Munsell Color Co., 2000. Munsell Soil Color Charts. Gretag Macberth, New York.

Nesbitt, H.W., Young, G.M., 1984. Prediction of some weathering trends of plutonic and volcanic rocks based on thermodynamic and kinetic considerations. Geochimica et Cosmochimica Acta. 48, 1523–1534.

Nesbitt, H.W., Young, G.M., 1982. Early Proterozoic climates and plate motions inferred from major element chemistry of lutites. Nature 299, 715–717.

Osher, L. J., Buol, S. W., 1998. Relationship of soil properties to parent material and landscape position in eastern Madre de Dios, Peru, Geoderma 83 (1–2), 143-166.

Pagotto, C., Remy, N., Legret, P., Cloirec, L., 2001. Heavy Metal Pollution of Road Dust and Roadside Soil near a Major Rural Highway Environmental Technology 22 (3), 307-319.

Plains, C. I., Srivastava, P., Parkash, B., 1998. Clay Minerals in Soils as Evidence of Holocene Climatic Change, *239*, 230–239.

Reth, S., Reichstein, M., Falge, E., 2005. The effect of soil water content, soil temperature, soil pH-value and the root mass on soil CO_2 efflux – A modified model**.** Plant and Soil 268 (1), 21-33.

Roberts D. L., Brink, J. S. 2003. Dating and correlation of Neogene coastal deposits in the Western Cape (South Africa): Implications for Neotectonism. South African Journal of Geology 105 (4), 337-352.

Ruhe, R. V., J. G. Cady, J.G., 1954. Latosolic soils of central African interior high plateaus. Transactions of the Fifth International Congress of Soil Science 4: 401-407.

Ruhe, R. V., 1959. Stone lines in soils. Soil. Sci. 87, 1959.

Sharpe, C. F. S., 1938, Landslides and related phenomena. New York, Columbia Univ. Press, 137 p.

Soil Survey Staff, 2006. Keys to Soil Taxonomy, 10th ed. USDA-Natural Resources Conservation Service,Washington, D.C. 341 pp.

Soil Survey Division Staff, 1993. Soil survey manual. Soil Conservation Service. U.S. Department of Agriculture Handbook, 18. 532 pp.

Soil Survey Staff, 1975. Soil Taxonomy: United States Department of Agriculture Handbook no. 436.Washington D.C., 754 pp.

Stiles, C.A., Mora, C.I., Driese, S.G., 2001. Pedogenic iron-manganese nodules in Vertisols: a new proxy for paleoprecipitation? Geology 29, 943–946.

Rawlins, B. G., Webster, R., Lister, T. R., 2003. The influence of parent material on topsoil geochemistry in eastern England. Earth Surface Processes and Landforms 28 (13), 1389–1409.

Retallack, G.J., 1999. Postapocalyptic greenhouse paleoclimate revealed by earliest Triassic paleosols in the Sydney Basin, Aus- tralia. Geological Society of America Bulletin 111, 52–70.

Rozendaal, A., Gresse, P.G., Scheepers, R. and Le Roux, J.P., 1999. Neoproterozoic to early cambrian Crustal Evolution of the Pan-African Saldania Belt, South Africa. Precambrian research, 97, 303-323.

Sariyildiz, T., Anderson, J. M., Kucuk, M., 2005. Effects of tree species and topography on soil chemistry, litter quality, and decomposition in Northeast Turkey, Soil Biology and Biochemistry 37 (9), 1695-1706.

Sawyer, E.W., 1986, The infl uence of source rock type, chemical weath- ering and sorting on the geochemistry of clastic sediments from the Quetico metasedimentary belt, Superior Province, Canada: Chemical Geology, 55, 77-95.

Schaetzl, R.J., Anderson S., 2005. Soils - Genesis and Geomorphology. Cambridge U. Press, U.K.

Schulze, D. G., Nagel, J. L., Van Scoyoc, G. E., Henderson, T. L., Baumgardner, M. F., Stot, D. E., 1993. Significance of Organic Matter in Determining In: Soil Colors. Bigham, J. M., Ciolkosz, E. J., (eds.) Soil Science Society of America Special Publication 31. p. 71-90.

Schwertmann, U., 1993. Relations Between Iron Oxides, Soil Color, and Soil Formation. In: Soil Colors. Bigham, J. M., Ciolkosz, E. J., (eds.) Soil Science Society of America Special Publication 31. pp 51-69.

Schreiber, B.C., El Tabakh, M., 2000. Deposition and early alteration of evaporites. Sedimentology, 47, 215–238.

Ségalen, P.,1994. Les sols ferrallitiques et leur re´partition ge´ographique. ORSTOM E´ditions, Office De La Recherche Scientifiqueet Technique d'Outre-Mer, Paris,Tome 1,198 pp.

Sheldon, N. D., 2006a. Abrupt chemical weathering increase across the Permian–Triassic boundary. Palaeogeography Palaeoclimatology Palaeoecology 231, 315–321.

Sheldon, N.D., 2006b. Precambrian paleosols and atmospheric CO_2 levels. Precambrian Research 147, 148–155.

Sheldon, N. D., Tabor, N. J., 2009. Quantitative paleoenvironmental and paleoclimatic reconstruction using paleosols, Earth-Science Reviews 95 (1–2),1-52.

Sheldon, N.D., 2009. Non-marine records of climatic change across the Eocene-Oligocene transition. In: Koeberl, C., Montanari, A. (Eds.), The Late Eocene Earth - Hothouse, Icehouse, and Impacts: Geological Society of America Special Paper 452, 241–248.

Simon, A., Larsen, M. C., Hupp, C. R., 1990. The role of soil processes in determining mechanisms of slope failure and hillslope development in a humid-tropical forest eastern Puerto Rico. Geomorphology 3 (3–4), 263-286.

Stokes, P. M., Campbell, P. G. C., Schroeder, W. H., Trick, C., France, R. L., Puckett, K. J., LaZerte, B., Speyer, M., Hanna, J. E., Donaldson, J., 1988. Manganese in the Canadian environment. Ottawa, Ontario, National Research Council of Canada, Associate Committee on Scientific Criteria for Environmental Quality (NRCC No. 26193).

Stoops, G., 1989. Contribution of in situ transformations to the formation of stone-layer complexes in Central Africa. Geo-Eco-Trop 11 (1–4), 139–149.

Stoops, G., 2003. Guidelines for the Analysis and Description of Soil and Regolith Thin Sections. SSSA. Madison, WI., 184pp + CD.

Srivastava, P., Parkash, B., Sehgal, J.L., Kumar, S., 1994. Role of neotectonics and climate in development of the Holocene geomorphology and soils of the Gangetic Plains between the Ramganga and Rapti rivers. Sediment. Geol. 92, 129–151.

Strawn, D., Doner, H., Mavrik, Z., McHugo, S., 2002. Microscale investigation into the geochemistry of arsenic, selenium, and iron in soil developed in pyritic shale materials, Geoderma 108 (3–4), 237-257.

Todisco, D., Bhiry, N., 2008. Micromorphology of periglacial sediments from the Tayara site, Qikirtaq Island, Nunavik (Canada), CATENA 76 (1), 1-21.

Tabor, N. J., Montañez, I. P., 2005. Oxygen and hydrogen isotope compositions of Permian pedogenic phyllosilicates: Development of modern surface domain arrays and implications for paleotemperature reconstructions, Palaeogeography Palaeoclimatology Palaeoecology 223 (1–2), 127-146.

Torrent, J., Schwertmann, U., Fechter, H. and Alferez, F., 1983. Quantitative relationships between soil color and hematite content. J. Soil Sci., 136(6): 354-358.

Torrent, J., Schwertmann, U., Schulze D. G.,1980. Iron oxide mineralogy of some soils of two river terrace sequences in Spain. Geoderma 23, 191-208.

Van Wambeke, A., Eswaran, H., Herbillon, A., Comerma, J., 1983. Oxisols. In: Wilding, L., Smeck, N., Hall, G. (Eds.), Pedogenesis and Soil Taxonomy. II. The Soil Orders. Elsevier, Amsterdam, pp. 325–354.

Vepraskas, M.J., Wilding, L.P., Drees, L.R., 1994. Aquic conditions for soil taxonomy: Concepts, soil morphology, and micromorphology. In: Ringrose-Voase, A.J., Humphries, G.S. (Eds.), Soil Micromorphology: Studies in Management and Genesis. Proceedings of the 9th Working Meeting on Soil Micromorphology, Townsville, Australia, July 12–17, 1992. Developments in Soil Science, vol. 22. Elsevier, Amsterdam, pp. 117–131.

Wagai, R., Mayer, L. M., 2007. Sorptive stabilization of organic matter in soils by hydrous iron oxides Geochimica et Cosmochimica Acta 71, 25–35.

Watson, J.P., 1961. Some observations on soil horizons and insect activity in granite soils. First Federal Science Congress, Proceedings, 1960, Salisbury, Southern Rhodesia, v. 1, pp. 271–276.

Williams, M.A.J., 1968. Termites and soil development near Brocks Creek, Northern Australia. Australian Journal of Science 31, 153–154.

Wilson, M. J., 1999. The origin and formation of clay minerals in soils; past, present and future perspectives. Clay Minerals 34(1), 7-25.

Yaalon, D. H., 1997. Soils in the Mediterranean region: what makes them different? CATENA 28 (3–4), 157-169.

CHAPTER SIX
SYNTHESIS AND CONCLUSION

6.1. Background

Given the size and incredible diversity which characterizes the physical geography of the Western Cape, South Africa, it might be assumed that most of its palaeosols would have been better characterised and described. More attention has been directed to its landscape geomorphology, geology, modern soils, climate, biodiversity and archaeology. Aside from the geochronology and stratigraphic correlations (Bateman et al., 2004, 2011; Dunajko and Bateman, 2010; Roberts et al., 2008, 2009, 2011), there is a marked lack of data on palaeosols from the region. Indeed, prior to this study, there has virtually been no palaeopedological characterisation of the studied location.

Though palaeosols are widely and reliably used for palaeoclimatic and palaeoenvironmental reconstructions, however, such detailed palaeosol studies are still lacking in the Western Cape. Chase and Meadows (2007) reviewed the dearth of continuous palaeoenvironmental proxies in South Africa. This is further evident from Jansen et al. (2007) work on palaeoclimate reconstructions were obtained from the Northern Hemisphere. Palaeosols represent a direct means of palaeoclimatic reconstruction because soils form at the Earth's surface, in direct contact with contemporary atmospheric and climate conditions (Sheldon and Tabor, 2009). The study of palaeosols has evolved from the "classic" qualitative field based comparisons to modern analogues to semi-quantitative and quantitative discipline. Palaeoenvironmental and palaeoclimate properties that have been successfully reconstructed include chemical weathering intensity, mineral provenance, nutrient fluxes in and out of the palaeosols, mean annual temperature and precipitation during pedogenesis.

Thus, seeing the importance of palaeosols in palaeoclimatic reconstructions and the lack of such studies in the geoarchaeological and geomorphological significant locations in the Western Cape, detailed palaeopedological investigations have been carried out so as to bridge

this gap in our knowledge. This chapter provides a synthesis of the four major components of a research focused on the palaeosol-sediment sequences and is the first of its kind. The overarching aim of this study is to demonstrate the potential of palaeosol analysis in improving the understanding of the palaeoenvironments and palaeoclimate dynamics in the region. The specific objectives include:

i) to characterise the selected palaeosols and pedosediments using their macro- and micro-morphological, physical, mineralogical and geochemical properties;
ii) to interpret depositional history, dominant pedogenic and geomorphic processes (autogenic and allogenic) that shaped the geomorphology of the study areas – landscape and palaeoenvironmental reconstruction including evaluation of selected geochemical climofunctions, weathering intensity and palaeohydrology;
iii) and to use C and O isotopic composition of palaeosol carbonate to reconstruct palaeoclimate through the estimation of ancient MAP and MAT conditions during pedogenesis.

6.2. Framework

One of the greatest limitations to the study of palaeosols is accessibility. This arises out of the fact that most palaeosols are buried under sedimentary successions, which means exposures are rate and examination may entail excavation, sometimes with heavy equipment. In this study however, palaeosols already exposed by quarry activities and natural processes have been sampled. The ages of the palaeosols have been assigned from the already published geochronological dates. Palaeosols were identified (cf. Chapter 1) and distinguished from pedosediments. The materials and methods applied in this research are documented fully in Appendix II. The palaeosols and pedosediments are described and named according to FAO (2006) and Soil Survey Staff (2010).The pedogenic horizons were selected in order to give a representative overview of Bw, Bt and Ck horizons. Larger

accumulations of pedogenic carbonates in a horizon are named as Bk horizons. Four locations were chosen for the study, viz:

a) Late Cenozoic coastal sedimentary environment at the West Coast Fossil Park, Langebaanweg (32°57′ S and 018°06′ E). LBW is well renowned for its rich geo-archaeological heritage. It is a pedocomplex with at least ten sequences of palaeosols and diagenetic pedosediments;
b) Late Quaternary palaeosols at Goukamma Nature Reserve (34°02′ S and 022°50′ E). This is a long stretch (~1km) of a coastal barrier whose steeper eastern escarpment is exposed to the warm Agulhas ocean current of the Indian Ocean and the western escarpment slopes more gradually inland;
c) Late Quaternary carbonate palaeosols exposed in a coastal cliff face at Koeberg (33°37′ S and 018°23′ E). The Western escarpment of the cliff is exposed to the cold Benguela currents of the Atlantic Ocean while the eastern escarpment slopes gradually inlands; and
d) A duplex soil profile that formed on deeply weathered Neoproterozoic metasediments on the Cape Peninsula (33°58′ S and 18°27′ E). Because there is no precise geochronology for this particular site, this study was limited to the use of qualitative and semi-quantitative approaches to infer palaeoenvironmental changes.

Palaeosol-based proxies explored in this thesis include selected physicochemical properties, micromorphology, total element geochemistry, clay mineralogy, and stable $\delta^{13}C$ and $\delta^{18}O$ isotope signatures in pedogenic of the carbonates. The justification and suitability of these proxies for palaeoenvironmental and palaeoclimate reconstruction are thoroughly explored in the respective chapters of the thesis where they were applied.

6.3. Synthesis of key findings

Suffice to say, this study has convincingly demonstrated, for the first time, that palaeosol-based proxies in the Western Café can be used to reinforce evidence of global palaeoenvironmental and palaeoclimatic oscillations reported in earlier studies (e.g. Adams et al., 1999; deMenocal, 2005; Fedorov et al., 2006; Thompson et al., 2006). It has been investigated in the study that quantitative palaeoclimate values for Western Cape can be calculated from geochemical climofunction models and the results are reasonably reliable and consistent with global trends. In line with the objectives, following are the specific contributions of the present work:

- Weathering intensities and pedogenesis infered from the geochemical properties suggest chemical weathering and soil formation at LBW was more pronounced in the mid-Miocence than in the Quaternary indicating a more humid and warmer climate with a more stable landscape that minimized erosion.
- For palaeosol-sediment-sequences with marine/ estuarine parent material as at LBW, the use of CIA and CIW to evaluate weathering intensity/ pedogenesis is more appropriate than the WI-1 and WI-2 weathering indices of Darmody et al. (2005) which gives inconsistent results.
- Various pedofeatures as revealed- from the micromorphological study of these palaeosols suggest cyclic patterns of erosion and deposition processes and are further well in conformity with past climate changes.
- Laterization are the principal pedogenic processes responsible for the red palaeosol formation at the Cape Peninsula, while calcification and salinization are accountable for all the Quaternary palaeosols. Inferences of gleization and lessivage are only evident in the mid-Miocene palaeosol at Langebaanweg.

- The fibrous clay minerals (palygorskite and sepiolite) common in the carbonate palaeosols suggest the Quaternary palaeoclimate of the Western Cape coast has been characterised by low precipitation (<300 mm yr^{-1}) and dry conditions. This is in agreement with the early reports obtained from marine records of the African continent (deMenocal, 2005). At precipitation values in excess of 300 mm yr-1, palygorskite and sepiolite is weathered into smectite.
- The palaeo-MAT computed from a palaeosol carbonate oxygen isotope is 14 ^{o}C and 12^{o}C for Koeberg and Goukamma respectively during pedogenesis, while the maximum MAP obtained from the cambic horizon (Bw) of Goukamma coastal barrier is 653 mm yr^{-1}. It should be recalled that the standard error (SE) of the MAP model is ±181 mm yr^{-1}. The details of the applied climofunctions are fully described in the respective chapters of the thesis where they were applied. The MIS 4 palaeoclimate of the Koeberg and Goukamma Nature Reserve therefore fall into cool and fairly moist.
- A cross plot of the $\delta^{13}C$ and $\delta^{18}O$ values of the pedogenic carbonate using Zeebe and Wolf-Gladrow (2003) model indicates they all formed under strong marine influence and C3 plants have been dominant since late Quaternary,
- In evaluating weathering/ pedogenesis for the Quaternary palaeosols at Koeberg and Goukamma, low levels of Aluminum (Al) in the parent materials invalidated the applicability of chemical weathering indices (CIA) to assess weathering intensity. In the case of chemical index of weathering (CIW), the age and sedimentary settings of the palaeosols overruled the possibility for K metasomatism and illitization by metamorphism. WI-1 and W1-2 of Darmody et al. (2005) found to be more consistent with results;
- the duplex soil on the Cape Peninsula gives evidence of that two major regional climate cycles are in evidence. A relatively warm and humid subtropical climate which gave rise

to the formation of the buried red vertic palaeosol and a drier, more seasonal humid Mediterranean climate under which the soils overlying the stone line are currently forming, as inferred from poor horizonation and translocation of colluvial materials. The stone layer appears to have been deposited as a lag by a palaeoriver as the energy decreased and the material was later mixed with the soil matrix by turbation;

6.4. Conclusion

African climate is influenced by major tectonic changes, global climate oscillations, and local variations in orbital forcing; better known as Milankovitch cycles and this study demonstrates that the palaeosols in the Western Cape are good indicators of climate change. Indeed, these palaeosols, if analysed with care and caution are very reliable terrestrial proxies for palaeoenvironmental and palaeoclimate reconstructions and ; in many ways, their results are in allignment with earlier studies using marine proxies. The results of the evaluated geochemical climofunctions suggest that more data are obviously needed for a more robust calibration of the models in the Western Cape palaeosols. Great care is required when using geochemical weathering indices for obtaining palaeoclimatic information from palaeosols sequences because these weathering indices are not only sensitive to climate but also to soil age. Moreover, the degree of weathering decreases with soil depth; in an eroded palaeosol profile, the most strongly weathered upper part may have been removed so that only the weathering index of the lower part is available. Overprints, most times, are typical of palaeosol sequences and this could compromise the data quality especially at the top horizons. Hence, both soil age and erosion need to be considered in order to obtain accurate palaeoclimatic information.

In combination with other proxies such as pollen and marine sediment-based isotopes, palaeosols may continue to provide a high spatio-temporal insight into the environmental and climate oscillations in the Southern Hemisphere.

6.5. Directions for future research

Most global scale reconstructions of palaeoclimates are from proxies obtained from Northern Hemisphere localities (e.g. Jansen et al., 2007). It is necessary also to use palaeoclimate data based on proxies from the Southern Hemisphere as a means of comparing global climate changes. The use of palaeosol-based proxies can augment the vast array of other global palaeoclimate studies. Palaeopedology has evolved from the "classic" qualitative description of soils and palaeosols to a more quantitative modelling approach. However, most of the models thus far available were developed from soil database mostly from the Northern Hemisphere. Obviously, the spatio-temporal variation of soils should be taken into account while applying these climofunction models in the southern hemisphere and South Africa in particular knowing that climate has a strong influence on soil formation. Research directed at collating a robust data set of soil properties including clay mineralogy, physico-chemical and geochemical properties of modern soils in Southern Africa would be step in the right direction. This would enable a more localized development and calibration of pedogenic models. Consequently, this would provide more detailed insights as to the rates of soil forming processes and also make for a development of a more accurate and applicable geochemical climofunction-based models for the region.

Reference

Adams, J., Maslin, M., Thomas, E., 1999. Sudden climate transitions during the Quaternary. Progress in Physical Geography 23(1), 1–36.

Bateman, M.D., Carr, A.S., Dunajko, A.C., Holmes, P.J., Roberts, D.L., McLaren, S.J., Bryant, R.G., Marker, M.E., Murray-Wallace, C. V., 2011. The evolution of coastal barrier systems: a case study of the Middle-Late Pleistocene Wilderness barriers, South Africa. Quaternary Science Reviews 30, 63–81.

Bateman, M.D., Holmes, P.J., Carr, A.S., Horton, B.P., Jaiswal, M.K., 2004. Aeolianite and barrier dune construction spanning the last two glacial–interglacial cycles from the southern Cape coast, South Africa. Quaternary Science Reviews 23, 1681–1698.

Baxter, A.J., Meadows, M.E., 1999. Evidence for Holocene sea level change at Verlorenvlei, Western Cape, South Africa. Quaternary International 56, 65–79.

deMenocal, P. B., 1995. Plio-Pleistocene African Climate. Science 270 (5233), 53-59.

Chase, B. M. and Meadows, M. E., 2007. Late Quaternary dynamics of southern Africa's winter rainfall zone. Earth-Science Reviews 84(3-4), 103-138.

Darmody, R.G., Thorn, C.E., Allen, C.E., 2005. Chemical weathering and boulder mantles, Kärkevagge, Swedish Lapland. Geomorphology 67, 159–170.

Dunajko, A.C., Bateman, M.D., 2010. Sediment provenance of the Wilderness barrier dunes, southern Cape coast, South Africa. Terra Nova 22, 417–423.

Food and Agricultural Organisation (FAO), 2006. Guideline for Soil Description, 4th edition. FAO, Rome, Italy (109 pp.).

Fedorov, a V, Dekens, P.S., McCarthy, M., Ravelo, a C., deMenocal, P.B., Barreiro, M., Pacanowski, R.C., Philander, S.G., 2006. The Pliocene paradox (mechanisms for a permanent El Niño). Science (New York, N.Y.) 312, 1485–9.

Jansen, E., Overpeck, J., Briffa, K.R., Duplessy, J.C., Joos, F., Masson-Delmotte, V., Olago, D., Otto-Bliesner, B., Peltier, W.R., Rahmstorf, S., Ramesh, R., Raynaud, D., Rind, D., Solomina, O., Villalba, R., Zhang, D., 2007. Palaeoclimate. In: Climate Change 2007: The Physical Science Basis. Contribution of Working Group I to the Fourth Assessment Report of the Intergovernmental Panel on Climate Change [Solomon, S., D. Qin, M. Manning, Z. Chen, M. Marquis, K.B. Averyt, M. Tignor and H.L. Miller (eds.)]. Cambridge University Press,

Cambridge, United Kingdom and New York, NY, USA.

Roberts, D.L., Bateman, M.D., Murray-Wallace, C. V., Carr, A.S., Holmes, P.J., 2008. Last Interglacial fossil elephant trackways dated by OSL/AAR in coastal aeolianites, Still Bay, South Africa. Palaeogeography Palaeoclimatology Palaeoecology 257, 261–279.

Roberts, D.L., Bateman, M.D., Murray-Wallace, C. V., Carr, A.S., Holmes, P.J., 2009. West coast dune plumes: Climate driven contrasts in dunefield morphogenesis along the western and southern South African coasts. Palaeogeography Palaeoclimatology Palaeoecology 271, 24–38.

Roberts, D.L., Matthews, T., Herries, A.I.R., Boulter, C., Scott, L., Dondo, C., Mtembi, P., Browning, C., Smith, R.M.H., Haarhoff, P., Bateman, M.D., 2011. Regional and global context of the Late Cenozoic Langebaanweg (LBW) palaeontological site: West Coast of South Africa. Earth-Science Reviews 106, 191–214.

Sheldon, N.D. and Tabor, N.J., 2009. Quantitative paleoenvironmental and paleoclimatic reconstruction using paleosols. Earth Science Reviews 95, 1-52.

Soil Survey Staff, 2010. Keys to Soil Taxonomy, Eleventh ed. USDA-Natural Resources Conservations Service, Washington, DC 341 pp.

Thompson, L.G., Mosley-Thompson, E., Brecher, H., Davis, M., León, B., Les, D., Lin, P.-N., Mashiotta, T., Mountain, K., 2006. Abrupt tropical climate change: past and present.

Proceedings of the National Academy of Sciences of the United States of America 103, 10536–43.

Zeebe, R.E., Wolf-Gladrow, D., 2003. CO2in Sea Water: Equilibrium, Kinetics, Isotopes. Elsevier Oceanography Series 65, Amsterdam: Elsevier, pp. 167-188.

APPENDIX I

Correlation matrix for the major oxides in palaeosols and sediments of LBW (n = 12)

	SiO_2	TiO_2	Al_2O_3	Fe_2O_3	MnO	MgO	CaO	Na_2O	K_2O	P_2O_5	SO_3	Cr_2O_3	NiO
SiO_2		0.796**	0.379	0.231	0.360	0.854**	0.961**	0.009	0.602*	0.008	0.856**	0.351	0.256
TiO_2			0.572	0.491	0.589*	0.525	0.849**	0.317	0.645*	0.189	0.560	0.367	0.088
Al_2O_3				0.588*	0.398	0.031	0.602*	0.847**	0.459	0.165	0.267	0.684*	0.177
Fe_2O_3					0.193	0.066	0.421	0.654	0.407	0.092	0.175	0.472	0.206
MnO						0.064	0.429	0.382	0.687*	0.148	0.348	0.564	0.135
MgO							0.702*	0.370	0.422	0.144	0.696*	0.069	0.397
CaO								0.245	0.659*	0.007	0.831**	0.508	0.171
Na_2O									0.391	0.291	0.116	0.622*	0.256
K_2O										0.004	-0.561	0.650*	0.099
P_2O_5											0.448	0.091	0.204
SO_3												0.481	0.285
Cr_2O_3													0.127
NiO													

* Significant at 0.05 probability level
**Significant at 0.01 probability level
Underline indicates inverse relationship

Correlation matrix for the major oxides in palaeosols and pedofacies of Glenhof Road (n = 6)

	SiO_2	TiO_2	Al_2O_3	Fe_2O_3	MnO	MgO	CaO	Na_2O	K_2O	P_2O_5	SO_3	Cr_2O_3	NiO
SiO_2		0.930**	0.986**	0.928**	0.318	0.906*	0.091	0.222	0.917**	0.063	0.636	0.977**	0.623
TiO_2			0.971**	0.739	0.461	0.853*	0.034	0.158	0.988**	0.135	0.798	0.863*	0.846*
Al_2O_3				0.857*	0.341	0.874*	0.114	0.257	0.960**	0.040	0.699	0.938**	0.738
Fe_2O_3					0.111	0.823*	0.175	0.259	0.705	0.036	0.352	0.974**	0.288
MnO						0.651	0.845*	0.768	0.548	0.913**	0.864*	0.202	0.559
MgO							0.330	0.208	0.880*	0.472	0.787	0.862*	0.587
CaO								0.965**	0.076	0.976**	0.509	0.182	0.094
Na_2O									0.075	0.952**	0.358	0.272	0.060
K_2O										0.227	0.865*	0.826*	0.875*
P_2O_5											0.614	0.020	0.202
SO_3												0.489	0.881*
Cr_2O_3													0.473
NiO													

* Significant at 0.05 probability level
**Significant at 0.01 probability level
Underline indicates inverse relationship

APPENDIX II
SELECTED DETAILED ANALYTICAL TECHNIQUES

A. Soil pH-H_2O and pH-KCl, EC

A modified method from Reeuwijk (2002) was used in measuring soil acidity and electrical conductivity. The pH of the soil was potentiometrically measured in the supernatant suspension of a 1:2.5 soil: liquid mixture. The liquid was either distilled water (pH-H_2O) or a 1 *M* KCl unbuffered solution. Ten grams air-dried fine soil (<2mm) each of the samples was weighed into a 50 mL beaker. Twenty-five millilitres of liquid was added and the soil-liquid suspension was put in a rotor shaker and extract for 2 hours. The suspension was allowed to stand for 30 minutes for equilibration. The pH electrometer (Martini pH55 pocket testers) was then standardised using buffer solutions of pH 4.0 and 7.0. The electrode was inserted into the supernatant to read the pH value of the samples. The above procedure was repeated for the measurement of soil pH in 1 M KCl solution. Electrical conductivity was read with the glass electrode of JENWAY 4070 conductivity meter in a distilled water supernatant.

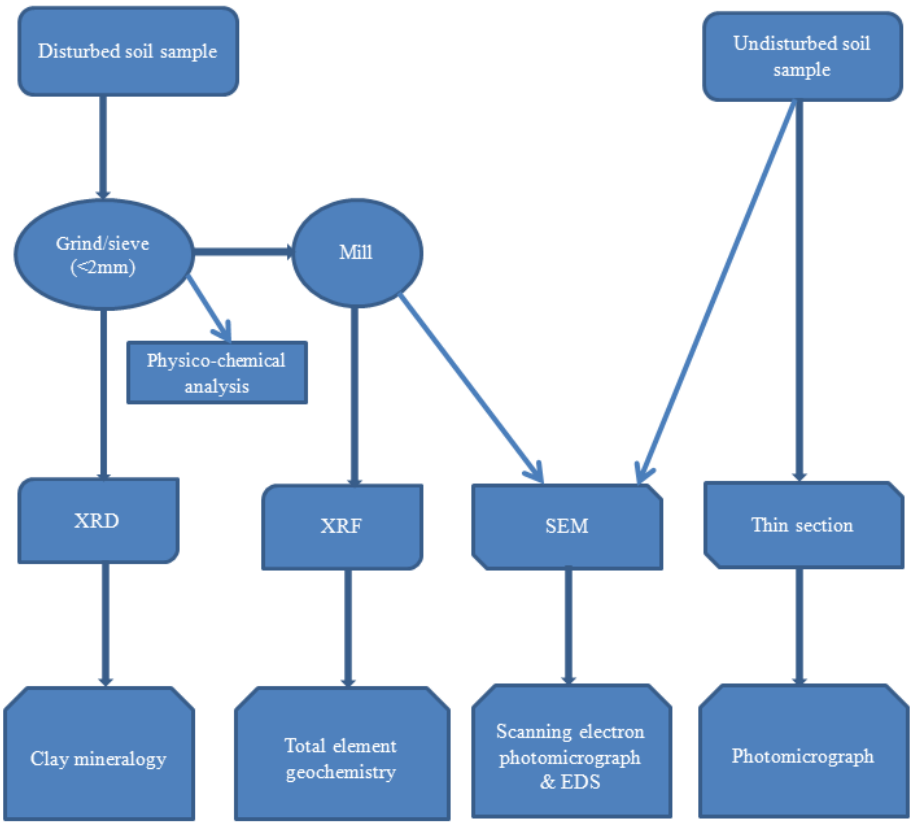

Flowchart of the analytical procedures

Table of laboratory analyses

Analysis	Method	Objective
a. pH (H_2O and KCl)	1: 2 soil: solution in pH meter	i) To measure the degree of acidity or alkalinity of the palaeosols and sediments ii) In KCl will give us an estimate of the exchangeable acidity brought about by Al iv) If pH KCl ≤ 5.2, exch Al is absent due to hydrolysis, polymerisation & precipitation
b. Electrical conductivity	EC electrode	i) This would tell us about the amount of dissolved salts in aqueous solution ii) EC and pH depends on bedrock and surficial geology, climate and local biota
c. Particle size	Laser diffraction And Bouyoucos method	i) to know the relative proportion of sand, silt and clay-sized fraction in soils. ii) To make a textural classification of palaeosols and sediments iii) This can also reveal the sedimentation patterns of the deposits in the basins. iv) Particle size affects physical and chemical properties of soils and sediments
d. $CaCO_3$ equivalent	Rapid titration	i) To measure the carbonate content of palaeosol (N.B. pH-H_2O MUST be ≥ 6.8) ii) Where relevant, this would be used to infer prevalent pedogenic pathways
e. C and O isotope	Spectrophotometry	i) To measure delta ^{13}C and ^{18}O isotopes in calcrete palaeosols ii) Results would be used to reconstruct palaeovegetation (C3 and C4 plants) iii) Results would also be used to estimate palaeoprecipitation and temperature
f. Bulk mineralogy	X-ray diffractometer	ii) This would reveal the constituent mineralogy of the palaeosols and sediments ii) Minerals form under varying environmental conditions and as such we infer this iii) This would also be useful in the palaeosols classification
g. Micromorphology	Thin section slides	i) To study the components of the palaeosols at microscopic and submacroscopic scale. ii) Help in identification of pedogenic processes.
h. Elemental composition	XRF	i) To measure major and minor elemental composition of palaeosols and sediments ii) Would be used to estimate weathering intensity and pedogenesis
i. SEM-EDS	SEM machine	i) To reveal solid grain/ pores relationship in the palaeosols and sediments ii) Monitor bio-accumulation of heavy metals root castes and palaeosols iii) To identify faunal structures at microscopic levels such as fungal hyphae, etc

B. Stable isotope spectrophotometry

New Gasbench method was used to analyse for stable isotopes ($\delta^{18}O$ and $\delta^{13}C$) composition of calcrete palaeosols at the Archaeometry Research Laboratory, Department of Archaeology in UCT. Samples were weighed into 12 mL borosilicate tubes and screw top lids containing a septum were used to close the tubes. The tubes were placed in a temperature controlled sampler tray set to 72^{o}C. Using the CTC Analytics A200S autosampler the tubes were flushed with helium to remove the atmospheric air present in them. 5 to 7 drops (according to sample size) of warm (72^{o}C) acid (85% orthophosphoric acid and phosphorus pentoxide, SG of solution = 1.92) were then manually added to each sample tube through the septum using a 1mL syringe. The samples were left to react for three hours before starting the run. The gas evolved from each reaction was sampled by the autosampler and passed to a Thermo Finnigan (Germany) model II Gasbench, where the sample gas was passed through a Nafion water removal unit. It then passed through the "Poraplot Q" GC column to separate the gas compounds released by the reaction, and then through a second Nafion water trap. The gas was then passed from the Gasbench to a Finnigan MAT 252 isotope ratio mass spectrometer (IRMS) computer controlled by Isodat software. The gasflow was controlled to give 10 sample peaks and 5 reference peaks. The CO_2 reference gas (99.995% purity) was also introduced into the mass spec via the Gasbench and was also controlled by the Isodat software.

Standards:

Cavendish Marble: crushed marble from Cavendish Square in Claremont. It was calibrated in our lab against a commercial reference gas. Mike Hall of Cambridge University also calibrated this marble. Discrepancy between the 2 measurements was 0.35 for the oxygen (-8.95 us, -8.60 them) and 0.05 (0.34 us, 0.39 them) for carbon. NBS 18, NBS 19, NBS 20 are from the US Department of commerce, bureau of standards samples. Carrara marble and Lincoln Limestone are commercial product, CarraraZ was calibrated at Cambridge by Mike Hall; the new Carrara marble value has been determined against CarraraZ.

C. Powder X-Ray diffraction (PXRD)

X-ray diffraction machine at Department of Geology of UCT was used for the mineralogical analyses of the samples. Powder XRD spectra were obtained by using a Bruker D8 Advance powder diffractometer with Vantec detector and fixed divergence and receiving slits with Co-Kα radiation. The phases were identified using Bruker Topas 4.1 software and the relative phase amounts (weight, %) were estimated using the Rietveld method.

D. Scanning electron microscopy (SEM)

Surface textures and features of the soil-palaeosol samples were studied by scanning electron microscopy at Microscopy Laboratory in Physics Department of UCT. Specimen was glued to an aluminium sample holder or "post". It was coated with thin layer of carbon (conductive material, gold can also be used for this purpose) and heated in an evaporation coater for 30 minutes. This is to enable the specimen endure the strong electric currents produced by the electron beam and prevent charge build-up at the point of analysis. After this initial treatment, the sample is placed in the SEM vacuum chamber, element dispersal spectroscopy (EDS), Oxford X-Max model and the electron gun is then switched on. The emission of secondary electrons in the vacuum gives rise to high-resolution images. The images were collected Nova NanoSEM 230 at a working distance (WD) of 5 mm, Landing E of 5.00 keV and varied magnifications ranging from 100 to ≥ 10000 (as may be deemed appropriate). Images were interpreted using Oxford INCA software.

E. Thin sectioning

Undisturbed hand samples were collected from the field. The delicate nature of soil demands careful sample preparation to avoid structural damage and disintegration. Before any processing, water was first removed from the soil. The sample was left in a well-ventilated area for several days until a constant weight is achieved and then dried on a hot plate at 40ºC for 48 hours. Thereafter, it was impregnated with epoxy resin to make it hard enough for cutting and polishing. The coated sample was allowed to cure at room temperature. Grinding, mounting on glass slide, grinding and lapping to final thickness (≤ 30 microns), and covering to dry up were other subsequent procedures. Petrographic light microscope was used in examining the slides at the Department of Geological Sciences at UCT.

F. X-Ray fluorescence spectroscopy

Eleven major elements, Fe, Mn, Ti, Ca, K, S, P, Si, Al, Mg and Na (with Ni and Cr when Ni and Cr concentrations exceed -2000 ppm or 0.2%) were determined using fusion disks prepared with LiT-LiM flux in the proportion 57:43 (Sigma chemicals) and LiBr as releasing agent, according to the method of Fernand Claisse (1999). The disks were analysed on a Philips PW1480 wavelength dispersive XRF spectrometer with a dual target Mo/Sc x-ray tube. All measurements were made with the tube at 50 kV, 50 mA. Fusion disks made up with 100% Johnson Matthey Specpure SiO_2 were used as blanks for all elements except Si. Fusion disks made up from mixtures of Johnson Matthey Specpure Fe_2O_3 and $CaCO_3$ were used as blanks for Si. Intensity data were collected using the Philips X40 software. All peaks

were corrected for background. Spectral overlap corrections are made for Br on Al, Cr on Mn, Al and Ca on Mg, and Mg and Ca on Na. Matrix corrections were made on all elements using the de Jongh model in the X40 software. Theoretical alpha coefficients, calculated using the Philips on-line ALPHAS programme, were used in the de Jongh model.

Trace elements were determined on powder briquettes in a series of analytical runs using a number of different x-ray tubes. The RhK" Compton or the MoK" Compton peak was used to determine the mass absorption coefficients of the specimens at the RhK"C wavelength or the MoK"C wavelength, and the Compton peak mass absorption coefficient values were used to correct for absorption effects on the Mo, Nb, Zr, Y, Sr, U, Rb, Th, Pb, Br, Se, Bi, As, W, Zn, Cu and Ni analyte wavelengths. Primary and secondary mass absorption coefficients for the Co, Mn, Cr, V, La, Ce, Nd, Ba, Sc, S and F analyte wavelengths were calculated from major element compositions using the tables of Heinrich (1986). Mass absorption coefficient corrections were made to the net peak intensities, (gross peak intensities corrected for dead time losses, background and spectral overlap), to correct for absorption differences between standards and specimens. No corrections were made for enhancement, which could be small but significant (<-5% relative) for the elements Cr, V, Ba and Sc in certain specimens, depending on their concentrations of Fe, Mn and Ti. Measured intensity data were processed through the computer program TRACE to correct gross peak intensities for background and spectral overlap and to make mass absorption coefficient corrections according to the methods outlined in Duncan *et al.* (1984). First order calibration lines with zero intercept were calculated using six or more international rock standard reference materials (SRMs) for each element. The one standard deviation error due to counting statistics and the lower limit of detection was calculated for each element in each soil-palaeosol specimen. Details of these measurements can be found at the URL: *web.uct.ac.za/depts/geolsci/facilities/xrf/X40CALIB.doc*

Reference

Claisse, F., 1999. “A new fusion technique for ferroalloys", presented at the 1999 Denver X-ray Conference.

Duncan, A. R., Erlank, A. J., Betton, P. J., 1984. Analytical techniques and database descriptions. Special Publications of the geologicala Society of South Africa 13, Appendix 1, 389-395.

Heinrich, K. F. J., 1986. Mass absorption coefficients for electron probe microanalysis. In: Proc. 11th Int. Congress on X-ray Optics and Microanalysis, London, Canada, J B Brown and R H Packwood (Eds).

APPENDIX III: SOIL AND SITE DESCRIPTION FORM (page #s in parens)

Persons Describing the Soil: _____ Pedon # _____

Date _____ Lat.(11) ____ . _____ Lon.(11) _____ . _____ (decimal degrees)

County _____ USGS Quad Sheet(11)_____ MLRA(11) _____

Site Properties: (13-14)

Current land use and vegetation: _____

Elevation (m): _____ Aspect (slope direction) (0^o to 360^o):_____

Slope gradient (%): _____ Slope length: (m) _____

Boulders on/in surface (%) _____ Stones on/in surface (%) _____

Physiography: (15) ___ Flood Plain ___ Stream terrace (level) ___ Stream terrace (dissected)
___ Upland ___ Closed Depression ___ Drainageway

Lanscape Position: (11) ___ Summit ___ Shoulder ___ Backslope
___ Footslope ___ Toeslope ___ Not Appl. (on < 2% slopes in coastal plains)

Land surface shape: (17) (First letter is down-slope profile, second letter is cross-slope profile)
L = linear V = convex C = concave
___ LL ___ LV ___ LC
___ VL ___ VV ___ VC
___ CL ___ CV ___ CC

Hydrology: (18-19)

Saturation type: endo or epi? _____ Wetland indicator plants? y/n ___ Artificial drainage: y/n ___

Depth of observed water: (cm) ____ Flooding evidence? y/n ____ Ponding evidence? y/n ____

SOIL PROPERTIES

Soil Drainage Class (15)	Depth Class: (59)	Parent Material(s): (20)
___ excessively drained	____ V. Shallow (< 25 cm)	___ Residuum (kind/s) _____
___ somewhat excessive	____ Shallow (25 – 50 cm)	___ Organic (not litter)
___ well	____ Mod. Deep (50 – 100 cm)	___ Alluvium
___ somewhat well	____ Deep (100 – 150 cm)	___ Marine (recent)
___ moderately well	____ Very Deep (> 150 cm)	___ Unconsol. Coastal Plain
___ somewhat poor		___ Beach
___ poorly drained		___ Lacustrine
___ very poorly		___ Loess
		___ Eolian sand (dune)
	Root-restricting depth: (59) (cm) _____	___ Colluvium

Texture:

Sand = S
Loamy Sand = LS
Sandy Loam = SL
Loam = L
Clay Loam = CL
Silt = SI
Silt Loam = SiL
Silty Clay Loam = SiCL
Silty Clay = SiC
Sandy Clay Loam = SCL
Clay = C
Sandy Clay= SC

ABBREVIATIONS (case sensitive)

Modifiers of Coarse Fragments:

Gravelly = GR (≥ 15%)
Cobbly = CB (≥ 15%)
Channery = CH (≥ 15%)
Stony = ST (≥ 15%)
Very (add V if ≥ 35%)
Extremely (add X if ≥ 65%)

Structure Grade:

Weak = WK or 1
Strong = ST or 3
Moderate = MO or 2
Structureless = SLS or 0

Structure Size: 1 through 5 (see Tab. 16, Fig. 44-47)

Structure Shape:

Granular = GR
Angular Blocky = ABK
Platy = PL
Subangular Blocky = SBK
Prismatic = PR
Massive = MA
Single Grain = SG

Consistence:

Loose = L
Firm = Fi
Very Friable = VFR
Very Firm = VFi
Friable = FR
Extremely Firm = EFi

Abundance:

Few (< 2% vol) = F
Many (≥ 20% vol) = M
Common (2 to < 20% vol) = C

Pore Linings or Masses:

Soil Profile _____ **Description Worksheet** (reference Field Book for Describing Soils or Soil Profile Desc. Manual)

Horizon			Depth	Bndry	Texture		Color			Redoximorphic Features (1 or 2 of each)					Structure			Consis-tence	Fine + V. F. Roots
#	% *	Name *	Bottom cm	Dis-tinct.	Rock Mod.	Fine-earth Class*	Moist Matrix* Hue	Val	Chr	Fe Depletions % vol.	Fe Depletions Full Color Hue V/C	Fe Concentrations % vol.	Fe Concentrations Full Color Hue V/C	Linings? or masses?	Gra-de	Size	Shape	Moist	Abun-dance F, C, M
1																			
2																			
3																			
4																			
5																			
6																			
7																			
8																			
Pg		24-31	32	31	39	38-41	33	33	33	37	37	37	37	37	45	46	47	50	50

Additional Description Worksheet (reference Field Book for Describing Soils or Soil Profile Desc. Manual)

Horizon		Rock fragments				Mn Conc.		Clay Films	Pores	Sandy or leached pockets	Rock-controlled structure?	Brittle?	Perching layer?	Root-limiting?
Hor #	Name	Gravel**	Cobbles**	Stones	Bldrs	Concre-tions	Films + masses							
				%	%	%	%	y/n	y/n	% vol	% vol	% vol	y/n	y/n
1														
2														
3														
4														
5														
6														
7														
8														
Page#	24-31	39	39	39	39	35-37	35-37	44	51	45	45(bottom)	53	18	50, 59

* If 2 major non-redox colors in the same horizon, split the boxes and give a vol. percentage of each. Also split if 2 separate horizon materials like E/A, E/Bt, or Bt/E.

** Channers are flattened but include gravel and cobble sized rocks. Comments:

APPENDIX IV

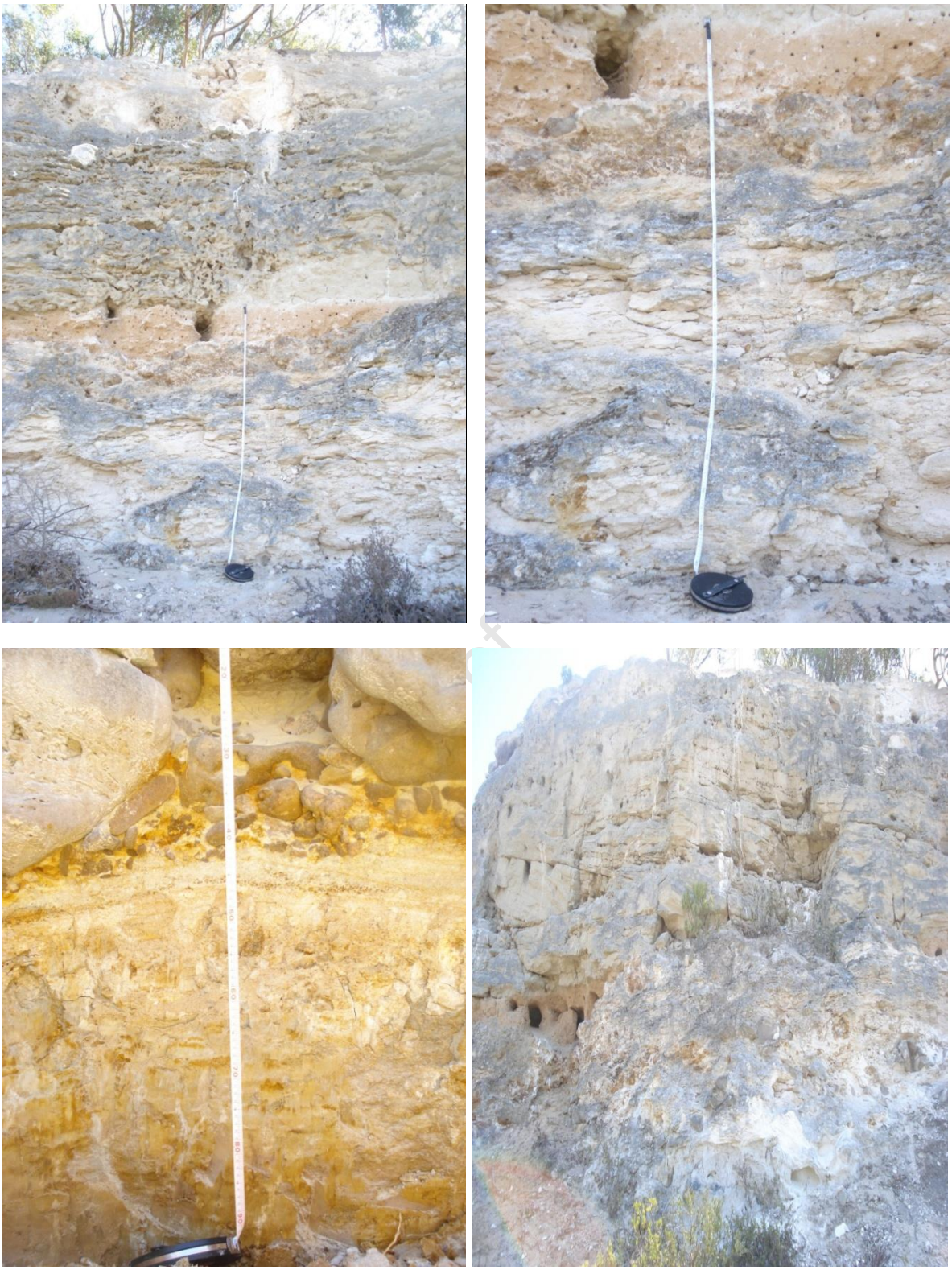

Views of Langebaanweg palaeosol sequences from different positions